UNIVERSITY OF CAPE TOWN

FACULTY OF ENGINEERING AND THE BUILT ENVIRONMENT
Department of Civil Engineering

Practical Application of the Torrent Permeability Test Method with the South African Durability Index Approach

---

Prepared by:
Sean T. Alfred

Supervisors:
Emeritus Prof. Mark Alexander
Prof. Hans Beushausen

CoMSIRU

A Thesis submitted in partial fulfilment of the requirement for award of the degree of Master of Science in Civil Engineering Specialising in Civil Infrastructure Management and Maintenance at the University of Cape Town.

[MAY 2025]

PLAGIARISM DECLARATION

Plagiarism is to use another's work and pretend that it is one's own. I know that plagiarism is wrong.

I have used the UCT Harvard convention for citation and referencing. I have attributed, cited, and referenced each significant contribution to and quotation in this thesis project from other people's work(s).

This thesis/dissertation is my work.

I have not allowed and will not allow anyone to copy my work to pass it off as their work.

This thesis/dissertation has been submitted to the Turnitin module (or equivalent similarity and originality checking software). I confirm that my supervisor(s) have seen my report, and any concerns revealed have been resolved with them.

Signature: Signed by candidate Date: 27/01/2025

Student Name: SEAN THABANI ALFRED

DEDICATION

I dedicate this dissertation to my late brother, **STEPHEN MWAI CHIDZERO.**
Your untimely passing was a sombre and challenging moment during my master's journey.
Continue resting in peace. I will keep striving to achieve the success we have always dreamt of.
I celebrate you with this achievement.

ACKNOWLEDGEMENTS

Firstly, I would like to thank **God** for blessing me with this opportunity to complete my master's thesis. You deserve all the praise and glory. You have carried me through it all, Lord.

I want to express my gratitude to my supervisor, **Prof. Mark Alexander,** for his unwavering support throughout my studies. I have drawn so much inspiration and encouragement from your wise and ever-insightful words, and I am forever thankful for your guidance and care.

To my co-supervisor, **Prof. Hans Beushausen,** thank you for the mentorship and unreserved advice. It has been an honour to learn much from you, both academically and professionally. I am humbled by your continued support.

I want to thank **Dr. Roberto Torrent** for the generous support and guidance in understanding the Torrent test method and use of the equipment. Your input was invaluable.

I want to extend my thanks to **Alwyn Carstens, Deo Kalala,** and **the team at Concrete Units** for their support and provisions, which made my field experiments possible.

I thank all the **staff** and my **colleagues** in the **Concrete Materials and Structural Integrity Research Unit (CoMSIRU)** for their input and constructive feedback during the research progress seminars. Your advice developed my presentation skills, built my confidence, and helped mould my research.

My heartfelt thanks go to **Nooredien Hassen** and the **UCT civil engineering laboratory staff** for their assistance and training for all the equipment I used and the experiments I conducted. A special mention goes to **Charles May** for being my right-hand man during my field experiments and for his support when I suffered my hand injury.

I greatly thank the **John Davidson Educational Trust, Shade Muluti,** and **CoMSIRU** for their financial assistance, enabling me to sustain myself and complete my studies.

To my friends **Shade, Tais, Areej, Meghan, Nadiya, Nicholas, Ichebadu, Saarthak, Aaron,** and **Sam,** I cherish all the memories we shared, the support and advice you gave me whenever required, and for making my stay in Cape Town memorable.

I am extremely grateful to my family: my mother, **Virginia;** my sisters, **Sonja** and **Judith;** and my brother, **Michael,** and his family**.** You believed in me when the chips were down and encouraged me to keep going. I love you all.

Finally, I would like to thank my wife **Victoria Mutongerwa** for always being supportive and motivating me in moments where I faced challenges during this journey.

ABSTRACT

Tests that assess the potential durability of concrete offer robust evaluation approaches for predicting its performance. The South African Durability Index Approach (SADIA) and the Torrent method are used in South Africa and Switzerland, respectively, to assess the potential concrete durability of the cover layer. Specifically, the Oxygen Permeability Index (OPI) test and the Torrent Permeability Test (TPT) are widely recognized as reliable techniques for evaluating the gas permeability of concrete. Studies have demonstrated the sensitivity of these methods to various factors that affect the properties of hardened concrete. Recent research has shown a strong correlation between the OPI and TPT methods in simulated environmental conditions. A combined approach using both methods has been suggested to improve existing practices for assessing concrete durability. However, the correlation has not been confirmed for site concrete elements, and practical guidelines have not yet been established.

This research aimed to develop practical guidelines for an integrated durability assessment strategy involving the OPI and the TPT methods on in-situ concrete elements. Five mixes consisting of two water-to-cement (w/c) ratios (0.5 and 0.6), two concrete grades (30 MPa and 40 MPa), and three binder types (100% CEM I 52.5N, CEM II/A-L 52.5N, and 70/30 CEM I + fly ash) were used to manufacture precast freeway median barriers and representative test panels. The concrete elements' early-age (28 – 56 days) gas permeability characteristics were tested under various environmental exposure conditions (summer and winter) in Cape Town, South Africa.

The OPI and TPT methods generally showed good sensitivity to the test variables (w/c ratio, binder type, age, and environmental exposure). There was a strong correlation between the two methods in the summer data but a weak association in the winter data. This difference was attributed to the pore-blocking effect of moisture on the Torrent test, emphasizing how surface moisture may affect the measured results even within permissible moisture levels. Nonetheless, the site correlation in the summer confirmed findings from previous studies.

Given this study's findings, it was determined that a combined approach using the Torrent and OPI methods can be implemented based on site-specific conditions. The initial assessment of the structure can be conducted using the Torrent test and, if required, substantiated by the OPI test in moist conditions. It is recommended that moisture correction methods be used to adjust the measured Torrent results in very dry conditions using reference surface moisture values.

However, to consolidate the proposed combined practical approach, the results of this research need to be validated through a more extensive study using larger sample sizes, a more comprehensive range of concretes, and varying environmental conditions.

TABLE OF CONTENTS

LIST OF FIGURES

LIST OF TABLES

LIST OF ABBREVIATIONS AND ACRONYMS

ACI	American Concrete Institute
ANOVA	Analysis of Variance
AS	Australian Standards
ASTM	American Society for Testing and Materials
BCP	Bulk Cement Paste
$Ca(OH)_2$	Calcium Hydroxide
$CaCO_3$	Calcium Carbonate
CCI	Chloride Conductivity Index
CCSA	Cement and Concrete South Africa
CIA	Concrete Institute of Australia
CIRSOC	Argentine structural concrete codes
CO_2	Carbon dioxide
COTO	Committee of Transport Officials
CoV	Coefficient of Variation
CS	Crusher Sand
CSA	Canadian standards
C-S-H	Calcium-Silicate-Hydrate
DI	Durability Index
DS	Dune Sand
DTS	Deemed-to-Satisfy
EN	European standards
FA	Fly ash
HCP	Hardened Cement Paste
IRAM	Argentine institute of standardization and certification
IRH	Internal Relative Humidity
ITZ	Interfacial Transition Zone
JSCE	Japan Society of Civil Engineers standard
kOPI	OPI permeability coefficient

kT	Torrent permeability coefficient
NaCl	Sodium chloride
NDT	Non-destructive test
OPI	Oxygen Permeability Index
P2P	Prescriptive to Performance
PB	Performance-based
PBD	Performance-based design
PC	Portland Cement
PC-I	CEM I 52.5N binder
PC-II	CEM II A/L 52.5N binder
RC	Reinforced concrete
RCPT	Rapid Chloride Permeability Test
RH	Relative Humidity
SADIA	South Africa Durability Index Approach
SANRAL	South African National Roads Agency Ltd.
SANS	South African National Standards
SCBA	Sugarcane bagasse ash
SCM	Supplementary cementitious material
SIA	Swiss standards
SL	Service life
SLM	Service life model
TPT	Torrent Permeability Test
UCT	University of Cape Town
w/c	Water-to-cement
WSI	Water Sorptivity Index

1. INTRODUCTION

1.1. Overview

Traditionally, design of structural concrete has relied on prescriptive standards. However, growing understanding of concrete durability has exposed the inherent limitations of this approach. Modern practices are now starting to emphasize performance-based specifications, considering the concrete's interaction with its environment, material choice and proportion, and concreting practices. This shift has led to the development of the so-called 'durability indicator' tests to assess concrete quality for durability. An 'indicator' represents a characteristic reflecting the status or degree of something. For example, concrete compressive strength can be seen as an indicator characterising the material's potential to resist applied stresses. Durability indicators assess the concrete system's status related to transport properties or deterioration mechanisms. The Oxygen Permeability Index (OPI) test (South Africa) and the Torrent Permeability test (TPT) (Switzerland) method measure gas permeability of the cover layer (Torrent, Neves & Imamoto, 2022b). Comparative studies by Beushausen and Alexander (2008), and Starck (2013; 2017) established that the OPI and TPT have similarities in assessing the concrete cover quality. The similarities present a basis for a correlation between the two methods.

However, no guidelines in local practices currently incorporate a combined approach using a non-destructive test (NDT) such as the TPT method. Therefore, this study proposed a practical implementation of the TPT method with the OPI test to allow for a faster approach to the durability assessment of concrete locally concerning gas permeability. This chapter introduces the study by providing a background and outlining the research problem, the aims, objectives, and related research questions, as well as the significance and limitations.

1.2. Background to the study

Reinforced concrete (RC) structures are ubiquitous in the built environment due to their strength and 'durability'. A concrete structure is considered durable if it can retain its strength and serviceability for its anticipated service life with minimum maintenance (Torrent, Neves & Imamoto, 2022b). Presently, parameters such as the compressive strength, water-to-cement (w/c) ratio, cement content, binder type, and cover depth are specified as proxies for concrete durability (Alexander, 2017, Beushausen, Torrent & Alexander, 2019). However, this approach is prescriptive and does not guarantee immunity from premature deterioration and loss in serviceability of the concrete structure (Alexander, 2018).

Over the years, a better understanding of deterioration mechanisms and mass transport processes in concrete has revealed the inadequacies of the prescriptive approach. As a result, codes and standards are beginning to adopt performance-based approaches towards the durability design of concrete (Torrent, Neves & Imamoto, 2022b). The performance-based approach is founded on assessing material attributes that can be connected to degradation

mechanisms under the predominant exposure environment. This enables a more rational way for durability prediction (Alexander, Otieno & Beushausen, 2021). One performance-based tool developed is Durability Indicators/Indexes (DI). The philosophy of durability indicators is to improve concrete durability by using specialized tests to assess transport properties in concrete, which influence deterioration. These indexes provide a more accurate evaluation of long-term durability, going beyond traditional specifications such as strength tests. The approach emphasizes early-age testing and the need for long-term monitoring, integrating practical solutions for real-world conditions to ensure better performance of concrete structures over time. (Alexander, Mackechnie & Ballim, 1999; Alexander, 2005; Alexander, Bentur & Mindess, 2017). Using these indicators, the material's potential can be considered during the design phase, and the structure's as-built quality can be assessed to predict its long-term performance.

In South Africa, a durability index (DI) approach has been developed, including three tests: Oxygen Permeability Index (OPI), Water Sorptivity Index (WSI), and Chloride Conductivity Index (CCI). These tests measure the concrete cover layer's resistance to gas, fluids, and ions, respectively (Alexander, Gouws & Maritz, 2001; Alexander, 2005). The South African Durability Index Approach (SADIA) has progressed to a point where the tests have been included in the current South African National Standards (SANS). Further, the methods are implemented extensively in significant national infrastructure projects by the South African National Roads Agency (SANRAL) (Nganga et al., 2016). The OPI test method will be discussed in greater detail for this study.

The OPI test involves the determination of a coefficient of permeability (*kOPI*) on cored and sliced concrete samples placed in a falling head permeameter (Alexander, 2005). The index values determined are defined as the negative logarithm (log) of *kOPI*; therefore, higher OPI values (above 9.5) indicate good permeability characteristics (less permeable) (Alexander, Santhanam & Ballim, 2010). However, the method is semi-invasive; the specifications require extracting core samples from the actual structure or 'mock-up' test panels manufactured from the same concrete batch and preparatory conditions as the real structure (Starck, 2013).

In Switzerland, the Torrent Permeability Test (TPT) is a standardized non-destructive test method, that measures the coefficient of air permeability (*kT*) of the covercrete (concrete cover layer) (Torrent & Frenzer, 1995). The method uses a portable instrument powered by a vacuum system. The TPT allows for quick determinations at multiple test locations, providing a comprehensive assessment of concrete permeability. However, the measured *kT* value can be affected by the moisture level of the tested surface, making interpretation challenging. (Starck, 2013).

Previous research by Beushausen and Alexander (2008), Torrent (2012), and Starck (2013; 2017) has shown that the OPI and TPT methods can successfully evaluate potential concrete durability characteristics. In particular, Starck (2013) investigated the potential of combining the two methods as a practical means for a faster DI approach to the local practice by introducing the non-destructive torrent method to supplement the OPI. Furthermore, the study established a general equation correlating the OPI and TPT based on the collected data, yielding an excellent relationship (R = 0.97).

1.3. Research problem

The OPI test and the TPT have emerged as reliable durability indicator tests that have been applied practically for many years (Alexander, 2017). In addition, researchers have demonstrated that the two methods have synergies that offer the potential for a combined approach (Beushausen & Alexander, 2008; Starck, 2013; Starck et al., 2017).

However, the existing body of research lacks practical guidelines for assessing concrete durability in-situ, incorporating the TPT method and OPI test together. Furthermore, implementing such an approach without applicable specifications negatively impacts confidence in obtaining reliable quality control assessments of RC structures, especially where the influence of environmental moisture conditions is involved. Thus, the on-site relationships between the OPI test and the TPT technique must be validated to develop practical guidelines.

1.4. Aim and objectives of the study

The principal aim of the research project was to develop a basis for a combined site durability index testing approach incorporating the Torrent method and OPI test. The study focused on the following objectives:

- Review the current state of the art in performance-based durability design and testing.
- Review the current state of practice of the OPI and TPT methods on site durability assessment of RC structures.
- Validate the relationship(s) (if any) between the DI results obtained from site elements tested using the OPI and TPT methods.
- Propose guidelines for a joint DI testing approach using the non-destructive TPT method with the local OPI test for site durability assessment.

1.5. Research questions

The specific research questions for the study are listed as follows.

- What methodologies are currently in use for performance-based durability definition and assessment?
- What practical challenges does the industry currently face with existing durability criteria and accompanying quality assurance testing that uses the OPI and TPT methods?
- What is the essential relationship between DI results achieved with the OPI test and the TPT method on site-tested elements?
- To what extent and how differently does the expected relationship depend on the site conditions and other identified influencing factors (if any)?

- How can in-situ durability testing using the TPT method supplement the local DI methodology (OPI test)?

1.6. Research significance

This study is expected to contribute to the growing knowledge of performance-based testing methodologies. Practical guidelines for a combined approach involving NDT in the local DI approach would allow faster and more comprehensive durability assessment of RC structures on site. In addition, the NDT may be substantiated by laboratory-based testing, where site conditions may influence the interpretation of results.

The approach will provide a more rational way for durability assessment in RC construction. Further, the research outputs can contribute towards valuable data inputs in service life modelling of RC structures in South Africa. The study's findings are expected to strengthen the industry's acceptance of the OPI and Torrent methodologies for evaluating concrete quality.

1.7. Scope and limitations

1.7.1. Scope

The thesis explored the practical application of the TPT method with the SADIA on RC structures. Two gas permeability test methods, the Oxygen Permeability Index and Torrent Permeability tests, were considered as per the SANS 3001-CO3-2:(2015) and the SIA 262/1-E:(2019) standards, respectively. The DI tests were performed on RC structural elements (freeway median barriers) and representative test panels constructed within the Cape Town area.

The study considered five concrete mixes comprising two grades (30 MPa and 40 MPa) of plain Portland cement and blended cement with 30% Fly ash replacement. The concrete elements were cast and tested during the summer and winter (to vary the exposure conditions) and subjected to natural curing.

1.7.2. Limitations

This research did not consider the following aspects:

- A wider range of concrete types. The selected mixes only simulated the most common mix designs for durability-critical structures in the local (South Africa) environment, where the primary deterioration mechanism is carbonation (inland).
- The effect of different curing methods on the DI tests; previous studies provide insight into this aspect (Surana, Pillai & Santhanam, 2017a,b).

1.8. Thesis outline

This research project comprises five chapters: Chapter 1: Introduction, Chapter 2: Literature Review, Chapter 3: Materials and Methods, Chapter 4: Results and Discussion, and Chapter 5: Conclusions and Recommendations. The following is a brief overview of the individual chapters.

Chapter 1 introduces the broad background of the research topic and then narrows down to the problem the thesis will address. It also discusses the objectives, related research questions, significance of the research, and study limitations.

Chapter 2 provides a literature review on concrete durability, including performance-based approaches, transport mechanisms, factors influencing durability, permeability, assessment techniques such as the Torrent method and oxygen permeability index test, and a critical analysis of previous relevant studies focused on the OPI and TPT methods.

Chapter 3 details the experimental methodology undertaken in this study, describing all the stages of execution involved and the considerations made to ensure that the practical objectives are addressed.

Chapter 4 provides a detailed analysis of the results obtained and critically discusses the data to answer the research questions.

Chapter 5 draws upon the data collected in the experimental work to propose a practical implementation strategy for an integrated approach to durability assessment in South Africa. Conclusions from the results and discussions are presented, and recommendations are made for future work.

2. LITERATURE REVIEW

2.1. Overview

This chapter aims to build an understanding of current durability indicator approaches used in the durability design of RC inland structures. Focus will be on permeability-related test methods, notably the Oxygen Permeability Index (OPI) and Torrent Permeability tests (TPT). Existing research on the methods will be evaluated, to explore the practicality of a combined approach. The chapter is presented as follows.

The chapter will cover the importance of concrete durability, transport properties in RC structures, gas permeability, carbonation, service life impact, durability design and specifications, and comparative studies on the OPI and TPT methods.

2.2. Understanding concrete durability

Concrete durability and sustainability have become key focus areas in recent times due to the increase in the use of concrete in infrastructure construction. The prevalent use of concrete is linked to its adaptability and economic efficiency in various construction applications, but most importantly, its high inherent durability (Alexander, Bentur & Mindess, 2017). However, current experiences with concrete, especially RC, indicate a lack of durability in many cases (Alexander, Ballim & Stanish, 2008). The problem has been linked to the misconception that durability largely relies on specifying permissible strength parameters (prescriptive approach).

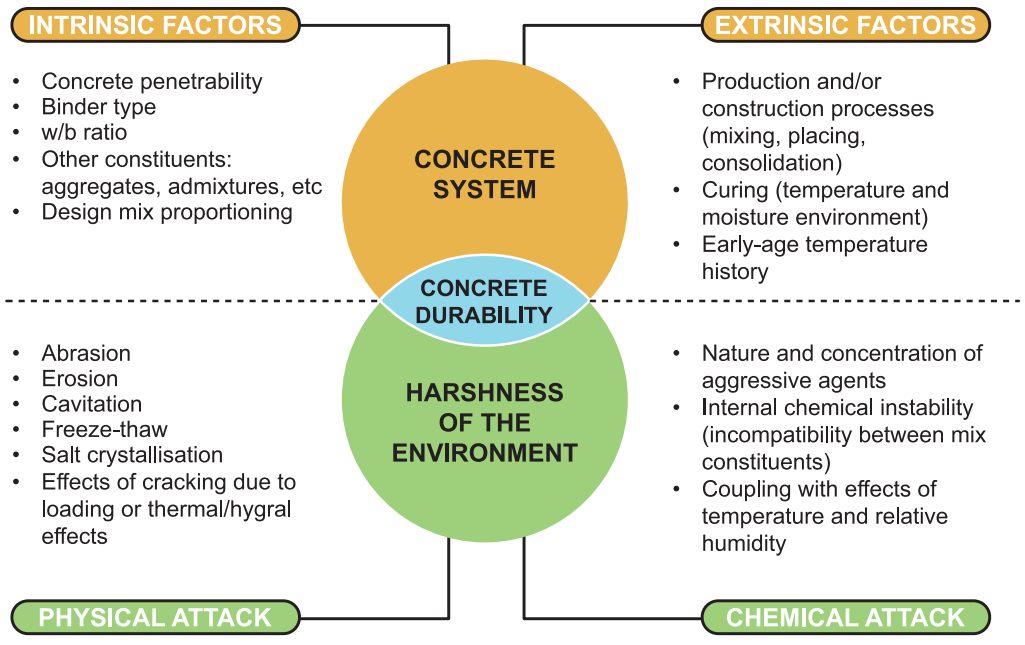

Figure 2-1 Factors influencing the durability of concrete (adapted from Alexander et al. (2021).

The concept of durability can easily be misunderstood because it is not a quantifiable characteristic or a material property. Durability depends on how well the concrete performs in its intended environment over its service life. (Nilsson, 2003). Figure 2-1 illustrates how durability depends on concrete's ability to resist deterioration from internal and external influences and withstand exposure to harsh environments. The prescriptive approach only considers certain internal factors in isolation.

When designing for durability, it is crucial to consider the mix design, construction practices, and environmental aggressiveness, which all influence concrete deterioration (Alexander, Otieno & Beushausen, 2021). Without a performance approach, durability cannot be optimised, and the concrete, especially RC, will be susceptible to premature deterioration. Thus, the durability of concrete depends on limiting the flow of destructive agents, particularly in the cover layer.

The following sections will discuss the concrete system and processes (transport mechanisms) that facilitate the flow of aggressive species through the concrete. The term ‘penetrability’ will be used frequently in these sections to cover various ingress mechanisms (permeation, absorption, diffusion, and migration). Penetrability is the ease with which aggressive agents can penetrate the concrete through the pore structure (Ballim, Alexander & Beushausen, 2009). Concrete penetrability is primarily controlled by the porosity of the cement paste, particularly at the interfacial transition zone (ITZ) (interface with the aggregate particles).

2.3. The concrete system and transport processes

2.3.1. Concrete microstructure

The microstructure of hardened concrete is essential in understanding how matter is transferred through the concrete. Once the mixture of the aggregates, binder, water and admixtures set, a solid concrete material is produced. It comprises three phases: aggregates, hardened cement paste (HCP), and the ITZ (Torrent, Neves & Imamoto, 2022b).

2.3.1.1. Aggregates

Aggregates comprise between 70% and 80% of the concrete volume and may have beneficial and detrimental effects on the concrete system (Mehta & Monteiro, 2001). According to Nilsson (2003), aggregates introduce twisted or distorted paths in the concrete matrix, which can affect species diffusion, reducing concrete’s penetrability. Aggregates can also possess properties that cause destructive reactions with hydration products, such as alkali-aggregate reactions (Torrent, Neves & Imamoto, 2022b). Generally, aggregates play a secondary role in the flow of matter in the concrete system but significantly influence concrete's penetrability.

2.3.1.2. Hardened cement paste

The hardened cement paste (HCP) is predominantly made up of calcium silicate hydrates (C-S-H) and calcium hydroxide ($Ca(OH)_2$), taking up about 60% and 25% of the HCP phase, respectively (Torrent, Neves & Imamoto, 2022b). The hydrates exist in the form of thin, long

crystals, contributing to the strength of HCP. Hydration products occupy twice the volume of the initially unhydrated cement crystals comprising solid (~72%) and porous (~28%) characteristics (Torrent, Neves & Imamoto, 2022b).

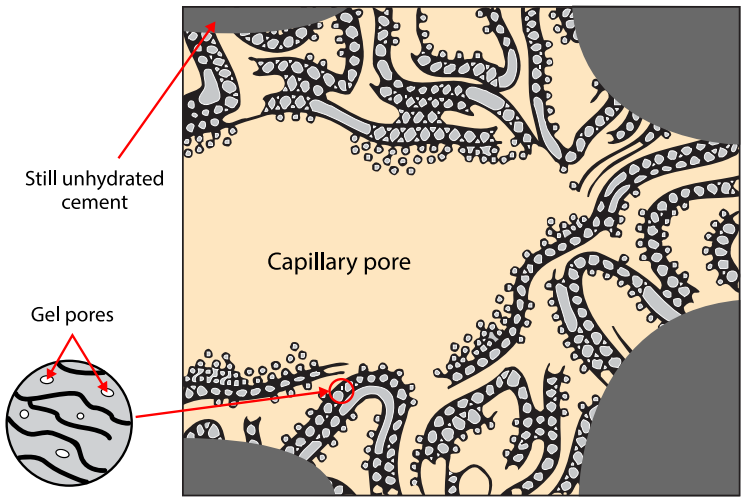

Figure 2-2 Pore structure of hydrated cement paste (adapted from Torrent et al.(2022).

Two types of pores exist within the HCP: gel and capillary (see Figure 2-2) (Mehta & Monteiro, 2006). Gel pores are small pores formed by the disordered arrangement of C-S-H crystal fibres during hydration. Gel pores are ingrained in the HCP and cannot be altered regardless of the extent of hydration (Torrent, Neves & Imamoto, 2022b). Capillary pores are voids created from previously water-filled spaces. They play a crucial role in concrete's ability to allow matter to move as they depend on the w/c ratio, cement type, and degree of hydration. Thus, larger capillary pores would provide an ideal medium for deleterious species to move through the concrete.

The influence of the w/c ratio on the evolution of hydration and formation of capillary pores is illustrated in Figure 2-3, from the unhydrated state (t = 0) to several weeks, when most hydration is achieved (about 70%) (Torrent, Neves & Imamoto, 2022b). Concrete mixes with a higher w/c ratio will have greater dispersion or distance between cement particles in water than those with a low w/c ratio. This difference translates to quicker stiffening and concrete setting in mixes with a lower w/c ratio due to the faster bonding of the hydration products with nearby particles (at t = hours). After several weeks (say 28 days), the hydration products of the concrete with a low w/c ratio take up more space (smaller and less capillary pores) than higher w/c ratio (larger, more capillary pores). Thus, lowering the w/c ratio can be beneficial in reducing the penetrability of the concrete.

The nature of the pore structure in the HCP depends on the physico-chemical characteristics of the cement and the use of supplementary cementitious materials (SCMs) (Torrent, Neves & Imamoto, 2022b). The discussion covered on the concrete system refers only to ordinary Portland cement (PC). Composite types of cement help achieve denser cement paste matrices, leading to a refined pore structure and reduced porosity of the ITZ in mass movement through the HCP (Torrent, Neves & Imamoto, 2022b).

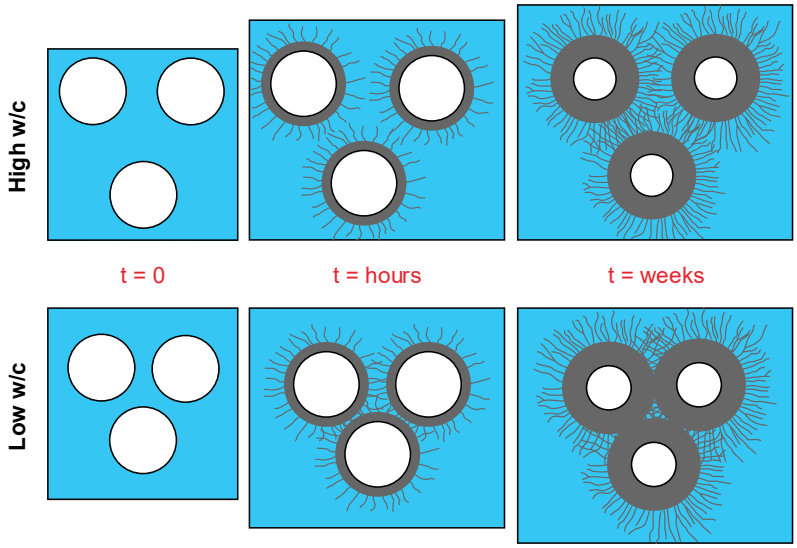

Figure 2-3 Evolution of cement hydration (adapted from Torrent et al. (2022).

2.3.1.3. Interfacial transition zone (ITZ)

The interfacial transition zone (ITZ) is the interface between the aggregates and HCP (Alexander et al., 2021). The contact zone is between 30 μm and 50 μm thickness, comprising $Ca(OH)_2$ crystals and ettringite needles (see Figure 2-4). The composition of the ITZ differs from the bulk cement paste (BCP) because of the film of water that forms around the aggregate particles following the compaction of fresh concrete. The local water-to-cement ratio (w/c) around those regions is altered from that of the BCP, producing larger portlandite crystals and ettringite (Angelucci, 2013). Further, the microstructure of the contact zone will be more open and porous than the BCP.

The ITZ microstructure makes the interface the weakest and most penetrable link in concrete, allowing for the movement of substances (Torrent, Neves & Imamoto, 2022b). The strength of the ITZ is influenced by the w/c ratio of the cement paste (lower w/c ratio = higher strength), concrete age (strength improvement with age), and trapped bleed voids. However, Scrivener et al. (2004) found that SCMs can enhance particle packing (fine-filler effect) and generate more hydration products, developing a more refined ITZ microstructure. Adding these binders with pozzolanic additions reduces bleeding, enhances pozzolanic reactions, and improves concrete durability by densifying the ITZ.

As the preceding discussion shows, the phases of the concrete system determine the concrete's strength and durability characteristics. The following section gives an overview of the different types of pores in the concrete, their size, and their contribution to the penetrability of concrete.

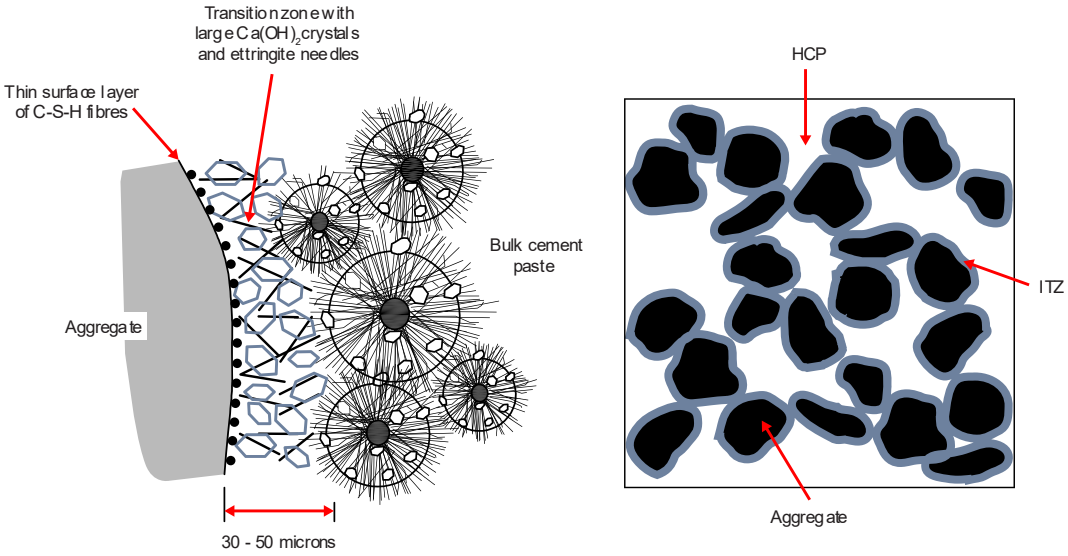

Figure 2-4 Schematic representation of the ITZ and its interaction with the aggregate particles and the cement paste (adapted from Alexander et al. (2021)

2.3.2. Concrete pore system

Three noteworthy types of pores exist in the concrete system (see Figure 2-5), viz. gel pores, capillary pores, and macropores (entrained air bubbles and entrapped voids). The pores in the HCP and ITZ account for a significant amount of material flow through the concrete (Torrent, Neves & Imamoto, 2022b). The size, volume, interconnectivity of the pores, and the number of penetrating agents dictate the permeability of the concrete. The pores are described as follows.

- ***Gel pores:*** exist as minute-sized voids, about the same order of 5 to 10 water molecules (Torrent, Neves & Imamoto, 2022b). Gel pores allow little mass flow through the concrete; thus, they have little effect on the penetrability of the concrete system (Richardson, 2002). High porosity in concrete paste does not necessarily mean high permeability due to the inability of the gel pores to allow ionic flow (Beushausen & Alexander, 2009; Angelucci, 2013).
- ***Capillary Pores:*** vary in pore radius over several orders of magnitude (0.01 µm – 1 µm for low w/c ratios and 1 µm – 100 µm for high w/c ratios). These vascular pores significantly affect the strength, permeability, and shrinkage at high relative humidity (for medium-sized pores) (Richardson, 2002; Mukadam, 2014). Capillary pores can create preferential paths for aggressive agents to penetrate if there is enough volume, size, closeness between pores, and the presence of microcracks (Mehta & Monteiro, 2001). Thus, the minimum requirement for improving the durability characteristics of concrete should be the specification of ideal low w/c ratios, achieving well-proportioned mix designs, and executing good construction practices (placing, compaction, finishing, and curing) (Starck, 2013).
- ***Macropores:*** exist because of entrained air and entrapped air voids formed during construction processes (mixing, placing, consolidation). Entrained air voids rely on the air-

entraining additives used in the mix, while the presence of entrapped air voids is mainly due to the degree of compaction achieved (Starck, 2013; Torrent, Neves & Imamoto, 2022b). The pore sizes are significantly larger than gel and capillary pores but carry a tiny portion of the flow of matter (Torrent, Neves & Imamoto, 2022b).

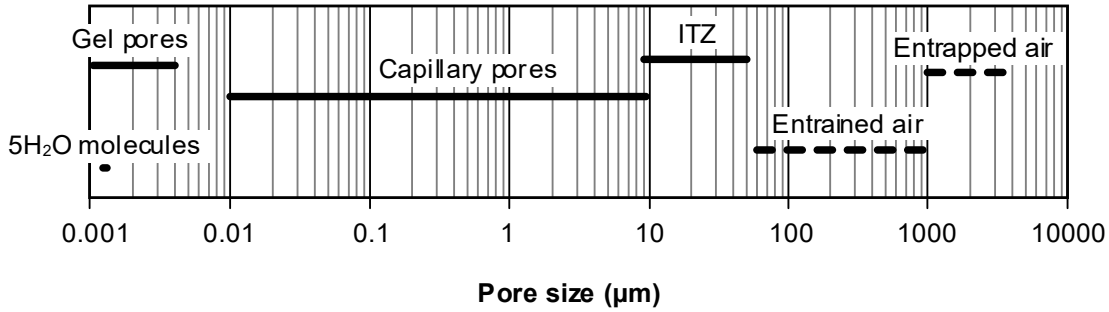

Figure 2-5 Pore size ranges found in concrete (adapted from Torrent et al. (2022).

2.3.3. Transport mechanisms that influence concrete durability

The flow of aggressive constituents in the concrete system is driven primarily by four processes: absorption, diffusion, permeation, and migration. Understanding these mechanisms is crucial because most concrete deterioration processes start with the penetration of gases, liquids, or solutions containing deleterious agents from the environment. This section describes each of the mechanisms with close attention to permeation and diffusion, which are closely linked to permeability.

2.3.3.1. Absorption

Absorption occurs when fluids enter the concrete through capillary suction in the unsaturated spaces. The pore geometry and saturation level within the concrete determine the extent of the capillary suction. The rate at which the wetting front moves through a porous medium is termed sorptivity (Alexander et al., 2021). Deeper into the concrete, the absorption mechanism diminishes and is only active near the surface.

Larger capillary pores, pore connectivity, and extrinsic factors (compaction, curing, mix composition) influence sorptivity (Kropp, 1995; Kropp & Alexander, 2007). Sorptivity is a valuable metric for evaluating concrete pore structure and absorption capacity. In evaluating concrete sorption characteristics, porosity must also be closely considered. Moore et al. (2021) claim that concrete with the same sorptivity can have different porosity levels. Concrete with lower porosity and the same rate of sorptivity will have better durability characteristics.

2.3.3.2. Diffusion

Diffusion in concrete is the unrestricted movement of ions, gases, and liquid molecules within the pore system due to a concentration gradient. The movement of these constituents happens in either a fully or partially saturated state, making the process a crucial mechanism for concrete

structures exposed to salts (Alexander et al., 2021). The diffusion rate is considerably higher in gases than in liquids and solids. However, the rates are affected by temperature, moisture content, diffusibility, and the type of diffusant (Alexander et al., 2021). The diffusion process can be detrimental to RC concrete as carbon dioxide (CO_2) gas influences carbonation processes, and the diffusion of chlorides (salts) can break down the passivation layer of embedded steel (Ballim, Alexander & Beushausen, 2009; Soutsos, 2010).

The diffusion theory is represented by Fick's first and second laws of diffusion. The first law is expressed by equation (2-1). It applies to steady-state diffusion into a uniformly permeable material, while the second law represents a non-steady ionic diffusion model equation (2-2) (Torrent, Neves & Imamoto, 2022b).

$$J = -D_{eff} \cdot \frac{\partial C}{\partial x} \qquad (2\text{-}1)$$

where J = mass transport (g/m^2s)
D_{eff} = effective diffusion (m^2/s)
$\partial C/\partial x$ = concentration gradient ($g/m^3/m$)
x = distance (m)
the negative prefix constitutes movement along a negative concentration gradient

Equation (2-1) is applicable for gas diffusion but is infrequently used for chloride diffusion due to the conditions and duration needed to attain a steady state. The penetration of CO_2, Cl^-, SO_4^{2-} substances occurs in an unsteady manner; thus, Fick's second law applies.

$$\frac{\partial C}{\partial t} = D \cdot \frac{\partial^2 C}{\partial x^2} \qquad (2\text{-}2)$$

where D = Diffusion coefficient (m^2/s)
t = time (s)
C = concentration of fluid (g/m^3)
x = distance (m)

Boundary conditions are introduced for the chloride concentration at a specific depth (C_x) and surface concentration (C_s) such that the apparent diffusion coefficient (D_a) can be determined using Crank's error function (Richardson, 2002; Alexander et al., 2021). However, this aspect is not discussed in this study.

The diffusion process is mainly related to the ingress of chlorides in marine structures, but it also influences the transport of oxygen (O_2) and CO_2 gases in concrete (Ballim, Alexander & Beushausen, 2009). Therefore, diffusion parameters are helpful in the prediction of service life for RC structures in marine environments.

2.3.3.3. Permeation

Permeation is the movement of gases or liquids through interconnected pores and cracks, driven by pressure changes. (Nilsson, 2003). The permeability of concrete depends on its microstructural properties, moisture content, and the characteristics of the penetrating fluid (Richardson, 2002; Ballim, Alexander & Beushausen, 2009; Starck, 2013). Permeability is considered the main influencing factor of the susceptibility of RC structures to extrinsic factors (Starck, 2013).

Gas permeability is determined experimentally by subjecting the test specimen to pressure cells with varying absolute gas pressure applied on opposite ends.(Kropp & Alexander, 2007). Suppose laminar flow is assumed for the movement of gas through the concrete. In that case, gas permeability can be evaluated using the Hagen-Poiseuille relation (equation (2-3)), which applies to Newtonian fluids passing through a cylindrical tube (Kropp & Alexander, 2007; Starck, 2013). The equation forms the foundation for the Torrent air permeability (discussed later in this chapter).

$$\boldsymbol{k = \eta \cdot \frac{Q}{t} \cdot \frac{L}{A} \cdot \frac{2P}{(P_1 - P_2)(P_1 + P_2)}} \qquad (2\text{-}3)$$

k = coefficient of permeability (m^2)

Q = volume of flowing gas (m^3)

η = viscosity of gas (Ns/m^2)

L = thickness of the sample (m)

A = permeated area (m^2)

P = pressure at which Q is measured (N/m^2)

P_1 = pressure at the entry of gas (N/m^2)

P_2 = pressure at the exit of gas (N/m^2)

t = time (s)

In terms of the durability of reinforced concrete (RC) structures, water infiltration is the most critical factor (Starck, 2013). Liquids can be considered fluids with negligible compressibility. When considering the viscosity of the permeating liquid, assuming laminar flow, the water permeability (K_w) can be obtained using D'Arcy's law (equation (2-4)). The law states that the flow of water, in this case, through a porous medium, is directly proportional to the hydraulic gradient (Mukadam, 2014).

$$\boldsymbol{K_w = \frac{Q}{t} \cdot \frac{L}{A} \cdot \frac{1}{\Delta h}} \qquad (2\text{-}4)$$

where K_w = coefficient of water permeability (m/s)
Δh = pressure head applied (height of water column)

Here, the viscosity is neglected, and the expression cannot be applied to other permeating fluids (Kropp & Alexander, 2007). The permeability coefficients determined from gas and water permeation are applicable in characterising the concrete rheology and, therefore, are useful in predicting deterioration mechanisms, like carbonation. This aspect is discussed in section 2.4.4.

2.3.3.4. Combined transport processes

Thus far, the discussion has highlighted each transport mechanism in isolation; however, in reality, more than one process can occur at any given time along the flow paths in the concrete (Kropp & Alexander, 2007; Ballim, Alexander & Beushausen, 2009). Even so, one transport process usually dominates; thus, in durability design approaches, the predominant transport mechanism governs evaluations for service life prediction (Alexander et al., 2021). For this study, carbonation is assumed to be the primary deterioration mechanism in the inland environment where the field experiments were executed. Therefore, carbonation and its related deterioration mechanism (carbonation-induced corrosion) are discussed in depth in the following sections.

Section 2.3 demonstrates how the concrete pore system significantly influences its durability by impacting the movement of fluids and gases through the concrete. Understanding these transport mechanisms within the pore system is crucial for predicting the service life of concrete structures.

2.4. An overview of carbonation

Carbon dioxide (CO_2) plays a vital role in the initiation of the corrosion of steel reinforcement. The atmospheric gas reacts with concrete pore water, specifically the cement hydration product ($Ca(OH_2)$), to form calcium carbonate ($CaCO_3$) precipitate (Alexander et al., 2021). The process is known as carbonation. Carbonation affects concrete's durability by lowering the pH of the pore solution (from 12.5 to 8.5), destabilizing the protective layer on the surface of the reinforcing steel. In the presence of sufficient oxygen and moisture, carbonation progresses (as a front) to a point where the steel will start to corrode (Figure 2-6), resulting in the loss of serviceability of the RC structure (Alexander et al., 2021).

The progression of the carbonation front is dependent on the depletion of calcium species ($Ca(OH)_2$) and hydrates in the pores. Thus, the amount of $Ca(OH)_2$) influences the carbonation rate (Torrent, Neves & Imamoto, 2022b). However, various factors have been found to influence the carbonation rate. The next section briefly discusses these factors.

Carbonation impairs the durability of RC structures but is not responsible for the loss in the structural integrity of concrete (Richardson, 2002; Starck, 2013). Nonetheless, it still causes unsightly degradation of concrete (cracking, spalling, delamination). The effect of carbonation is known to alter concrete properties (increase in hardness, decrease in permeability) due to the deposition of $CaCO_3$ (reaction product) in the pores (Dhanya, 2015). This alteration is beneficial only to unreinforced concrete.

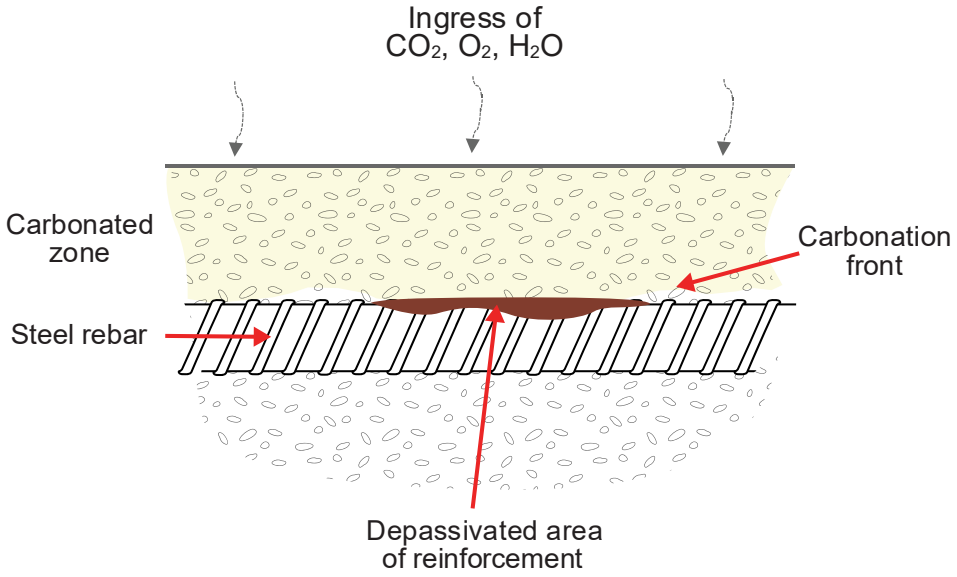

Figure 2-6 Schematic of carbonation leading to steel corrosion.

2.4.1. Factors affecting the rate of carbonation

The factors that influence the carbonation depth are often interrelated but can be classified according to exposure influences and concrete properties, excluding concrete age.

2.4.1.1. Environmental influences

Relative humidity (RH)

Carbonation processes are most active at 50-70% relative humidity. (Richardson, 2002; Starck, 2013; Zhou et al., 2015). At lower RH, the dry conditions limit the dissolution of $Ca(OH)_2$, slowing down the carbonation rate. At more than 80% RH, the diffusion of CO_2 matter is restricted by the filled pores. However, the rate of corrosion at this level or higher is at its greatest (Zhou et al., 2015).

CO_2 concentration

A higher CO_2 concentration in the surrounding atmosphere allows for greater availability of CO_2 and a steeper concentration gradient, facilitating faster carbonation rates. However, CO_2 concentration should not be considered in isolation as an influence on carbonation rates, as other factors such as temperature, reaction kinetics, and pore structure may also play a role. In particular, the exposure environment of the concrete makes it difficult to generalise CO_2 content for any one structure; the local condition (for example, enclosed parking, submerged concrete) will inevitably influence the rate of carbonation (Zhou et al., 2015; Stefanoni, Angst & Elsener, 2017; Li et al., 2018; Gopinath, 2020).

CO_2 diffusivity

The diffusivity of CO_2 in the concrete system is controlled by the degree of saturation (moisture content), the pore network, and the voids present (Starck, 2013). In saturated concrete, the pores are blocked, slowing the diffusion rate into the concrete. Concretes with advanced or deeper carbonation fronts allow CO_2 gases to penetrate the concrete easily, prolonging or accelerating carbonation (Gopinath, 2020).

Temperature

Gopinath (2020) posits that a slight variation in temperature in the surrounding environment does not significantly affect carbonation rates. However, higher carbonation rates are expected at elevated temperatures (say above 30 °C) due to lower activation energy threshold to cause carbonation reactions (Nilsson, 2019; Alexander et al., 2021). Increased energy and collisions between molecules accelerate reaction kinetics. However, excess heat may inhibit carbonation rates by evaporating the pore solution and slowing the reaction process.

2.4.1.2. Influence of concrete properties

Binder type

Plain Portland cement (PC) is reported to have better carbonation resistance than concrete with SCMs (Starck, 2013; Zhou et al., 2015; Stefanoni, Angst & Elsener, 2017; Gopinath, 2020). This resistance is attributed to the reduced amounts of $Ca(OH)_2$ by pozzolanic activity and dilution in blended cement (Alexander et al., 2021). However, the carbonation resistance in blended cement, for example, with the addition of fly ash, can be improved if the pore structure of the concrete is dense and the replacement levels are controlled (Stefanoni, Angst & Elsener, 2017; Barbara et al., 2020).

Water-to-cement ratio (w/c)

Lower w/c ratio concretes may contain more cement content, increasing the $Ca(OH)_2$ (increased pH buffer) and carbonation resistance. On the other hand, some authors (Starck, 2013; Zhou et al., 2015) concede that various competing factors, such as cover thickness, curing condition, cement type and composition, can affect the carbonation rates of low w/c concretes.

Curing

Early age and extended moist curing are crucial in improving concrete's resistance to carbonation. Curing encourages hydration, especially in the outer layer, reducing pore size and limiting carbonation (Gopinath, 2020; Alexander et al., 2021). Prolonged curing facilitates extended hydration development, especially in blended cement concrete (Leemann & Moro, 2017; Gopinath, 2020).

2.4.2. Measurement of carbonation

Understanding carbonation is crucial for predicting the period for reinforcement steel to be affected. This process is slow, often taking years to reach the steel. Therefore, carbonation resistance is typically assessed using lab or site specimens. Commonly used methods involve assessing the pH sensitivity of phenolphthalein indicator solution sprayed on a freshly exposed concrete specimen or specimens exposed to accelerated carbonating conditions (Alexander & Beushausen, 2019; Gopinath, 2020). More sophisticated approaches involve thermogravimetric analysis and X-ray diffraction. The methods of determination are not discussed in this study. However, Gopinath (2020) details various test approaches for assessing carbonation. Carbonation models for predicting carbonation rates, particularly models related to gas permeability, are relevant to this study.

2.4.3. Overview of carbonation prediction models

An extensive body of literature on carbonation modelling has been published, proposing various models (Ekolu, 2018). The models can be categorised as empirical, statistical, numerical, and simulation-based.

Statistical models use mathematical correlations derived from data analysis, including power and exponential equations, regression of multiple variables, and fitting of mathematical functions. (Ekolu, 2018). However, they require significant data inputs to accurately predict patterns and trends that can inform the carbonation behaviour of concrete (Elsalamawy, Mohamed & Kamal, 2022).

Numerical models are applied to conduct a more complex concrete carbonation analysis. Such models are built on theoretical knowledge of the carbonation process (thermodynamic reactions and transport processes taking place). They rely on computational procedures (Ekolu, 2018). While numerical models are extensive, they require complex iterative processes and assumptions of boundary conditions, which may lead to residual errors (Gopinath, 2020). However, Saetta (2005) and Kwon (2010) have documented the usefulness of numerical models.

Simulation models utilise constructed input and output parameter algorithms based on an artificial neural network approach. The algorithm can make predictions of carbonation in concrete for new input data as the neural network learns to produce expected outputs. Like statistical and numerical models, simulation models require extensive input data and the aid of different software. These demands make the practical implementation of the models very challenging (Ekolu, 2018; Gopinath, 2020). Studies have experimented with simulation approaches, highlighting the merits and limitations (Kwon & Song, 2010; Luo, Niu & Dong, 2014).

Empirical models are based on experimental data and focus on mixing or composition parameters (w/c ratio, cement content) or concrete material properties. (Ekolu, 2018). The parameter used in a model is assumed to be heavily linked with the penetration of CO_2 into the concrete. Literature classifies empirical models as permeability, diffusion, strength, or composition-based (Ekolu,

2018; Torrent, Neves & Imamoto, 2022b). Empirical models often lack parameter variations, limiting their accuracy in predicting carbonation for diverse concrete systems (Gopinath, 2020). However, some models reported in the literature show considerable development and refinement to address the limitations (Parrot, 1994; Salvoldi, Beushausen & Alexander, 2015; Ekolu, 2018; Gopinath, 2020).

The various models described have merits and limitations. Empirical models strongly correlate with carbonation, particularly diffusion, permeability, and compressive strength-based ones. (Parrot, 1994; Ekolu, 2018; Belgacem, Neves & Talah, 2020; Gopinath, 2020; Torrent, Neves & Imamoto, 2022b).

2.4.4. Carbonation models related to gas permeability

This section describes models related to the OPI and TPT permeability indicators or coefficients with carbonation. An in-depth discussion of the models will not be given here as carbonation models are not a focus of the study. Instead, a chronological development of relevant models is given.

2.4.4.1. Models related to OPI

Early contributions by Ballim (1996) and Mackechnie and Alexander (2002) presented a predictive model for carbonation using the OPI and WSI. However, the models were limited to performance prediction in marine environments and did not consider the role of the chemical composition of concrete affecting the carbonation chemistry (Fotso Lele, 2021). Lampacher (2000) proposed a model based on structures in an inland environment (average carbonation rate of 3.16 $mm/year^{0.5}$). The empirical value does not correlate with the parameters influencing carbonation or show a relationship between carbonation depth and the OPI.

Recently, Salvoldi et al. (2010; 2015) developed a model based on Parrot's service life model (1994), where the coefficient of diffusion is represented by the gas permeability of the cover layer (Gopinath, 2020). Though different mechanisms drive permeation and diffusion, they occur in the same pore structure; therefore, permeability can be used to describe the pore system and estimate the diffusion parameter (Kropp, 1995). The Salvoldi model allows an estimation of carbonation progression based on parameters displayed in Table 2-1 using accelerated tests. A correlation between permeability and diffusion coefficient established in Salvoldis' study is presented in Figure 2-7. In contrast, Gopinath (2017; 2020) contends that Salvoldi's model underestimates carbonation behaviour in areas with varying climatic conditions. Thus, Gopinath proposed an extension of Salvoldi's model.

Table 2-1 Carbonation model parameters defined by Salvoldi and Fotso Lele (adapted from Fotso Lele et al. (2023).

Parameters	Input data	Output parameter
Concrete mix	Binder type, binder content	Molar concentration of carbonatable material
Exposure	Land use	Molar concentration C02
	Project location	Relative humidity factor
Geometric parameters	Concrete cover	Concrete resistance depth
Concrete micro-structure	OPI value	Concrete diffusion coefficient

An updated computer-based model was developed by Fotso Lele (2021; 2023). The approach can predict the performance of new structures, covering parameters like the Salvoldi model. The SLM includes probabilistic inputs for estimating the service life of RC structures expressed in a limit-state function. It is presented in a user-friendly program with decision-making tools for optimizing durability (Fotso Lele, Beushausen & Alexander, 2023). The model is limited to the local case but provides a basis for further development of computer-based or simulation models, which have not been widely explored.

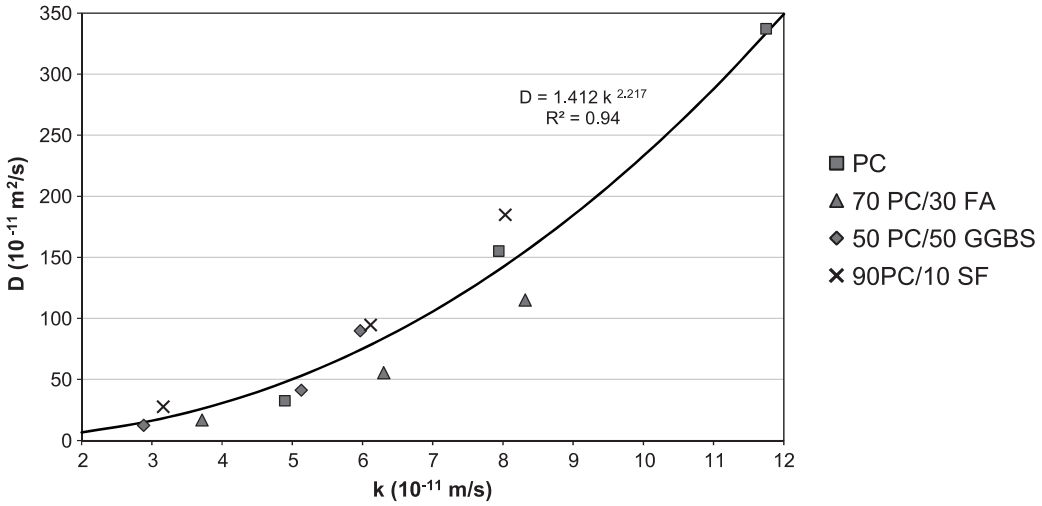

Figure 2-7 OPI permeability relation with effective dry diffusion coefficient for different binder types (adapted from Salvoldi et al. (2015).

2.4.4.2. Models related to TPT

Various approaches have been proposed, linking air permeability with carbonation parameters (Torrent, Neves & Imamoto, 2022b). Initially, Torrent (2013, 2015) hypothesised the 'Exp-Ref' method (Figure 2-8) for chloride-induced corrosion and modified it for carbonation-related deterioration (Torrent & Luco, 2014). The model comprises three principles viz;

- Experimental assessment of the as-built concrete structure (cover thickness, air permeability using TPT).
- Defining reference conditions linked to a specified service life, prescribed by EN 206: 2013 parameters.

- Correlation between measured permeability coefficient and carbonation rate.

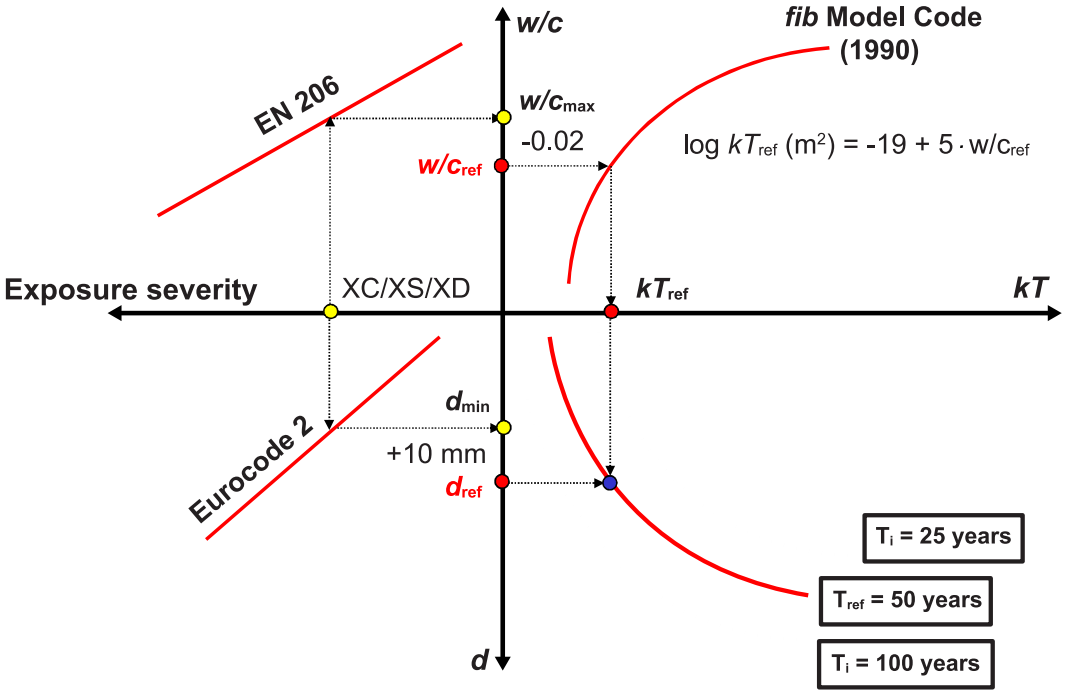

Figure 2-8 Concept of Exp-Ref method for service life prediction (adapted from Torrent et al. (2022).

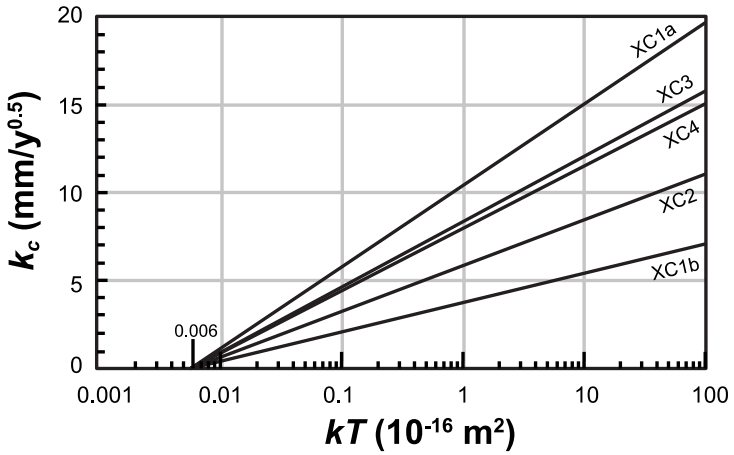

Figure 2-9 kc-kT relation defined by the Exp-Ref method for EN carbonation exposure classes (adapted from Torrent et al. (2022).

Figure 2-8 and Figure 2-9 show the concept of the Exp-Ref method. The parameters obtained are inputs for the model equations to predict service life, initiation period, and corrosion occurrence period, as Torrent et. al (2013, 2015; 2022b) documented. Torrent asserts that the model shows a rational probabilistic prediction model for the service life of new RC structures.

Another carbonation model was presented by Kurashige and Hironaya (2015) based on air permeability and accelerated carbonation tests. Relations for the carbonation depth, rate,

accelerated carbonation index, permeability, w/c ratio, and cement type were established and used to generate nomograms (Torrent, Neves & Imamoto, 2022b). The model needs to be recalibrated for different types of concrete to assess the structure's service life during testing. This involves complex equations and data fitting, making the approach somewhat impractical.

A full probabilistic SLM based on site *kT* measurements was developed by Belgacem et al. (2020). The approach assumes that the depassivation of steel reinforcement defines the end of service life caused by carbonation. The model presents a probabilistic correlation between the concretes' resistance to carbonation and air permeability established using a log-normal conditional probability density function (Torrent, Neves & Imamoto, 2022b). The model includes an environmental aspect to address the difference in carbonation progress between moderate humidity (XC3) and cyclic wet and dry (XC4) exposure classes of EN 206 (Belgacem, Neves & Talah, 2020). Belgacem reports a fair agreement between the model and other performance design methods. The proposed approach applies only to CEM II A/L mixes and favours natural carbonation rates estimated directly from measured *kT* rather than indirectly through accelerated carbonation rate.

Given the preceding discussions on carbonation models, the literature suggests a growing interest in SLMs that use permeability parameters, such as the OPI and TPT indicators, to provide more realistic predictions of the diffusion process of carbonation. Thus, the application of the OPI and TPT methods is bound to increase for performance assessments of RC structures.

2.5. Concrete permeability

The discussion in sections 2.3 and 2.4 revealed how the concrete system's microstructure affects the concrete's permeability with respect to the flow of matter. It was established that the flow of matter primarily occurs through the pores in the HCP and ITZ. Permeability is the characteristic that controls the speed at which a fluid or gas passes through a material with pores (Alexander et al., 2021). Under pressure, the movement of liquids through the concrete depends on the pore saturation, while gas flow requires sufficiently dry pores. Thus, saturation level and moisture content influence the permeability of concrete.

This section discusses test methods for measuring concrete permeability. It focuses on gas permeability techniques, particularly the oxygen permeability index and Torrent air permeability tests. Key factors affecting concrete permeability are also presented.

2.5.1. Gas permeability test methods

2.5.1.1. Overview

Gas permeability measurements are routinely used to characterise the transport properties of concrete. Considerable literary evidence has linked this metric with diffusion coefficients and water absorption rates.(Torrent, Neves & Imamoto, 2022b). The intrinsic permeability of concrete to gas flow is substantially higher than that of water; thus, gas-permeability methods can be conducted in shorter periods to water-permeability tests (Beushausen & Luco, 2015; Torrent,

Neves & Imamoto, 2022b). Gas permeability tests offer a useful durability indicator that can guide concrete mix design decisions and quality control for structural concrete (Beushausen & Luco, 2015).

Various experimental approaches have been developed to measure gas permeability in laboratory and in-situ settings. The tests can be carried out under various flow conditions (steady or non-steady states); this is necessary for site measurement where maintaining constant gas pressure is difficult (Beushausen & Luco, 2015). Gas permeability methods can be non-invasive (surface) or invasive (destructive).

Surface methods typically use a vacuum system to create an air pressure gradient between the concrete surface and the underlying pore network in the cover layer. Intrusive methods may involve hole-drilling for injecting or withdrawing air and core-drilling for saw-cut samples to be tested. The air permeability index or coefficient can be determined by monitoring pressure changes over time due to air penetration into the pore system or from the steady gas flow rate, depending on the system (Zhang & Li, 2019).

Laboratory-based test methods are advantageous from a control perspective, as specimens can be preconditioned to minimise the influence of moisture on permeability results. Site methods lack control over the ambient conditions in the test environment, which may produce larger dispersions in recorded values and interpretations of results. Site measurements provide a more representative measure of the actual compactness of concrete in real-world conditions.

Table 2-2 presents several gas permeability methods, including recently developed methodologies. This study intends to combine the OPI and TPT to propose a more rational practical approach to local durability assessment. Therefore, the following sections will discuss the OPI test and Torrent air permeability method in more detail.

Table 2-2 Summary of various gas permeability test methods.

Test Method	Test Type and Environment	Mechanism / Concept	Merits	Demerits	References
Cembureau	- invasive - laboratory (in-situ cores, lab specimen)	- volumetric gas flow meter	- easy to handle - reliable (good) repeatability	- laborious - time-consuming	(Kollek, 1989; Li, 2022)
Autoclam	- semi-invasive - in-situ	- single vacuum system	- quick - applicable to high-performance concrete	- difficulty in achieving a surface seal - uncontrolled gas flow	(Basheer & Nolan, 2001; Yang et al., 2014)
Figg	- invasive - in-situ	- intrusive porosiscope	- quick - cost-effective	- difficulty in achieving a surface seal - variations in test protocols	(Figg, 1973)
Hong-Parrot	- invasive - in-situ	- drilled hole test	- easy to use. - quick	- uncontrolled gas flow - lack of standardised procedure	(Parrott, 1989; Parrott & Hong, 1991)
Kurashige	- non-invasive - in-situ	- triple vacuum system	- does not require pressure regulation	- sophisticated equipment - model estimations yet to be validated	(Kurashige, 2015; Torrent, Neves & Imamoto, 2022b)
Oxygen permeability index	- semi-invasive - laboratory (in-situ cores, lab specimen)	- oxygen permeameter	- realistic simulation of concrete performance - good correlation with carbonation	- sensitive to specimen preparation - not reliable for tests on high-performance concrete	(Alexander, Gouws & Maritz, 2001; Alexander, Ballim & Stanish, 2008)
Seal method	- non-invasive - in-situ	- rubber-latex seal flow meter	- easy to handle	- not well understood - The assumed model is yet to be validated	(Ujike, Okazaki & Nakamura, 2009)
Torrent air permeability	- non-invasive - in-situ, laboratory	- double vacuum system	- portable equipment - quick - applicable on-site and laboratory	- sensitive to surface moisture conditions and ambient conditions	(Torrent, 1992, 2012; Torrent, Neves & Imamoto, 2022b)

2.5.1.2. Oxygen permeability index (OPI) method

The OPI test assesses the quality of the as-built structure or lab-manufactured specimen by monitoring the pressure drop as gas passes through the concrete sample (see Figure 2-10). It provides insight into the microstructure and macrostructure of the concrete cover layer. It demonstrates particular sensitivity to macro voids and cracks, creating preferential gas permeation passages (Alexander et al., 2021).

The OPI method has been developed rigorously, gaining wide acceptance as a standardised approach in the SANS 3001-CO3-2:2015 code. The test result, a permeability coefficient (durability indicator, *kOPI*), is already considered in performance-based design for concrete durability (Alexander et al., 2021).

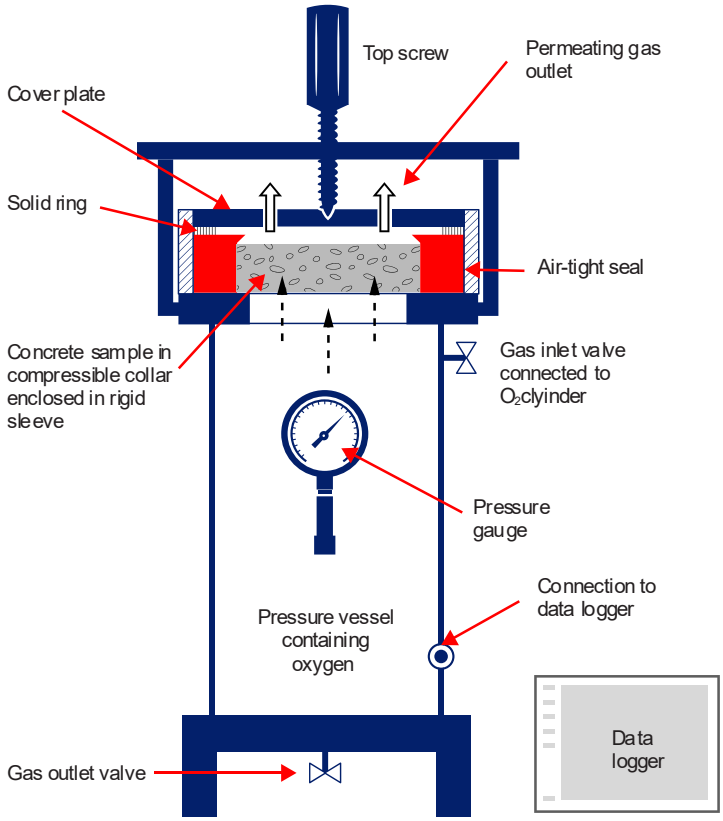

Figure 2-10 Schematic diagram of OPI cell (after Alexander et al. (2021).

The permeability coefficient is transformed into a unitless index value (OPI value) by taking the negative logarithm of the coefficient. This compresses the wide range of variability resulting from small changes into a more manageable scale.(Alexander, Mackechnie & Ballim, 1999). The OPI value quantifies the “impermeability” of the concrete. Typical ranges of *kOPI* for structural concrete mixes range between 10^{-9} m/s (9) and 10^{-11} m/s (11).

Further details on the test procedure can be found in section 3.6.3.2 and the SANS and DI manual (2018, 2023). Additionally, section 2.6.3.1 discusses the practical application of the method and its relevance as a quality and conformity assessment approach.

The permeability coefficient of the test is calculated using the following formula.

$$kOPI = \frac{w \cdot V \cdot L \cdot z}{R \cdot T \cdot A} \qquad (2\text{-}5)$$

kOPI = Darcy's coefficient of oxygen permeability (m/s)
w = molecular weight of oxygen gas (w = 0.313 N/mol)
V = volume of oxygen vessel (m^3)
L = thickness of the specimen (m)
R = gas constant (R = 8.314 J/K/mol)
T = mean temperature (K)
A = area of the specimen cross-section (m^2)
z = relative pressure decay rate (ln P_o/P_t)

2.5.1.3. Torrent air permeability (TPT) method

The TPT method is a non-destructive approach for assessing air permeability in situ and laboratory settings. A vacuum is created on the concrete surface, and the device monitors the rate of pressure rising in the isolated test chamber (Torrent, Neves & Imamoto, 2022b). The method incorporates a double chamber cell and a pressure regulator (Figure 2-11).

The TPT technology enhances traditional vacuum systems. Older methods are unable to control airflow over porous concrete areas. This fault causes inconsistencies in pressure changes and incorrect permeability measurements (Torrent, 1992; Torrent, Neves & Imamoto, 2022b). The TPT method uses a guard ring to balance air pressure, enabling unidirectional airflow into the test chamber. By measuring the rate of pressure increase in the central chamber, the air permeability coefficient (*kT*) can be determined using equation (2-6) Torrent et al. (2022b) demonstrate the derivation of the equation.

The TPT technique was one of the first approaches to be accepted as a standard gas permeability methodology by the Swiss standards (2013, 2019). Due to its high sensitivity to in-situ moisture and temperature, extensive research has been conducted to enhance the methods' reliability. Various literature and the Swiss standard provide comprehensive documentation on limiting values, sampling criteria, and conditions under which the test can be conducted on-site and in a laboratory environment (Torrent, Neves & Imamoto, 2022b).

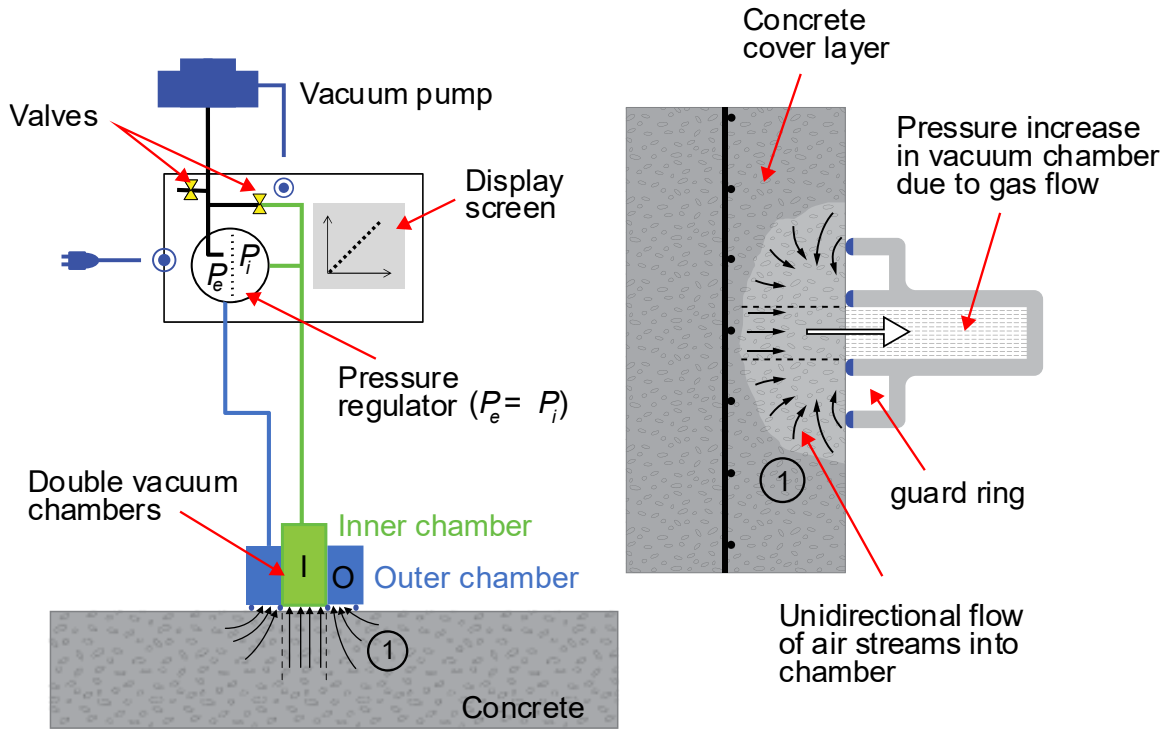

Figure 2-11 Schematic diagram of TPT (3rd generation - PermeaTorr) setup (after Torrent et al.(2022).

$$kT = \left(\frac{V_c}{A}\right)^2 \cdot \frac{\mu}{2 \cdot \varepsilon \cdot P_a} \cdot \left[\frac{ln\left(\frac{P_a + \Delta P}{P_a - \Delta P}\right)}{\sqrt{t_f} - \sqrt{t_0}}\right]^2 \qquad (2\text{-}6)$$

kT = coefficient of air permeability (m^2)

V_c = volume of the inner chamber pneumatic system (m^3)

A = area of inner test chamber (m^2)

μ = dynamic viscosity of air (Ns/m^2)

ε = open porosity of the concrete (0.15)

P_a = atmospheric pressure (N/m^2)

ΔP = increase of effective pressure in the inner chamber (N/m^2)

t_0= time at which pressure rise is initiated (t = 60 s)

t_f = time at the termination of the test (s)

The Torrent equipment has improved over five models, featuring electronic pressure control and remote capabilities. These advances add to the methods' portability and time efficiency, making it a convenient and fast approach. Further details on the testing procedure are discussed in section 3.6.4 and Torrent et al. (2022b).

The South African OPI test and the Swiss Torrent method are two of the most developed approaches in terms of gas permeability (Starck et al., 2017; Beushausen, Torrent & Alexander, 2019; Dlamini, 2019; Sangoju, Gopal & Bhajantri H, 2020; Al-haddad, 2022). Both methods are

used for durability design specifications, with local codes setting limits for various conditions. The OPI and TPT exhibit synergies that can be utilised in a combined approach in South Africa.

2.5.1.4. Relating the OPI and Torrent test method

The OPI and TPT offer valuable insights into concrete's air permeability but employ distinct approaches. In the OPI test, the whole concrete sample (70 mm diameter x 30 mm thickness) is tested, whilst in the TPT, a test area, 50 mm diameter x penetration depth of the vacuum front, is assessed. The OPI measures the rate of oxygen gas permeation over a pressure decay, and the TPT measures the rate of increase in air under a vacuum (negative pressure). These tests target different aspects of the pore network: OPI emphasises diffusivity, and TPT focuses on airflow and connectivity. The differences lead to distinct mathematical descriptions of gas transport in each test.

Directly linking the OPI and TPT methods through their derived formulae may be a new approach to developing a more fundamental association. However, it would necessitate intricate mathematical manipulations. Existing studies investigating connections between the OPI and TPT have been based on developing empirical correlations from laboratory data.

Both approaches demand meticulous effort to achieve reliable outputs. Empirical correlations require robust datasets and statistical analysis, whereas mathematical derivations may involve assumptions that require verification using existing data. This study explores in-situ empirical correlations to advance previous work on linking TPT and OPI methods.

The OPI and Torrent methods indicate a refinement of gas permeability approaches, addressing execution time factors and apparatus reliability, where methods like the Cembureau and Autoclam are limited. A significant drawback of most methods presented in Table 2-2 is the lack of harmonization due to their varied approaches. This makes developing general acceptance criteria challenging as their data and associated variabilities impact their comparability. While OPI and Torrent approaches have gained wider acceptance, they still require further refinement, particularly their use in SLMs to model the actual performance of concrete in the field.

2.5.2. Factors affecting concrete permeability

2.5.2.1. Compressive strength

Data from several studies reported by Torrent et al. (2022b) suggest a reasonably good correlation between compressive strength and coefficients from different permeability tests (for example, the Cembureau method). However, literature also shows a contrasting relationship between the same parameters when permeability tests are conducted on in-situ concrete (Figure 2-12) (Nganga, Alexander & Beushausen, 2013; Alexander & Beushausen, 2019). The lack of correlation with compressive strength highlights why strength should not be considered a durability indicator. Further, handling of fresh concrete and the execution of construction on site highlight the difference between as-built quality and laboratory concrete.

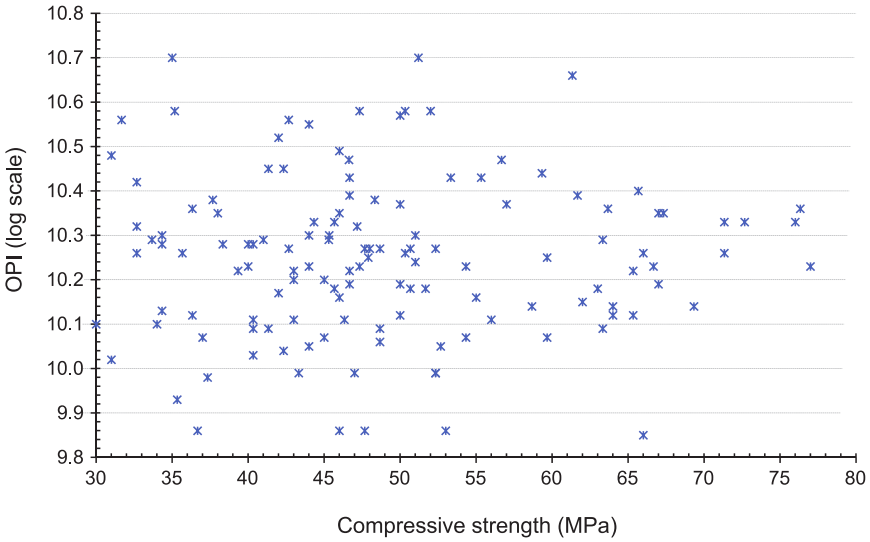

Figure 2-12 Disassociation between compressive strength (measured on lab specimen) and oxygen permeability (OPI), measured on the as-built structure (adapted from Nganga et al. (2013).

2.5.2.2. Water-to-cement (w/c) ratio

Low w/c ratios generally translate to impermeable, high-strength concrete. This is due to the water in the concrete mix determining the extent of the capillary pores in the HCP. The transport characteristics, including the pore volume and dimensions, are also affected. Findings by Torrent et al. (2022b) show PC mixes merging well within a w/c range of 0.4 – 0.7 against the OPI, Cembureau, and TPT.

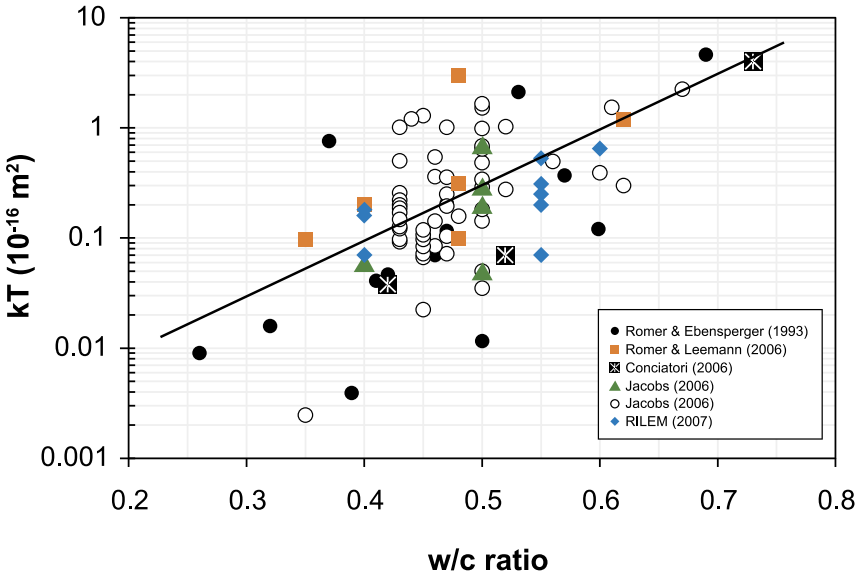

Figure 2-13 Relation between air permeability (kT) and w/c ratio (adapted from Torrent et al. (2022).

In contrast, several data sources by Jacobs et al. (2009) reveal a large scatter (Figure 2-13) attributed to experimental variabilities. Jacobs et al. show that the relationship between the w/c

ratio and permeability is influenced by the properties of the binder, leading to significant variations in penetrability among concretes with the same w/c ratio (Torrent, Neves & Imamoto, 2022b). The full benefits of low w/c ratios can only be harnessed if the concrete achieves a high hydration level (Starck, 2013).

2.5.2.3. Binder type

Cement extenders can reduce concrete permeability when the mix design is carefully proportioned (Starck, 2013; Bahurudeen & Santhanam, 2014; Bustos et al., 2015; Zhang & Li, 2019). A study by Zhang (2019) found that 30% replacement level of fly ash improves the concrete microstructure over time, resulting in ideal pore size distribution significantly reducing permeability. Bahurudeen (2014) and Bustos (2015) also report the benefits of using natural pozzolans and bagasse ash, respectively. However, SCMs have also been linked to high carbonation rates (due to low $Ca(OH)_2$ products). Thus, the net benefit of cement extenders depends on the replacement levels and the quality of curing methods (Bahurudeen & Santhanam, 2014). In a separate study, Dhanya (2015) could not conclusively differentiate the gas permeability characteristics between PC and blended cement specimens.

2.5.2.4. Aggregates and the ITZ

The ITZ facilitates movement of substances in concrete. Bustos (2015) and Wu (2021) argue that the interaction of aggregates with the ITZ affects permeability; an increase in aggregate volume weakens the ITZ, attributed to microcracks present in the ITZ. Additionally, Wu reports that PC concretes produce weaker ITZs than those with mineral additives. However, isolating the ITZ effect is challenging because of the concurrent factors influencing the concrete system. Densifying the ITZ with appropriate binders and aggregates can significantly enhance concrete permeability.

2.5.2.5. Handling

Poor placement and compaction can result in surface and internal defects such as honeycombing, excessive voids, bug holes, and sand streaks (Torrent, Neves & Imamoto, 2022b). Some researchers have found that poor compaction efficiency increases sorptivity and porosity, but the relationship between compaction degree and permeability is unclear, especially in laboratory settings (Neves, Santos & Valente-Monteiro, 2011; Starck, 2013; Nishimura, Kato & Mita, 2015). Other studies reported by Torrent et al. (2022b) suggest that bleeding channels may enhance pore connectivity, thus increasing gas permeability. Bleeding-induced segregation in concrete elements can increase permeability in upper sections. Proper mixing and compaction are vital for the durability of concrete structures, underscoring the need for in-situ assessments due to varying on-site handling.

2.5.2.6. Curing

Inadequate curing significantly increases capillary porosity, particularly in PC mixes (Torrent, Neves & Imamoto, 2022b). Surana et al. (2017b) found that air curing and wax emulsions (curing

compounds) can lead to poor gas and water permeability among different curing methods. In contrast, other curing compounds (e.g. resin-based) can produce favourable permeability characteristics.

Curing aims to keep the concrete saturated or near-saturated to support hydration and pore-filling (Nganga, 2012). Wet curing, especially in the first seven days, is crucial for concrete to reach its full potential. Curing temperature negatively affects transport characteristics and compressive strength, with some trends reversed in short-term and continuous curing scenarios (Surana, Pillai & Santhanam, 2017b).

Field studies also confirm that air-curing and curing compounds, to some extent, exhibit poor permeability characteristics compared to wet methods (Starck, 2013; Surana, Pillai & Santhanam, 2017a). Further research is needed to validate these findings across different concrete types and conditions. The durability parameters *kOPI* and *kT* are more sensitive to curing methods than compressive strength, making them useful for assessing curing compounds and efficiency. This study applied a wax-emulsion compound to all concrete elements, which were then air-cured.

2.5.2.7. Temperature

The concrete microstructure is unaffected by temperatures between 0 °C – 50 °C (Torrent, Neves & Imamoto, 2022b). However, higher air permeability is expected at higher temperatures due to alterations and microstructure damage (Figure 2-14). Van der Merwe (2019) reported increased gas permeability by as much as four orders of magnitude at extreme temperatures (several hundred degrees). Coarse aggregates and cement expand significantly at high temperatures, but data on gas permeability at sub-zero temperatures is limited.

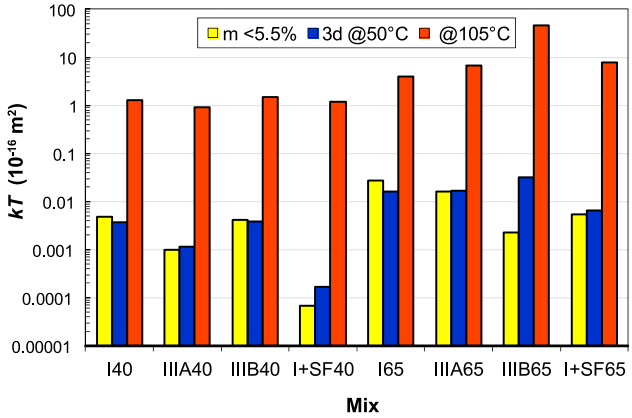

Figure 2-14 Effect of specimen drying temperature on measured kT (adapted from Torrent et al. (2014).

Torrent et al. (2014) developed a preconditioning procedure for laboratory-based TPT measurements. Results showed that oven-drying at 105 °C until constant mass caused high measured *kT* values. The evidence supports Van der Merwe's research and Torrent et al. (2019). Torrent et al. found that such temperatures do not represent field conditions and can harm the

concrete's microstructure. A temperature of 50°C is recommended for conditioning lab specimens.

2.5.2.8. Moisture

Moisture content in the field can vary due to daily and seasonal factors such as temperature and rainfall. Thus, preconditioning is required for most permeability tests on site-drawn specimens. Knowing the surface moisture content of concrete during permeability tests is crucial for accurate data interpretation (Torrent, Neves & Imamoto, 2022b). Drier concrete typically has more pore space for the flow of gases, associated with higher permeability (Starck, 2013). However, substance flow only occurs after the open pores are filled with water under capillary suction. The saturation degree of the pore network affects capillary pressure and *kT*.

Various studies have addressed moisture issues in field tests (Nnodim, 2020; Torrent, Neves & Imamoto, 2022b). Early methods for measuring moisture in concrete relied on a conversion factor involving air permeability and relative humidity (RH), such as the Hong Parrot and Autoclam methods. These approaches require determining the internal relative humidity (IRH) using a probe, which can be intrusive and warrants IRH readings below 80% at each location. However, this method is impractical for field use and fails to reflect moisture influence accurately (Nnodim, 2020; Torrent, Neves & Imamoto, 2022b).

The H_2O meter, a surface moisture device, was initially used for the TPT approach. Although it had a pressing sensor head for detecting moisture on concrete surfaces, it produced inaccurate measurements on specimens with varying moisture levels. Torrent and Ebensperger (1993) then proposed a new method combining *kT* measurements and resistivity. Unfortunately, the approach became unreliable on concretes with SCMs. This is due to the effect of SCMs on resistivity measurements, which consequently yields incorrect correction factors for site concrete. Even so, Balyssac and Bonnet (2018) assert that the combination of the TPT and resistivity measurements can be helpful in the assessment of carbonation depth and saturation degree under controlled conditions.

The standard approach for on-site moisture accounting uses an impedance-based moisture meter (see Appendix B.2). It is prescribed that air-permeability measurements can be taken when the moisture content is 5.5% or lower. Paulini (2015) contested that the value is too high. However, other studies, including those by Torrent et al. (2014), support the limiting value, finding it aligns with that of an oven-preconditioned specimen after three days. (Figure 2-15). Furthermore, Torrent et al. consider the limit acceptable for new structures (28 – 90 days).

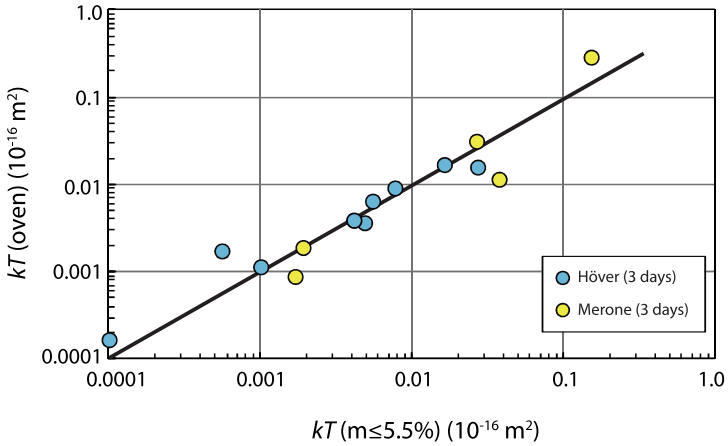

Figure 2-15 Correlation between oven-dried and lab-dried test specimens on measured kT (based on samples from two different cement clinkers) adapted from Torrent et al. (2014, 2022b).

Bueno et al. (2021) posited a moisture correction relation between *kT* and moisture content using a 5% moisture content reference. The moisture value is derived from findings by Torrent et al. (2014). The correction is represented by equations (2-7) and (2-8). and is valid for surface moisture between 1:0% ≤ m ≤ 6:0%.

$$\boldsymbol{kT_5 = F_5 \cdot kT_m} \qquad (2\text{-}7)$$

$$\boldsymbol{F_5 = e^{1.45(m-5.0)}} \qquad (2\text{-}8)$$

where kT_5 = coefficient of air permeability at m = 5% (m^2)
kT_m = permeability coefficient at recorded moisture content
F_5 = correction factor
m = surface moisture content (%)

According to Bueno et al., the difference between measured kT_m and corrected kT_5 values is expected to be insignificant when surface moisture is between 4.5% and 5.5%. However, the approach proposed by Bueno et al. still lacks validation based on site data. Therefore, the present study will investigate the correction on measured *kT* values.

This section has highlighted the relevance of gas permeability in assessing durability performance and outlining the many factors that can affect concrete's durability characteristics. Next, the approaches used in different countries for designing and specifying concrete durability are discussed.

2.6. Performance-based approaches towards concrete durability

The goal of durability design for reinforced concrete structures is to ensure a long service life by choosing appropriate materials, construction techniques, and structural details that prevent

harmful substances from entering (Beushausen & Luco, 2015). There are two approaches to achieving this objective: prescriptive design concepts and performance-based concepts (Nilsson, 2019). The prescriptive approach sets limits on concrete mix design parameters like compressive strength, w/c ratio, and cement content. The performance approach assesses material properties related to deterioration mechanisms under current exposure conditions. (Beushausen, Torrent & Alexander, 2019).

Previous sections in this chapter have discussed the crucial factors governing concrete durability and demonstrated that the commonly employed prescriptive approach fails to address durability concerns.

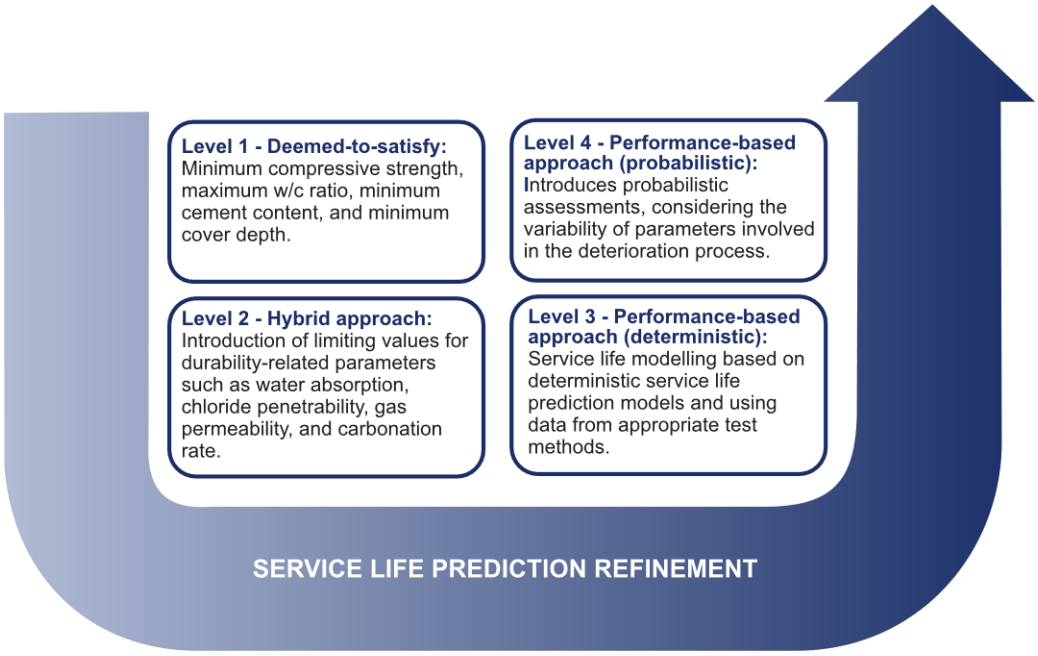

Figure 2-16 Different levels for specifying concrete durability performance (adapted from Wally (2022).

Figure 2-16 shows the various levels of durability specifications applicable in the service life design of concrete (Wally et al., 2022). Several methods exist for evaluating durability. One approach uses durability indicators as a supplementary evaluation mechanism by combining levels 1 and 2. Another is implementing probabilistic service life models at levels 3 and 4, as suggested by Beushausen & Luco (2015) and Wally et al. (2022). The progress towards adopting performance-based approaches (P2P has been slow and conservative, particularly regarding the inclusion and implementation of the approaches in international standards and national codes. The gradual change results from a limited understanding of the complex deterioration processes in reinforced concrete structures and a lack of reliable correlations between performance tests and actual durability (Beushausen, Torrent & Alexander, 2019).

The following sub-sections provide an overview of current performance approaches across various regions. While not exhaustive, they offer a brief insight into the state of the art. Additionally, two case studies illustrate the use of OPI and TPT methods in engineering projects.

2.6.1. Current approaches

2.6.1.1. South Africa

Existing standards SANS 10100-2:2014 and SANS 2001-CC1:2012, primarily rely on prescriptive design requirements for strength and cover depth based on exposure conditions (Dlamini, 2019). However, performance indicator tests termed the South African durability index approach (SADIA) have been developed, utilising the OPI, WSI, and CCI to assess the durability potential of concrete. The tests have been trialled rigorously to improve their reliability and account for variabilities, resulting in the inclusion of the OPI and CCI tests in the SANS standards (SANS CO3-2:2015; SANS CO3-3:2015). Ongoing research is being conducted on the WSI for its inclusion in future codes of practice (Beushausen, Torrent & Alexander, 2019; Sugandhini et al., 2022; Torrent, Neves & Imamoto, 2022b).

Table 2-3 Nominal OPI specifications used in South Africa for structures in carbonating environments (adapted from COTO (2020a).

Environmental class	Exposure condition	Cover (mm), as specified	OPI (log scale)
		For 100 year service life	
XC1a, and XC1b	mild	40	9,15
		50	9,00
		60	9,00
XC2	moderate	40	9,40
		50	9,10
		60	9,00
XC3		40	9,65
		50	9,35
		60	9,05
XC4	severe	40	9,65
		50	9,35
		60	9,05

The South African DI approach has also been linked to SLMs for carbonation and chloride ingress, enabling the prediction of durability characteristics based on relevant parameters like binder chemistry, mix composition, diffusivity, and environmental conditions (Salvoldi, Beushausen & Alexander, 2015; Gopinath & Alexander, 2018; Beushausen, Torrent & Alexander, 2019; Fotso Lele, Beushausen & Alexander, 2023). Further, the South African National Roads Agency (SANRAL) have implemented durability specifications in national road infrastructure projects for over a decade specifying limiting OPI values based on EN206-adopted exposure categories (SANS 50206, 2015) applicable to the local context (see Table 2-3 and Appendix A.2). Govender (2019) proposed a data model for managing DI data for national road infrastructure. Such a database is believed to provide project-specific numerical summaries of critical parameters affecting concrete durability, aiding evaluative processes, decision-making, and improving material design and construction practices. Further, there is optimism that the data model can be

integrated with bridge monitoring systems. On the other hand, recent studies by Nganga et al. (2022) have proposed a refined approach for determining target OPI values for concrete mix designs based on a specified or characteristic OPI value.

Limited literature exists concerning approaches applied in other parts of Africa. However, an ongoing study in Kenya proposes P2P approaches as an alternative directive to the outdated local prescriptive codes (Nganga, Mumenya & Abuodha, 2020).

2.6.1.2. The Americas

The American Concrete Institute (ACI) codes are widely utilised in American and Middle Eastern countries (ACI Foundation, 2020). The current code for structural concrete requirements (ACI 318:19) mainly provides prescriptive solutions for addressing specific exposure classes based on anticipated levels of exposure. Alongside the ACI 318 code, the ACI 201.2R serves as a guide for concrete durability design. While some provisions within the codes specify performance-based alternatives, the absence of defined limits or comprehensive performance criteria poses challenges in comprehending and implementing the provisions (Kessy, Alexander & Beushausen, 2015; Hooton, 2019; Al-haddad, 2022). For instance, in cases where low permeability concrete is required (such as sulphate exposure), the ASTM C1202:2002 (Rapid chloride permeability test (RCPT)) is required for the performance assessment of the concrete; however, no limits or performance criteria are given (Kessy, Alexander & Beushausen, 2015).

In other parts of the Americas, progressive approaches have been studied and implemented to varying extents. Argentina's CIRSOC 201:2005 durability specifications are based on water permeability tests. Moreover, specific limits for sorptivity are defined for aggressive environments (Torrent, Neves & Imamoto, 2022b). In Canada, the CSA A23.1/A23.2 and CSA S3001 standards allow performance specifications in severe exposure conditions (ACI Foundation, 2020). The specifications can be supported by standardised test methods, including the RCPT, sorptivity (ASTM C1285:2004), and chloride bulk diffusion (ASTM C1556:2004), among others (Beushausen & Luco, 2015; Alexander, 2018). While these test methods have varying degrees of reliability, not all are suitable for routine quality control purposes, according to Alexander (2018), especially where test duration is concerned.

Some countries in North America use SLMs (for example, LIFE 365) to estimate corrosion initiation and assess lifecycle costs based on chloride diffusion (Alexander, 2018). It is essential to acknowledge that such models assume a primary degradation mode and may thus be limited to specific exposure environments.

2.6.1.3. Asia

Unlike the American approach, the Japanese guidelines (JSCE) predominantly employ PBD techniques. Quantitative design procedures based on Fickian deterministic models are utilised (Kwon, Ahn & Rosen, 2017). The diffusion coefficient is determined through field investigations and laboratory data; cover depths are proposed for varying service life spans (20 to 100 years) using critical chloride content and safety factors. South Korea adopts similar approaches to

Japan, with modifications for regional conditions (Kwon, Ahn & Rosen, 2017; Torrent, Neves & Imamoto, 2022b).

In contrast, the Chinese code (GB/T50476) is generally prescriptive, with requirements for minimum strength, cement content, cover depth, and air content for various aggressive environments (marine, freezing) (Hooton, 2019). Additionally, maximum limits for w/c ratio and crack widths for various exposure classifications are specified. The limit values are derived from chloride migration (Nordtest NT492) and freeze-thaw tests (ASTM C666) (Hooton, 2019).

In India (IS 456-2000), exposure conditions are defined ambiguously, limiting distinct classification of exposure classes (Sugandhini et al., 2022). However, revisions of the exposure categories have been proposed (Alexander, Santhanam & Ballim, 2010; Kessy, Alexander & Beushausen, 2015; Sugandhini et al., 2022). The Torrent air permeability test method has also been adopted for non-destructive testing of bridges (Torrent, Neves & Imamoto, 2022b).

2.6.1.4. Europe

The EN 206 set of codes allows for a hybrid approach wherein prescriptive (deemed-to-satisfy (DTS)) or performance techniques can be applied. Several European countries (e.g., Switzerland, UK) and non-European nations like South Africa have adopted the EN exposure classes. The adopted exposure classes are added as annexes, specifying local requirements. However, the concrete must attain the equivalence performance to reference concrete conforming to DTS specifications relevant to the exposure classes (Kessy, Alexander & Beushausen, 2015).

In Switzerland, the SIA 262/1:2019 specifies non-EN standard tests and requirements for relevant exposure classes. The Torrent air permeability test (TPT) is a commonly applied test method. The cover concrete is evaluated based on specified limiting kT values corresponding to the relevant exposure conditions, as shown in Table 2-4. However, one limitation of the current SIA 262/1 is the omission of guidelines on assessing laboratory specimens. Nevertheless, the Argentinian code (IRAM 1892:2021) and Torrent (2022b) provide guidelines to address this gap.

Like the South African DI approach, the TPT method has undergone significant development and refinement over the years, resulting in its implementation in various countries such as Chile, China, India, Japan, and Spain, particularly for evaluating road infrastructure (Torrent, Neves & Imamoto, 2022b). Additionally, the test has been linked to the OPI test and is considered for integration into the South African approach (Starck, 2013; Starck et al., 2017; Torrent, Neves & Imamoto, 2022b).

Table 2-4 kT specifications for various exposure conditions, according to SIA 262/1:2013 (adapted from Torrent et al. (2022).

	Concrete type						
Description	*A*	*B*	*C*	*D*	*E*	*F*	*G*
Strength classes[a]	C20/25	C25/30	C30/37	C25/30	C25/30	C30/37	C30/37
Exposure classes[b]	XC1 XC2	XC3	XC4 XF1	XC4 XD1 XF2	XC4 XD1 XF4	XC4 XD3 XF2	XC4 XD3 XF4
Minimum cement content (kg/m^3)	280	280	300	300	300	320	320
Max w/c ratio	0.65	0.60	0.50	0.50	0.50	0.45	0.45
Air-permeability kT_s (10^{-16} m^2)	-	-	2.0	2.0	2.0	0.5	0.5

[a] The indicated values correspond to the required characteristics strength (MPa) at 28 days, measured on clylinders/cubes

[b] Correspond to the exposure classes defined in EN 206-1. The combinations of exposures are those typically found in Switzerland.The limits for XD classes can be applied to equivalent XS classes for marine environments, absent in Switzerland.

The UK and French codes are limited in prescribed methods for assessing the equivalent performance for concretes deviating from the regular EN 206 specifications. However, extensive studies have been undertaken in France, particularly the PERFDUB French National project, to develop methodologies for evaluating concrete durability using PBAs (INSA Toulouse, 2022). The project aimed to consolidate existing knowledge and stakeholder input to make the performance-based approach more practical and widespread. The outcomes of the investigations were synthesized into a guideline, the pr FD P18-480. Meanwhile, Spain has numerous performance tests in the local codes to evaluate gas permeability, chloride ingress, and resistivity (Beushausen & Luco, 2015). In other parts of Europe, provisions are made for probabilistic models.

Various predictive models have been developed to quantify the service life of structures based on key input parameters. For instance, the Norwegian approach utilises the DURACON model (Alexander, 2018). The model is set on a 10% serviceability risk level for corrosion occurrence for the specified period (Alexander, 2018; Sangoju, Gopal & Bhajantri H, 2020). The input parameters for the model an environmental component, concrete cover, and concrete quality, whereas concrete resistivity and chloride diffusivity are included for environments like the North-sea offshore. Similarly, the Netherlands also employs the DuraCrete model. Within the Scandinavian region, a transport interaction model, viz. ‘ClinConc’ chloride ingress model simulates chloride transport in the concrete pore system. All the models discussed here commonly apply the rapid

chloride migration test to determine the diffusion coefficients (Alexander, 2018; Alexander & Beushausen, 2019; Sangoju, Gopal & Bhajantri H, 2020).

2.6.1.5. Oceania

The Australian code (AS 3600) specifications are typically DTS but allow for specific exposures (classified as U) to be performance-based according to the nature and aggressiveness of the environment (ACI Foundation, 2020). Under these conditions, the user specifies the concrete properties to ensure durability performance. The durability requirements in the Australian codes are fragmented and conflicting; for example, concrete cover specifications between the AS 3735 and AS 3600 are different for the same exposure conditions. Further, no guidelines on associated assessment methods are provided (Papworth, 2018). Recent developments reported by Papworth et al. (2016, 2018) and Freitag (2016) show that the Concrete Institute of Australia (CIA) has compiled a series of documents (Z7 series) that provide consistent and comprehensive guidelines to support current standards. The documents are focused on concrete durability planning, modelling, performance tests, and exposure classes.

2.6.2. A general critique of current approaches

This section has highlighted that most of the codes are traditionally prescriptive and exhibit a conservative attitude towards adopting performance-based approaches. The classical ‘recipe-like’ approach conspires against durability and sustainability, mainly where harsh environments and new concrete blends are used (Torrent, Neves & Imamoto, 2022b; Wally et al., 2022).

The codes that have adopted performance approaches like the South African and modified European regulations show progressive development towards delivering durable concrete structures. However, there is still a lack of clarity and agreement on interpretation criteria and consistent testing procedures among these codes, which presents a barrier to universal acceptance of performance approaches. The RILEM Technical Committee state-of-the-art report 230-PSC (Beushausen & Luco, 2015) reports many performance indicator approaches that apply to quality control and conformity assessment of RC structures. Even so, most documented techniques have been limited to laboratory studies and have little practical implementation (Beushausen, Torrent & Alexander, 2019).

The transition to whole performance-based approaches is an achievable yet complex process. However, more engagement between the academic and industrial spheres is required for a full transition. This is particularly important for further developing and refining existing performance indicator techniques up to a point where best practices can be formulated. Much research is also required to develop and validate SLMs linked to performance indicator inputs. Concerted efforts are being made by committees such as the ACI, CIA, and fib task groups to develop more holistic guidelines for the design and construction of durable structures (Papworth, 2018; Papworth & Matthews, 2018; Hooton, 2019; ACI Foundation, 2020). Thus, there is an anticipation that future codes of practice will reflect more performance-oriented guidelines.

This section has reviewed the current approaches adopted in different parts of the world to specify the durability performance of concrete. A summary of some of the commonly known performance test methods (DI and SLMs) is shown in Table 2-5. Based on the literature on performance-based approaches, the South African and Swiss approaches present significant advances in the P2P transition. The following section details two case studies that exemplify the state-of-the-practice of the OPI and TPT methods.

Table 2-5 Summary of durability performance techniques in various countries (based on durability indexes) (adapted from Alexander (2018).

Country	Durability parameter	Service life model	Durability test method
Canada	Chloride ion penetrability	None Identified	ASTM C 1202 (Chloride penetration test)
France	Chloride diffusion coefficient - Effective and apparent - Apparent gas permeability - Liquid water permeability - Initial Ca(OH)2 content - Water-accessible porosity	LCPC Empirical models	Chloride diffusion – migration and diffusion tests Air and water permeability
Netherlands	Chloride ion penetration	DuraCrete Probability-based durability design	NT Build 492 (Rapid chloride migration test) Two electrode method (TEM)
Norway	Chloride diffusivity	DuraCon Probability-based durability design	NT Build 492 (Rapid chloride migration test) Two electrode method (TEM)
Spain	Electrical resistivity	LIFEPRED Resistivity-based model	Two-point or four-point (Wenner) resistivity test
Switzerland	Chloride migration Accelerated carbonation Air-permeability *(on-site)*	Exp-Ref Chloride and carbonation-induced corrosion initiation models	Max limits: SN 505 262/1-B (NT Build 492) Max limits: SN 505 262/1-I Max limits: SN 505 262/1-E
South Africa	Oxygen permeability* water sorptivity* Chloride conductivity* **Lab or site*	Chloride and carbonation-induced corrosion initiation models	Oxygen permeability index (OPI)) Chloride conductivity index (CCI) Water sorptivity index (WSI)

2.6.3. Practical implementation of the South African and Swiss approach

This section discusses some case studies where the South African and Swiss durability indicator approaches have been applied, as well as some challenges faced when applying the methods in practice.

2.6.3.1. Swakopmund-Walvis freeway bridge (SADIA)

Otieno and Walter (2022) investigated the practical implementation of the SADIA against the DTS durability design on upgrading the Swakopmund-Walvis freeway bridge. The verification process included three steps: durability index testing of the as-built concrete, measurement of in-situ cover depth, and service life estimation using the South African chloride ingress model (Otieno & Walter, 2022). Table 2-6 shows a summary of the DTS specifications. The target DI values listed are specified by SANRAL in the Committee of Transport Officials (COTO) guidelines for road infrastructure to enforce quality control.

Table 2-6 Summary of DTS design and performance specifications (adapted from Otieno et al. (2022)

Concrete mix	On-site concrete production	Target DI values*
▪ Binder type: 50/50 PC/GGBS	▪ Minimum cover depth: 50 mm	▪ Minimum OPI: 9.10
▪ Minimum binder content: 380 kg/m^3	▪ Adequate compaction	▪ Maximum WSI: 10 mm/hr0.5
▪ Maximum w/c ratio: 0.50	▪ Curing: impermeable membrane	▪ Maximum CCI: 2.2 mS/cm

**DI targets based on SANRAL specifications (COTO, 2020)*

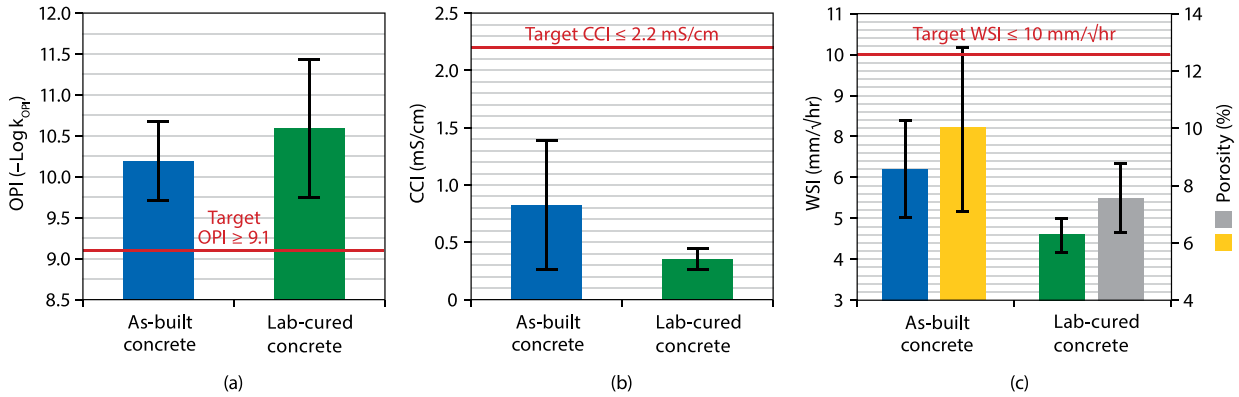

Figure 2-17 OPI (a), CCI (b), and WSI (c) test results for the as-built and lab-cured concretes (adapted from Otieno et al. (Otieno & Walter, 2022).

The findings from the investigations (see Figure 2-17) show that the target DI values were met, 30% of the cover measurements were below the target (50 mm), and most of the tested bridge elements surpassed the design service life (100 years). Otieno and Walker convincingly showed the usefulness of a hybrid approach using DTS specification with durability indicators and SLMs. Such an approach permits corrective measures to be implemented on the structure in cases where the specifications are not met and penalties can be imposed on conditional acceptances.

2.6.3.2. Port of Miami tunnel, USA (TPT)

The TPT method was used to resolve a dispute on the Port of Miami tunnel construction. During the prefabrication process of the concrete segments (tunnel lining), it was discovered that some segments were not cured according to specifications, which required an extended curing period (Torrent, Neves & Imamoto, 2022b). It was assumed that these segments would not achieve the desired performance, prompting rejection of the elements.

Table 2-7 Estimated carbonation depth of concrete segments (adapted from Torrent et al. (2022).

Curing time (hours)	Predicted carbonation depth at 150 years (mm)		
	Analytical	Based on *kT* site measurements	
	DuraCrete/DARTS	Parrott	Exp-Ref
18	35	19	43
72	24	14	28

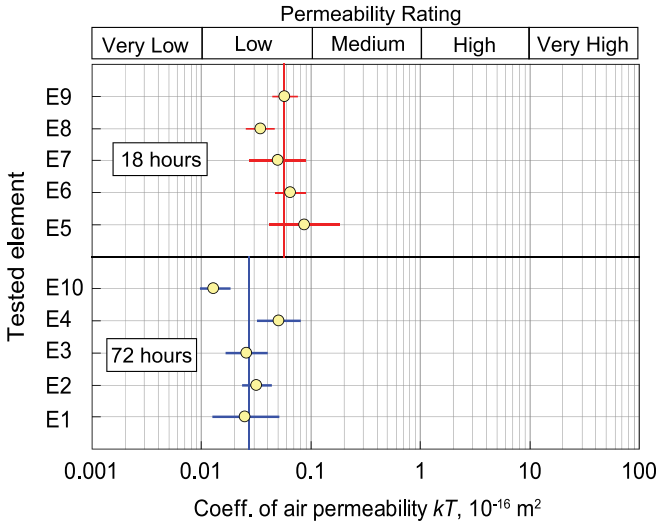

Figure 2-18 Summary of kT results for the tested concrete segments (adapted from Torrent et al. (2022).

An investigation was conducted to assess the durability performance of the affected concrete segments against the fully cured elements. The TPT, DuraCrete service life models, and two other prediction models were employed. The affected segments had slightly higher permeability values compared to the reference elements. However, both sets of the *kT* results had the same permeability classification (Figure 2-18). Based on carbonation depth estimations, the service life predictions from the three models showed that all the segments would meet the performance requirements regardless of the differences in the curing (Table 2-7). Ultimately, the affected concrete elements were accepted, avoiding significant financial consequences on the project. The

study highlights the value of on-site air permeability measurements as a quality control tool and the benefits of assessment of service life data from the actual structure.

2.6.4. Challenges experienced with the OPI and Torrent methods

Challenges still exist, particularly for site-based OPI and Torrent investigations. Over the years, the OPI method has experienced inconsistencies in data collection from various laboratories, attributed to insufficient documentation of information relating to the tested concrete samples. The inconsistencies have made it challenging to analyse trends in the growing database of OPI investigations. DI testing report spreadsheets have been developed to compute the data and capture important information on the tested samples (Nganga, 2012; Nganga, Alexander & Beushausen, 2017). The most recent updates to the spreadsheet (v5.00) were made in 2023, indicating continued progress and refinement of the SADIA approach's data collection and analysis process.

Moyana (2016) and Nganga et al. (2017) reported an increase in the OPI data variability between 2008 - 2015, linked to material variabilities and construction quality variations. These challenges highlight the need for ongoing OPI investigations to better understand the behaviour and effect of these evolving materials on gas permeability. Section 2.6.1.1 highlighted studies to develop an approach to estimate target OPI values at the pre-construction stage for specifying acceptable minimum OPI values to be achieved on-site. The approach can increase confidence in understanding variabilities in site practices for concrete construction and encourage contractors to provide assurances of achieving OPI targets.

Ambient conditions continue to influence site Torrent measurements (Jacobs et al., 2009; Bueno et al., 2021; Nguyen, Nishio & Nakarai, 2022; Torrent, Neves & Imamoto, 2022b), as well as the misinterpretation of collected data (Torrent, Neves & Imamoto, 2022b). Ongoing studies show the evolution of approaches aimed at compensating for the effect of environmental conditions, particularly moisture, to supplement the Torrent testing protocol. A growing database is needed for site Torrent investigations in varying environmental conditions to better understand the air permeabilities of in-situ concrete. Further, approaches utilising the Torrent method with other durability assessment methodologies can help increase confidence in interpreting data collected on site. This study attempts to develop such an approach for local durability assessment.

Overall, increased investment in training and education for technicians and engineers is required to build the capacity for a wider adoption of concrete durability performance methodologies. The advancement of concrete durability management and the construction of more resilient and sustainable infrastructure will rely heavily on approaches like the OPI and TPT methods soon; thus, the economic costs of implementation challenges presented above need to be addressed through a collaborative effort between the subject matter experts and governing bodies controlling the standardisation of test methods and practices.

2.7. Review of previous studies on gas permeability tests

The section reviews studies carried out by Romer (2006), RILEM TC (2007), Beushausen (2008), Wieland (2009), Starck (2013; 2017), and Bahurudeen (2014) to qualify the TPT and OPI methods as sound gas-permeability approaches.

Romer (2006) and the RILEM TC (2007) assessed the sensitivity of various indicator tests to concrete transport properties and curing effects. Six concrete mixes were used to produce concrete specimens (200 mm x 200 mm cubes) of varying quality and subjected to different environmental conditions in the laboratory. After one year of storage in a controlled environment (20°C, at 35%, 70%, and 90% RH), the samples were tested for permeability using the OPI and TPT methods. The TPT and OPI demonstrated comparable sensitivity to concrete quality and curing effects.

The RILEM TC (2007) examined the correlation of in-situ gas permeability with reference laboratory tests. The comprehensive study involved manufacturing concrete panels (300 mm x 900 mm 1200 mm). The panels were subjected to simulated field conditions and later tested. Samples were acquired and disseminated to various research facilities, including one in South Africa (UCT), to assess the sustainability metrics. The study found that the reference and 'site' tests (TPT) successfully differentiated penetrability levels with high significance (see Table 2-8). Beushausen (2008) presented a good correlation between the OPI and TPT (Figure 2-19), highlighting the similarities in sensitivity to the variables tested.

Table 2-8 Extract of significance of reference tests (UCT tests) vs significance of site tests (adapted from Torrent et al. (2022). (o – not significant; + - significant; ++ - highly significant).

Compared sets	*1 – 2*	*2 – 3*	*1 – 3*	*4 – 5*	*2 – 6*
Variable tested	*w/c* OPC	*w/c* OPC	*w/c* OPC	*w/c* BFSC	Curing
Expected "penetrability"	2 > 1	3 > 2	3 > 1	5 > 4	6 > 2
Reference test	**Differentiation capability**				
O_2 permeability (OPI)	++	++	++	++	++
Water sorptivity (WSI)	++	--	++	+	o
Site test	**Differentiation capability**				
Autoclam air	--	++	++	o	++
Torrent air-permeability	++	++	++	o	++
Hong-Parrott	o	++	++	++	+

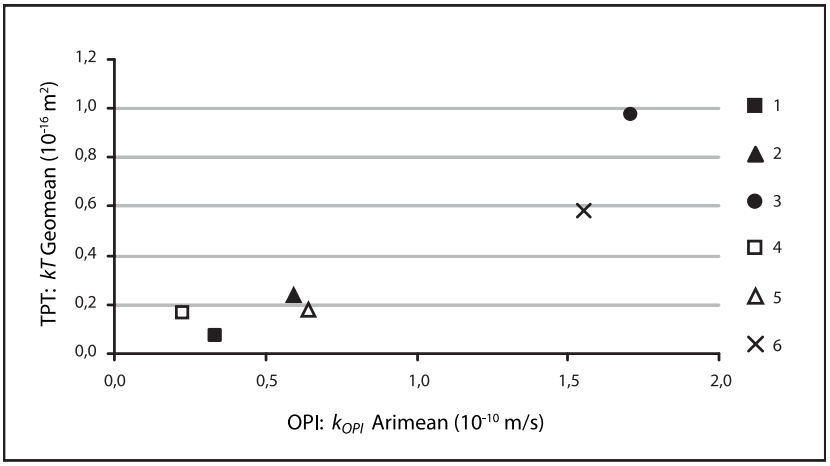

Figure 2-19 Correlation between OPI and TPT methods from UCT results (adapted from (Beushausen & Alexander, 2008).

Wieland's (2009) findings did not correlate the OPI and TPT well. The study involved mixes with various cement extenders and w/c ratios, which produced impermeable concrete characteristics. However, the qualitative classification led to the same conclusions concerning durability potential. It is fair to assume that the OPI and TPT methods do not share a causal relationship even though previous studies have obtained good correlations. Instead, the correlation may be influenced by the association of the parameters which they measure.

Bahurudeen (2014) also examined the durability performance of concrete with supplementary materials, specifically sugarcane bagasse ash (SCBA). A reduction in permeability was observed with the increase in replacement levels. The author attributed the enhanced performance to the pozzolanic effect on the pore structure. Interestingly, the recorded Torrent air permeability values significantly reduced permeability compared to the control specimen, yet the effect was less pronounced in the OPI values. Nonetheless, both methods demonstrated their sensitivity to SCMs.

Starck (2013; 2017) recently conducted a comprehensive comparative study to correlate *kT* and *kOPI*. A set of 150 mm cubes was produced using two binder types (PC and 50% PC and GGBS) and three w/c ratios (0.5, 0.65, 0.8). Starck simulated dry and wet conditions resembling the Cape Town seasons by soaking the cubes daily for 35 days during the winter and storing them in a dry room (20 °C, 53% RH) between 35 and 90 days in summer. Figure 2-20 shows the resulting correlation between the OPI and Torrent indexes from Starcks' study, which yielded an excellent correlation (R^2 = 0.95). Previous studies indicated good correlations to varying degrees, except for Wieland (R^2 = 0.39). Starck's study deviated from the cluster of other studies. The discrepancy was attributed to the experimental conditions in the previous studies (Starck, 2013; Torrent, Neves & Imamoto, 2022b).

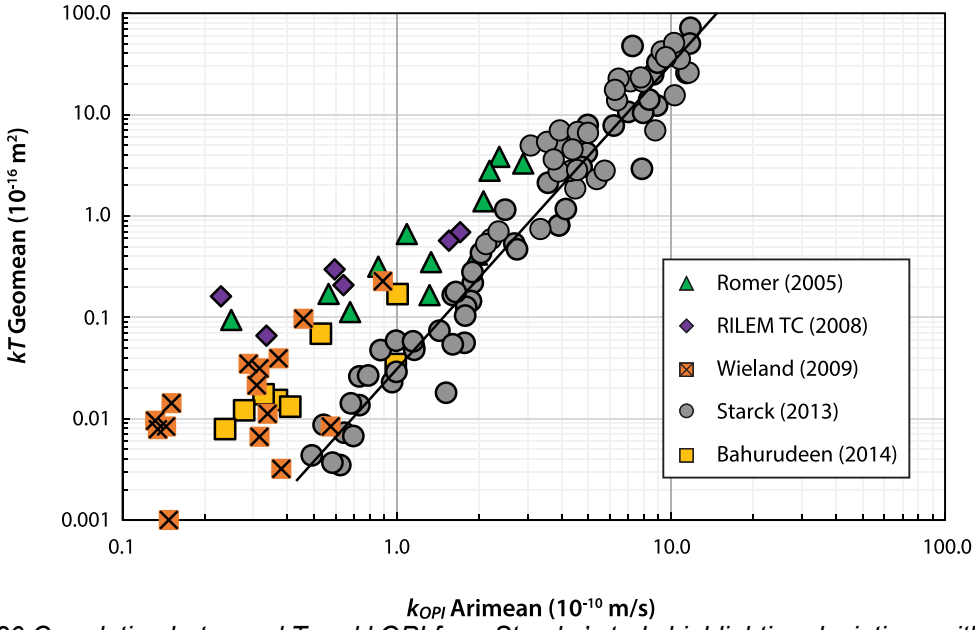

Figure 2-20 Correlation between kT and kOPI from Starcks' study highlighting deviations with previous studies (after Starck (2013).

One of Starck's primary deductions was a general equation relating the OPI and TPT (equation (2-9)) and a permeability classification relationship between the two methods (see Figure A-1). Additionally, Starck attempted to address the influence of moisture on the measured *kT* values. However, the analysis could not improve the established correlation. Starck proposed using a correlation curve to predict the likelihood that the prediction of the *kOPI* would be undervalued (see Figure 2-21), where the lower bound curve represents the worst *kOPI* estimation. Stark conceded that the correlation chart may be unreliable in practice and, therefore, must be validated.

$$\boldsymbol{kOPI = 3.1 \cdot kT^{0.31}} \qquad (2\text{-}9)$$

where kOPI (10^{-10} m/s); kT ($10^{-16}m^2$)

The consensus from previous studies suggests that the two methods possess a good correlation and a solid basis for a combined approach. However, the OPI and TPT interrelationships have not been investigated on structural elements in the field to validate the reported findings. Therefore, the present study aims to address this gap in the literature.

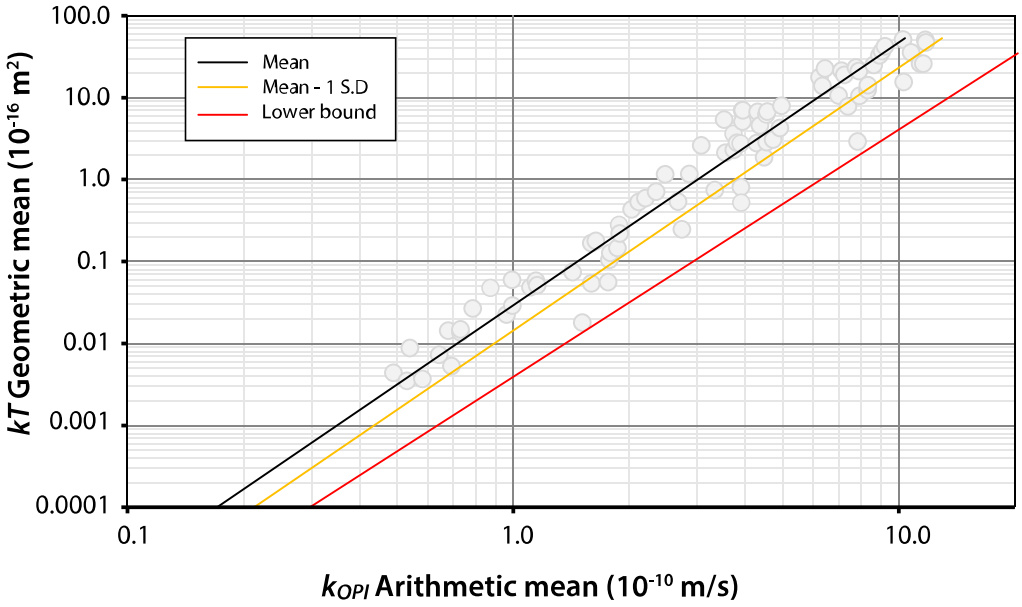

Figure 2-21 kT - kOPI Correlation curves showing limiting boundaries (after Starck et al. (2017).

2.8. Summary

This literature review focused on concrete durability assessment methods, particularly gas permeability indicator tests. The key findings from the review chapter are summarised below:

1. Prescriptive design approaches are insufficient in specifying and designing for concrete durability. Instead, durability is closely related to the ability of the concrete system to resist the penetration of aggressive species in specific exposure environments.
2. Transport mechanisms acting in concrete have been quantified using durability indicator tests, with gas permeability tests providing reliable results in shorter periods.
3. The OPI and TPT have been reported to be widely accepted gas permeability test methods for durability assessments.
4. The transition from prescriptive to performance (P2P) approaches is slow despite various performance indicator test methods and service life prediction models being developed worldwide.
5. Past studies have shown the synergies between the OPI and TPT methods, with a good correlation established on laboratory-manufactured specimens. An integrated approach utilising the OPI and TPT tests has been proposed for practical implementation in South Africa. However, a comparative study has not been done on concrete as-built to validate the correlation.
6. Further research is therefore required to establish the interrelationships between the OPI and TPT methods on site concrete.

3. MATERIALS AND METHODS

3.1. Introduction

The chapter describes the experimental procedures, materials and equipment, and methodology employed for the current study. The practical aim was to quantify the air permeability of site structural elements using the Torrent Permeability test method and the Oxygen Permeability method. This would allow a deeper insight into the interrelationships between the two processes and propose guidelines for practically implementing both methods in the local practice of durability index testing.

3.2. Overview

Three binder types, Portland Cement (PC) CEM I 52.5N, Portland limestone CEM II A/L 52.5N, and a blend of PC CEM I 52.5N and 30% fly ash (FA), were used. Five concrete mixes were made from the chosen binders with varying water-to-cement (w/c) ratios (0.50 and 0.60) and concrete grades (30 MPa and 40 MPa). Five median barriers and representative test panels were cast at a local precast manufacturer's site in the Boquinar industrial area in Cape Town (coordinates: -33.97830066774946, 18.584109577591832). The concrete elements were manufactured during the summer (February 2022) and winter periods (June 2022). The rationale behind this schedule was to expose the test specimens to different environmental conditions representing the 'worst-case' natural curing period (summer, which generally is hot, windy and dry in Cape Town) and 'best' natural curing conditions (winter, which is usually characterized by moderate temperature, high humidity and frequent rain). A curing compound, Glade 6251, was applied to the concrete elements after de-moulding at 24 hours. The samples were left to air-cure under natural environmental conditions on site and tested at 28 and 56 days. The TPT was carried out on the median barriers and the test panels, while the OPI test was carried out on extracted core samples from the test panels. The following sections of this chapter present a detailed description of the procedures followed in the experimental programme. Table 3-1 summarises the durability indicator tests conducted on the concrete specimens, and Figure 3-1 shows a summary of the experimental programme.

Table 3-1 Test methods used in the Experimental Programme.

Test performed	Test method	Standards
Compressive strength (cube)	Cube crushing	SANS 5863 (2006)
Durability Index	Oxygen permeability (OPI)	SANS 3001-CO3-1 (2015) SANS 3001-CO3-2 (2015) UCT DI Manual (2018,2023)
Durability Index	Torrent Air permeability	SIA 262/1-E:2019
Surface resistivity	Four-point (Wenner) probe	-
Concrete surface moisture	Electrical Impedance	ASTM F2659 (2010)

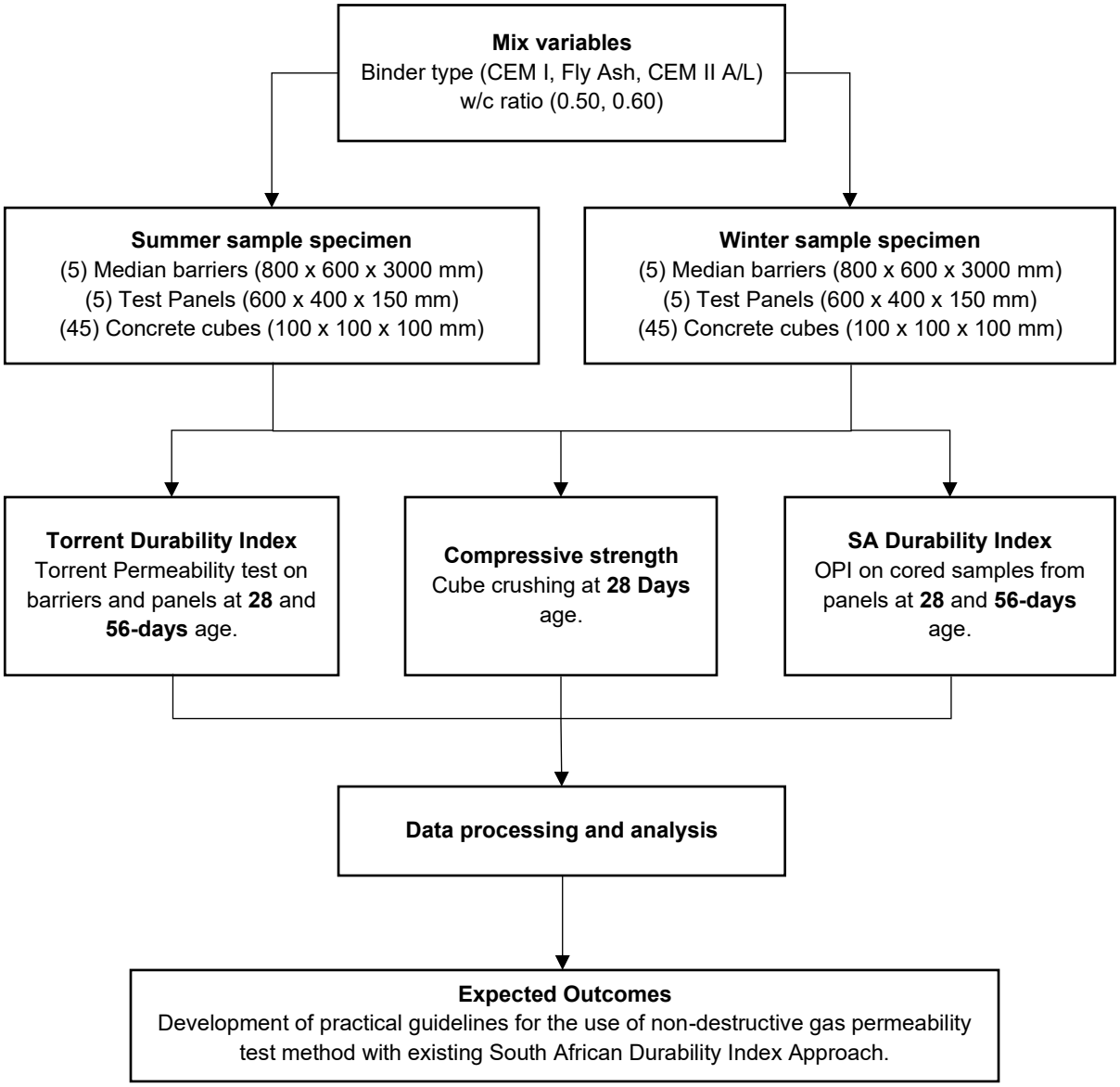

Figure 3-1 Schematic chart of the experimental programme.

3.3. Materials

3.3.1. Cement

The primary binders used in the study were Plain Portland Cement (PC) CEM I 52.5N and PC CEM II A/L 52.5N (comprising 8.9% limestone) supplied from the PPC Cement Riebeeck West and De Hoek plant, respectively. The cement types conform to the 52.5N strength class under the SANS 50197-1 standard for ordinary cement. Table 3-2, and Table 3-3 show the chemical properties of the clinker in the two binders.

Table 3-2 Chemical compositions of CEM I 52.5N Binder (courtesy of PPC (Esau, 2022)).

Oxide		% Composition
Silica	SiO_2	19.95
Alumina	Al_2O_3	4.10
Iron Oxide	Fe_2O_3	3.50
Lime	CaO	64.95
Magnesia	MgO	0.90
Sulphate content	SO_3	2.50
Chloride content	Cl^-	0.01
Potassium Oxide	K_2O	0.68
Sodium Oxide	Na_2O	0.57

Table 3-3 Chemical compositions of CEM II 52.5N A/L Binder (courtesy of PPC (Esau, 2022)).

Oxide		% Composition
Silica	SiO_2	22
Alumina	Al_2O_3	4.2
Iron Oxide	Fe_2O_3	3.3
Lime	CaO	67.2
Magnesia	MgO	1.1
Sulphate content	SO_3	2.3
Chloride content	Cl^-	0.01
Potassium Oxide	K_2O	0.72
Sodium Oxide	Na_2O	0.25

3.3.2. Fly ash (FA)

FA, a by-product from furnaces fired with pulverised coal (Jacobs & Kiliswa, 2021), was partially replaced for the CEM I cement. FA has been reported to improve the properties of fresh and hardened concrete due to its ability to form additional cementitious products (hydrates), thereby reducing permeability in concrete (Constro Facilitator, 2022). A blend of 70% CEM I and 30% FA was used to analyse how the durability parameters of the concrete would be influenced. The FA used in this study was a classified fly ash product (Durapozz) supplied by Ash Resources. The chemical composition of the cement extender is shown in Table 3-4.

Table 3-4 Chemical compositions of Fly ash (Ash Resources, 2009).

Oxide		% Composition
Silica	SiO_2	54.33
Alumina	Al_2O_3	32.91
Iron Oxide	Fe_2O_3	3.11
Lime	CaO	4.25
Magnesia	MgO	1.07
Sulphate content	SO_3	0.25
Chloride content	Cl^-	0.01
Potassium Oxide	K_2O	0.71
Titanium Dioxide	TiO_2	1.66
Strontium Oxide	SrO	0.12
Phosphorus Pentoxide	P_2O_5	0.50
Manganese (III) Oxide	Mn_2O_3	0.04
Sodium Oxide	Na_2O	0.21

3.3.3. Water-to-cement ratio

The water-to-cement ratio (w/c) refers to the ratio of water mass to the mass of cement (Owens, 2009). The w/c influences the strength and permeability characteristics of concrete. Though the relation between w/c and strength is not linear, increasing the w/c decreases concrete strength and increases permeability (Omar, 2018). In this study, two ratios were used, 0.50 and 0.60. The design water content was 175 L/m^3 for all the concrete mix designs. Note, this value is the "effective water" (excludes the water absorbed by the aggregates). The water content could not be achieved in some instances. Some mixes were retempered to achieve the desired consistency, and the water content was adjusted during winter batching due to perceived aggregate moisture from rainfall. It was decided to continue testing the affected concrete mixes to understand the effect of the altered w/c ratios on the performance of the concrete.

3.3.4. Chemical admixture

A water-reducing plasticiser, Chryso® Plast Omega 174, was added to all the mixes. The plasticiser improves the workability of fresh concrete (Chryso South Africa, 2020). Modern high-performance concretes often use chemical admixtures to improve workability and durability. However, the chemical interactions between binders and admixtures are complex, making it difficult to empirically determine the right combinations to assure long-term durability, especially in aggressive environments (e.g., coastal environments). Nonetheless, this study utilised dosages between 0.60% and 0.65% of the plasticiser by cement mass.

3.3.5. Fine aggregates

Dune Sand (DS) from Macassar Olympic, supplied by Afrimat, and quartzitic sandstone Crusher Sand (CS) from the Villiersdorp quarry were blended to make up the fine aggregate material used in the study. The fines were combined to compensate for the angular-shaped, rough-textured, and coarser particle sizes of CS with the well-rounded, very fine particles of DS (Park et al., 2018).

The particle size grading of the DC and CS are illustrated in the grading curves shown in Figure 3-2. The properties of the fine aggregates are displayed in Table 3-5.

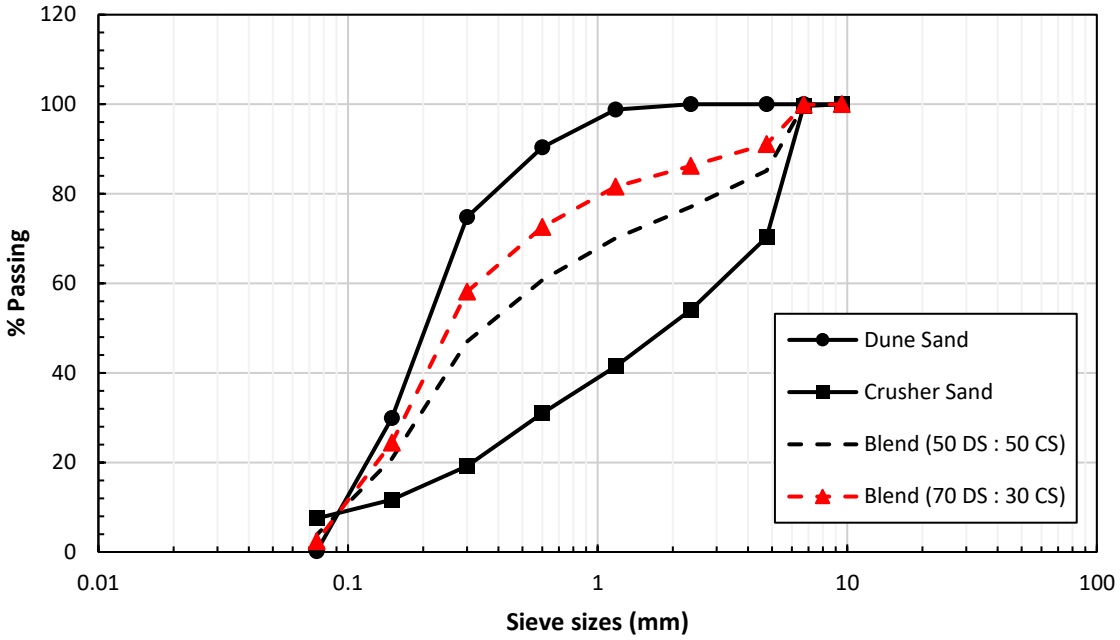

Figure 3-2 Grading curves for fine aggregate (data from Megamix (2022)).

Table 3-5 Properties of fine aggregate (data from Megamix (2022)).

Fine aggregate	Fineness Modulus	Relative Density	Loose Bulk Density (g/cm^3)	Aggregate Crushing Value	Absorption (%)
Dune Sand	1.06	2.63	2.32	-	-
Crusher Sand	3.72	2.64	1.62	20.4	0.9

3.3.6. Coarse aggregates

Quartzitic sandstone is a popular aggregate choice within the Western Cape of South Africa due to its cost-effectiveness and availability (Mackechnie, 2003). The sedimentary rock comprises quartz grains and other mineral fragments accumulated from water and wind action. Studies conducted by Mackechnie (2003) and Kumar et al. (2016) found that sandstone aggregates tend to exhibit less desirable properties in terms of their strength and stiffness compared to traditional coarse aggregates (greywacke and granite). Nonetheless, sandstone aggregates are widely accepted for most structural concrete works, with supplementary cementitious material (SCM) as an alternative to depleting natural aggregates. This study used 19-mm quartzitic sandstone acquired from the Villiersdorp quarry. The properties of the aggregates are summarised below in Figure 3-3 and Table 3-6.

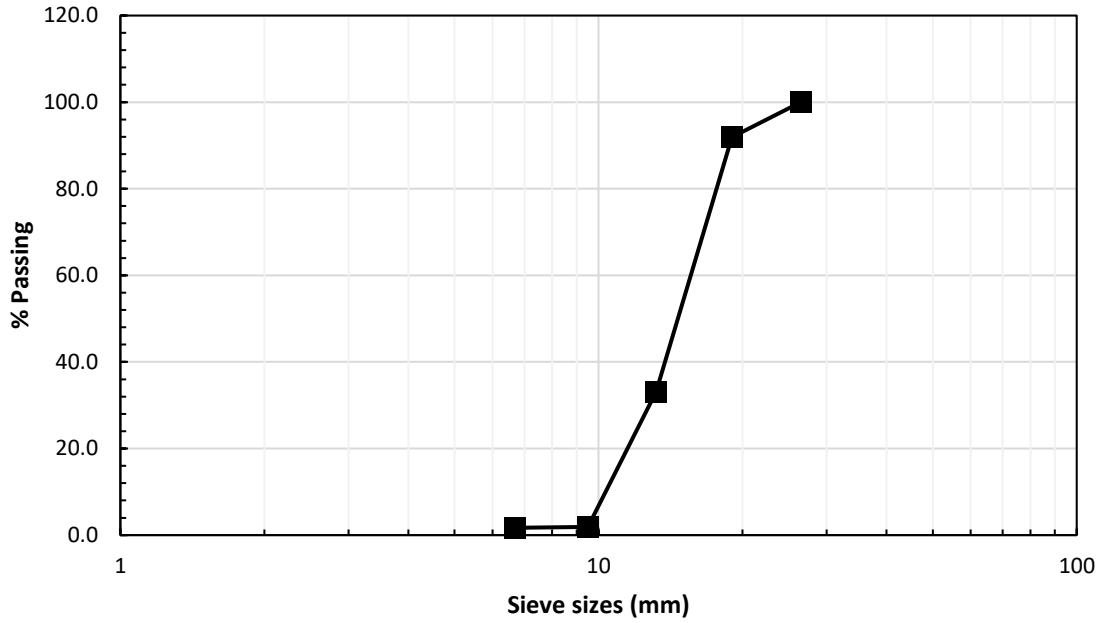

Figure 3-3 19-mm Quartzitic Sandstone grading curve (data from Megamix (2022)).

Table 3-6 Physical properties of coarse aggregates (data from Megamix (2022)).

Coarse aggregate	Flakiness Index (%)	Relative Density	Loose Bulk Density (g/cm^3)	Aggregate Crushing Value	Absorption (%)
Quartzitic Sandstone	17.0	2.64	1.38	20.4	0.9

3.4. Concrete mix designs

The concrete mix designs for this research study adopted the Cement & Concrete SA (CCSA) method. Five mixes were selected, resembling commonly used mix design specifications for durability-critical structural concrete. The targeted slump for all mixes was 75 ± 50 mm. Table 3-7 shows a breakdown of the mix specifications used for this study. Concrete mixes were classified by binder type (PC-I: CEM I 52.5N, PC-II: CEM II/A-L 52.5N, FA: 70% CEM I 52.5N + 30% fly ash) and grade (e.g., 40-PC-I for 40 MPa with CEM I binder). Note that Winter mix proportions were adjusted to compensate for cold weather and wet aggregates. Thus, the mix compositions presented in Table 3-7 are nominal. Details on the actual mix proportions achieved on site are presented in Appendix B.1.

Table 3-7 Design mix proportions (materials in kg/m³) (data from Concrete Units).

Description	Mix Designs				
	Mix 1	**Mix 2**	**Mix 3**	**Mix 4**	**Mix 5**
Mix designation	**40-PC-I**	**40-PC-II**	**30-PC-I**	**30-PC-II**	**30-FA**
Design Strength (MPa)	40	40	30	30	30
CEM I 52.5N	355	0	285	0	210
CEM II/A-L 52.5N	0	355	0	285	0
Fly Ash	0	0	0	0	90
Coarse aggregate	1100	1100	1080	1080	1080
Dune Sand	515	515	570	570	615
Crusher Sand	220	220	245	245	215
Omega 174 (% Binder)	0.60	0.60	0.65	0.65	0.60
Water	175	175	175	175	175
W/C	0.50	0.50	0.60	0.60	0.60

3.5. Sample preparation

3.5.1. Concrete batching and mixing

The concrete mixes were prepared at a ready-mix batch plant near the test site (Figure 3-4). The plant employs a central-mix system, combining all materials centrally before discharging into the mixer truck. Batching is either manual or automated. Manual batching relies on operator control, while automated batching uses computer-controlled weighing. The PC-II mixes were batched automatically, while the PC-I and FA mixes were batched manually due to cement silo limitations. After batching, each mix containing 1 m³ of concrete was discharged into a delivery truck. Each mix was sampled to observe the consistency before being delivered on site.

It was observed that some mixes were retempered to achieve better consistency before placing and casting. This presented challenges in ascertaining the true composition of batches, specifically the water content. Uncontrolled addition of water directly elevates the w/c ratio. This may create a deceptive improvement in workability but masks a cascade of detrimental effects on the concrete mix, including incomplete mixing, localised zones of high w/c, and segregation, which introduce inherent flaws into the concrete microstructure.

The resulting concrete microstructure will have a higher total porosity, enlargement of pore sizes, and the establishment of more interconnected pore networks, adversely affecting the hardened concrete's mechanical properties and durability performance.

3.5.2. Casting

Concrete was discharged into a hopper suspended on a gantry crane before placement. The concrete was then placed in steel moulds of the median barriers measuring 800 mm height by

600 mm width by 3000 mm length. The moulds contained steel reinforcement fixed in place and propped by 50 mm cover blocks. Concrete was also placed in the test panel moulds (600 mm x 400 mm x 150 mm). An industrial poker vibrator was used to compact the concrete, ensuring good distribution and removing entrapped air voids. The concrete was also sampled for the compressive strength test and slump test. The same procedure for casting was followed for all the concrete combinations, resulting in each mix having a median barrier and representative test panel. Figure 3-5 shows the concrete and cast elements placed on-site.

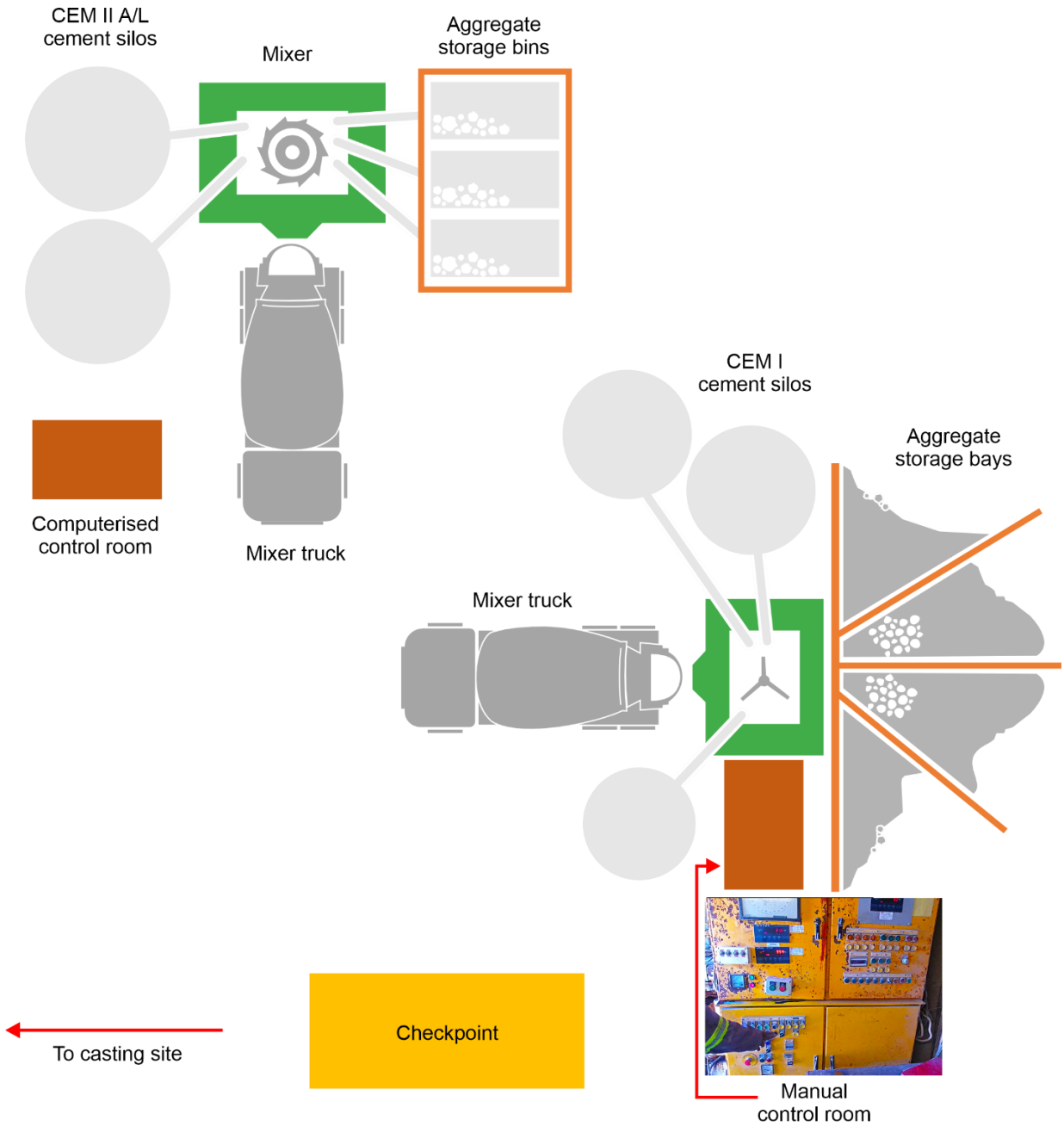

Figure 3-4 Schematic plan view of the plant used for batching and mixing of the concrete mixes used in the study.

Figure 3-5 Cast median barriers and 'mock panel' (bottom), placed concrete in steel formwork, panels (top-left), and barriers (top-right).

3.5.3. Curing

A curing compound (Glade 6251) was applied on the cast surface of the freshly placed concrete members per the manufacturer's instructions. The curing admixture was used to prevent excessive water evaporation and ensure efficient cement hydration during curing. After the stripping of the formwork (after 24 hours), an additional curing compound was applied to the exposed surfaces of the concrete samples. The samples were left to air cure until the testing time. The elements cast during the winter period were also exposed to wetting cycles due to the rainfall prevalent in the winter months.

The cube specimens for the compressive strength tests were cured in a temperature-controlled (23 ± 2°C) water tank in the testing laboratory on-site.

3.5.4. Exposure

In summer, the median barriers and test panels were kept on-site and exposed to the outdoor environment. The specimens were oriented North-easterly where the testing face/plane would be exposed to the sun. This strategy was employed to ensure worst-case natural curing on-site. At 28 days, the panels were transported to the UCT Civil Engineering laboratory for the DI tests. After testing, the panels were kept in a controlled environment to observe the sensitivity of the OPI and TPT methods to age. The median barriers remained on-site for the entirety of the testing program.

Similarly, during winter, the barriers were kept on-site for the experimental investigations. The panels were moved to the UCT lab at 28 days and then exposed to the outdoor environment on the rooftop of the UCT New Engineering building until the next testing age at 56 days. This was done to ensure exposure to rainfall and lower temperatures.

Table 3-8 shows the storage locations of the test specimen during the experimental program.

Table 3-8 Site locations for concrete elements during the testing period (weather data from Meteostat.net and UCT Department of Geological Sciences).

Site location	Site condition	Test specimens on site
Concrete Units precast yard, airport industria, Cape Town	Summer: Exposed to the outdoor environment with average conditions of 20.3°C, 70% RH, and 24.4 mm total precipitation	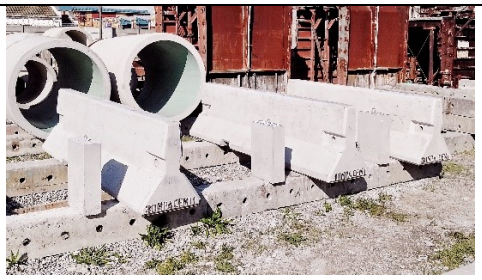
UCT Civil Engineering Laboratory	Summer: Exposed to the indoor environment (after 28 days) with average conditions of 22°C, 60% RH	
Concrete Units precast yard, airport industria, Cape Town	Winter: Exposed to the outdoor environment with average conditions of 13.1°C, 75% RH, and 68.2 mm total precipitation	

Site location	Site condition	Test specimens on site
The roof of the New engineering building, UCT, Cape Town	Winter: Exposed to outdoor environment (after 28 days) with average conditions of 13.0°C, 80% RH, and 129.2 mm total precipitation	

3.6. Experimental tests

3.6.1. Compressive strength

Nine cubes per mix were used to measure the compressive strength development of the concrete mixes. The cubes were crushed at 3, 7, and 28 days using a hydraulic compression testing machine per the SANS 5863:2006 standard.

3.6.2. Slump test

The slump test was carried out to check the consistency of the mixed concrete from the ready-mix truck. The procedures set in the SANS 5862-1 (2006) standard was followed. The concrete mixes from the truck were sampled at the discharge point as per SANS 878 (2012). This allowed for a reliable representative sample of the mixes to be tested.

3.6.3. Oxygen permeability index test (OPI)

3.6.3.1. Sample preparation and conditioning

At 28 days, the five test panels were transported to the UCT Civil Engineering Laboratory. All efforts were made to protect the panels from damage and inter-alia during transportation. However, there was some exposure to rainfall during transportation to the lab. The elements were kept at ambient conditions in the laboratory for three days before coring the test specimen. This is because there was no immediate access to the coring machine. Nonetheless, the coring of the samples was still within the period recommended by the DI manual (28-35 days).

Four cores were extracted from each panel at a depth of 150 mm per SANS 3001-CO3-1:2015. The coring was done perpendicular to the casting direction to eliminate discrepancies due to bleeding and segregation. The samples were then saw-cut so each disc measured 70 ± 2 mm in diameter and 30 ± 2 mm thick. Four discs were taken for the OPI test.

After coring and cutting (Figure 3-6), the disc specimens were preconditioned in an oven at 50 ± 2°C for seven days before conducting the DI tests.

The same procedure was followed for the tests conducted at 56 days.

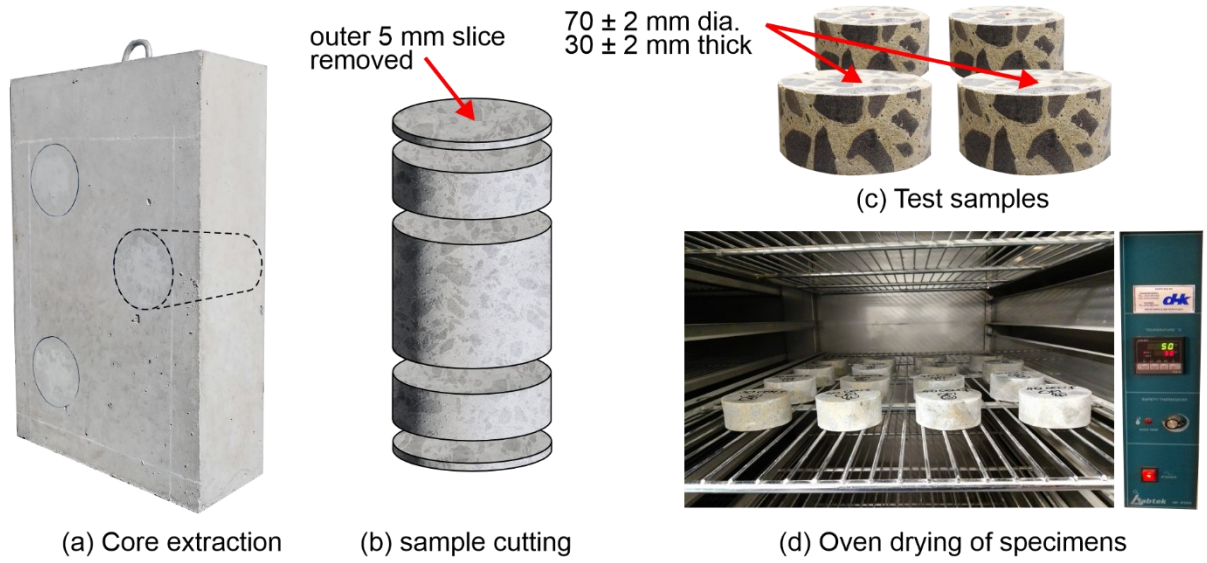

Figure 3-6 Preparation of test specimens for DI testing.

3.6.3.2. Oxygen permeability index (OPI) test

Section 2.5.1.2 describes the OPI test, and further details are available in the DI manual and SANS 3001-CO3-2:2015.

Instrumentation

The gas permeability of the concrete specimens was evaluated using a falling head permeameter - the equipment assembly consisted of the following components.

i. A permeability cell (5 L capacity ± 5% tolerance) with inlet and outlet valves
ii. Oxygen supply with a pressure regulator
iii. Cover plate
iv. Rubber collar
v. Rigid sleeve

Figure 3-7 shows the assembly of the components and placement of the concrete samples. Multiple permeameters were used simultaneously for the test and connected to a data logging device recording the pressure drops in each permeability cell. Additional apparatus for the OPI test included a digital vernier calliper for measuring sample dimensions and a desiccator for storing specimens after removal from the oven.

Testing procedure

After preconditioning, the samples were placed in a desiccator to cool as prescribed in the DI manual and SANS 3001-CO3-2:2015. Each sample was then fitted in the apparatus as shown in

Figure 3-7. Once the samples were secured, the permeability cells were pressurised with oxygen gas (100 ± 5 kPa). The pressure decay of the gas passing through the concrete sample was monitored on the data-logging device. All the data points generated were recorded until the test was terminated (each test ran for six hours). The data on the logging device was transferred to calculation sheets to determine the coefficient of permeability of each tested sample. A detailed description and explanation of the OPI test used in this study can be found in SANS 3001-CO3-2:2015 and the DI manual.

Figure 3-7 OPI test set-up.

3.6.4. Torrent permeability test (TPT)

Instrumentation

Air permeability was measured using a Permea-Torr device (described in section 2.5.1.3). The instrument is the third generation of five models. It features automatic operation, calculations, and graphic plots of the measurements during the test. Comparative tests conducted on the older generation devices (second and third) versus the newer fourth and fifth-generation instruments showed that the measured permeability results yielded comparable results (Szychowski & Torrent, 2017; Torrent et al., 2018). The equipment (depicted in Figure 3-8) consists of:

i. A two-chamber vacuum cell with a test chamber and guard ring.
ii. Soft rubber-like rings attached on the circumference of the chambers for vacuum sealing
iii. A display and control unit fitted with a pressure regulator and sensors.
iv. Vacuum pump
v. Power supply
vi. Impermeable polycarbonate plate (for conditioning and calibration)

Other equipment (see Figure 3-9) used in the testing procedure is categorised as follows.

Equipment for surface preparation

- Markers and chalk
- Cover meter/scanner for the localisation of reinforcement location.
- Dry sponge and brush for surface dedusting
- Sandpaper
- Gypsum filler for sealing surface defects.

Equipment for surface moisture condition checks

- Surface moisture meter (0.0% - 6.9% scale) – Tramex concrete moisture encounter (CME4)
- Surface resistivity meter – Proceq Resipod
- Infrared thermometer

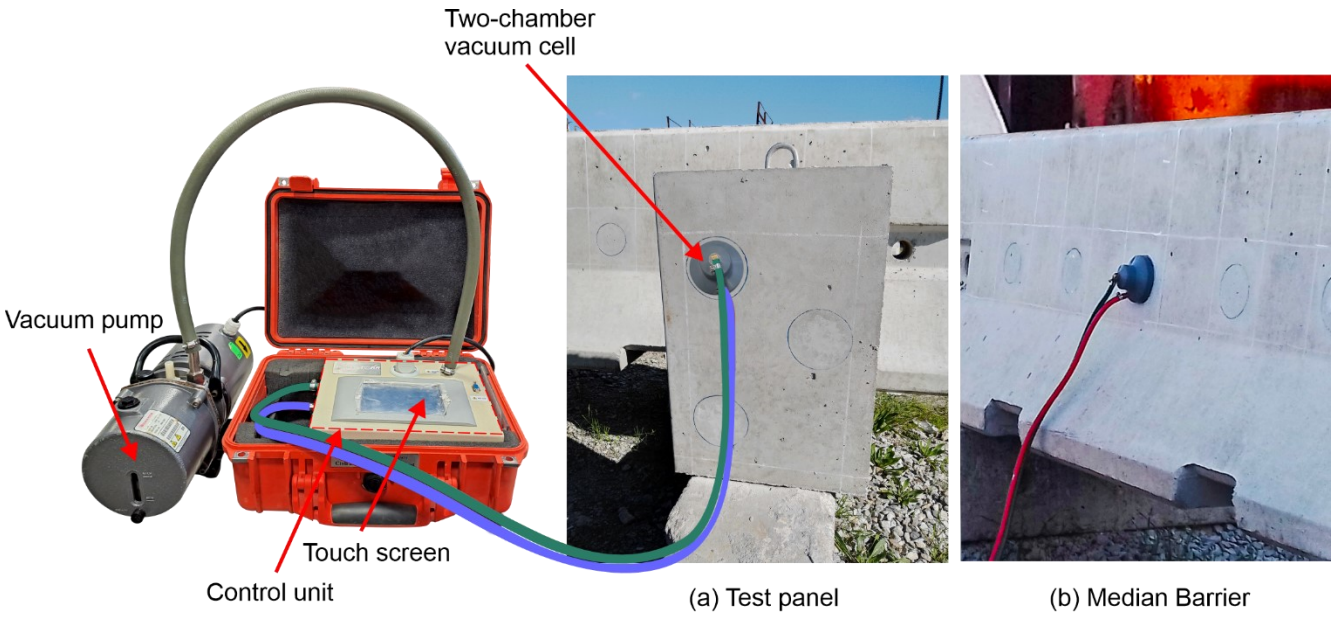

Figure 3-8 Torrent permeability set up on site.

(a) (b) (c) (d)

Figure 3-9 Instruments used in surface preparation and moisture condition checks: (a) resistivity meter, (b) infrared thermometer, (c) concrete moisture meter, (d) concrete scanner (rebar locator).

3.6.4.1. Sample and equipment preparation

The Hilti scanner was used to locate and mark out the reinforcement to make it easier to select the test area. Six measurement points were marked on each barrier, 200 mm apart, adhering to the sampling guidelines set in the SIA 262/1:2019 standard. On each test panel, three testing points were selected. Only three test locations were chosen on the panels due to the specimen size. A visual inspection of the surface of the barriers and test panels was made to record any defects on or near the test areas.

Areas with surface defects at the marked test points were sealed with gypsum paste (Figure 3-10). This action was taken to prevent any air infiltration between the contact of the chambers of the vacuum cell and the concrete surface.

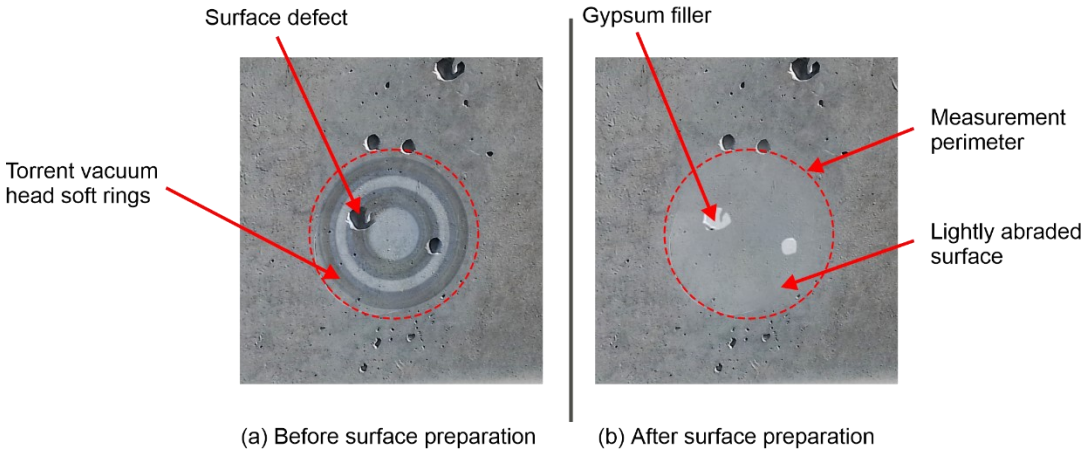

Figure 3-10 Surface preparation for Torrent permeability measurement.

Test point surfaces were lightly abraded to remove the curing compound layer and ensure smoothness. The influence of surface protective systems (curing compounds) on the

measurement of gas permeability is yet to be investigated. Lastly, the surface of the test points was de-dusted using a dry sponge and brush.

The Torrent tester was conditioned by placing the vacuum head on the calibration plate and creating a vacuum suction to flush the pneumatic system. The equipment was calibrated per the SIA standard. The equipment was shielded from direct sunlight during testing to prevent elevated system pressure.

Testing procedure

The concrete temperature and surface moisture content were measured to assess whether the surface conditions were met before testing.

3.6.4.2. Concrete temperature measurement

An infrared thermometer was used to measure the temperature at the surface of each testing location. The Swiss guidelines require the surface temperature of the element to be between 5°C – 50°C. Temperature measurements were taken before and after the permeability test and recorded.

3.6.4.3. Surface moisture measurement

The Argentine (IRAM 1892:2022) and Swiss (SIA 262/1:2019) standards specify that the surface moisture content of the test specimen should be ≤ 5.5% for site measurement. A moisture meter device (Tramex CME4) was used to quantify the moisture content at each test point. The device uses the electrical impedance principle, where the electric resistance of a material varies proportionally to its moisture content (Tramex, n.d.).

Electrical impedance is a suitable NDT method for assessing surface moisture, correlating with oven-dried specimens (Torrent, Moro & Jornet, 2014; Torrent et al., 2018; Bueno et al., 2021). The 5.5% limit was deemed to correspond to 3-days oven-dried samples at 50°C. The findings make the method acceptable for new structures (28-90 days age).

A detailed explanation of the moisture meter can be found in Appendix B.2. Moisture measurements were taken clear from steel reinforcement to avoid any interruption of the transmitted signals from the device (Figure 3-11). The surface moisture of each tested area was taken as the highest recorded value. This was done to account for the erratic drying behaviour of concrete (Tramex, n.d.).

Resistivity measurements were taken at each test location as a secondary method for the moisture condition investigation. The TPT method previously relied on resistivity measurements but now uses electrical impedance due to the sensitivity of resistivity to concretes with SCMs, which complicates result interpretation (Torrent, Neves & Imamoto, 2022b).

Nevertheless, the measured resistivity values were used in this study to monitor the moisture condition and sensitivity of the method to the different concrete blends used. A Proceq Resipod meter was used for resistivity measurements. Details on the measurement procedure can be found in Appendix B.3.

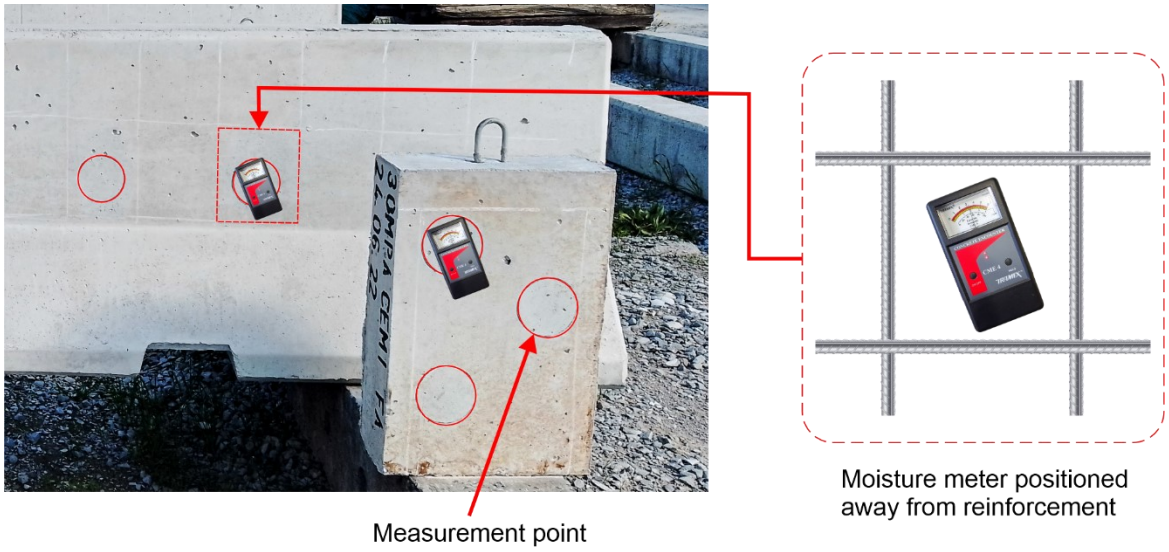

Figure 3-11 Surface moisture measurement on site.

3.6.4.4. Torrent permeability measurement

Following the moisture and resistivity measurements and the Torrent tester calibration, Torrent measurements were taken. Six determinations were made per barrier and three per representative panel. To take a measurement, the vacuum head was placed over the marked points (Figure 3-8), and a vacuum was automatically created in the chambers through the pump. The pressure increase in the chamber due to air in concrete pores was recorded.

At the termination of the test, the instrument recorded the coefficient of permeability in m^2. The recorded kT value is based on equation (2-6). The kT value for each tested element was taken as the geometric mean (kT_{gm}) of the six individual results from the barriers, and three from the panels, respectively. Air permeability measurements typically exhibit lognormal distribution linked to the test methods' sensitivity to the pore structure of the material under test. Thus, robust statistical treatment is required to handle the scatter of air permeability coefficients. Taking the geometric mean of the kT measurements reduces the impact of outliers in skewed data as it directly relates to the central tendency of the log-transformed data.

Torrent permeability was measured at the same test points at 28 and 56 days in summer and winter, using consistent preparation and testing procedures. During the winter period, the surface moisture content of the test elements was higher than the 5.5% limit during the morning due to morning condensation. Therefore, the moisture readings were taken regularly until the moisture level fell below the limit (around midday) before any torrent measurement was taken.

Rainfall data from Meteostat and UCT Geological Sciences was collected for the entire curing and testing period to observe weather patterns. Detailed information can be found in Appendix C.2.

3.6.5. Summary of the DI test program

Table 3-9Testing schedule for the durability index measurements.

Test performed	Testing events*	Number of determinations	Number of tests
OPI	4	4	20
Surface moisture	4	18**	20
Resistivity	4	18**	20
TPT	4	9**	20

** The testing events involve two testing ages (28 and 56 days) in the winter and summer.*

*** Includes the measurements on the test panels and median barriers.*

3.7. Data Processing and Analysis

3.7.1. Processing of OPI results

The OPI test data were recorded on the data logging unit. The information was transferred to the DI calculation spreadsheets in Microsoft Excel software. Bar charts and scatter plots were generated to depict the patterns and trends of the data.

3.7.2. Processing of TPT data

The measured Torrent values were captured on the Permea-Torr device and later transferred onto the TPT recording sheets. A sample of the data recording sheets can be found in Appendix D.1. Microsoft Excel software was used to enter the recorded data and perform calculations of the permeability coefficients (kT) as outlined in the Swiss standard. Bar charts and scatter plots were also generated to present the data for trend analysis.

3.7.3. Treatment of data outliers

Caution was taken to identify outliers in the gas-permeability data obtained. Neves et al. (2012) report that gas permeability measurements are prone to large variability due to microstructural defects, which can inflate results by up to ten times. Due to the expected variabilities and small dataset used in the study, all the determinations were retained to observe the extent of variabilities in the data.

3.8. Statistical analysis

This study employed different statistical methods to analyse the observed trends in the results. Inferential statistics enable the use of sample data to draw conclusions about the broader population from which the sample was drawn. Hypothesis tests such as the t-test and analysis of

variance (ANOVA) are commonly used to analyse differences between groups that assume normality (data points cluster around the mean value). Non-parametric tests are used where the data does not follow a normal distribution.

The differences in compressive strength results were analysed using the t-test and ANOVA. The *kOPI* and *kT* data were analysed using non-parametric tests, particularly the Mann Whitney/U-test, Wilcoxon-signed rank, and Kruskal Wallis tests. This is because the coefficients of permeability are logarithmic, which tends to skew the data's distribution (Neves, Branco & De Brito, 2012; Nganga, 2012; Torrent, Neves & Imamoto, 2022b). Non-parametric tests assume no particular data distribution, making them a robust alternative applicable to a wider range of data types.

A correlation test was also carried out to analyse the strength of the relationship between the OPI and TPT results. The statistical methods used in the study are briefly described as follows.

3.8.1. t-test

The t-test measures the differences between the sample means of the two groups. The test assumes that the data is normally distributed, independent, and of similar variance (Bevans, 2022). Three main types of t-tests are commonly used in hypothesis testing: paired samples, independent samples, and one-sample tests. The paired-sample test compares the means of data groups from the same population. For instance, this study compared permeability values of the same panels at 28 and 56 days.

The independent-samples t-test evaluates the means of two separate groups of data. The environmental exposure (summer vs winter) and w/c ratio (0.5 vs 0.6) variables were investigated using the independent samples t-test. The evaluations were based on the null hypothesis that the sample means were equal. Further description and calculations of the test are provided in Appendix B.4.1.

3.8.2. ANOVA test

The ANOVA checks the statistical significance among three or more groups in a data population. The test is an extension of the t-test on independent samples. A one-way ANOVA was carried out to compare the means of the compressive strength test results based on the different binder types. It was hypothesised that the means were the same regarding the different binder types. The DATAtab software tool was used to compute the ANOVA tests.

3.8.3. Mann-Whitney / U-test

The U-test is the non-parametric equivalent of the t-test for independent samples. The test checks the rank sum difference of the samples instead of analysing the means of the samples (Bernstein & Bernstein, 1999). The rank sum is calculated by sorting the data from the smallest to the largest recorded value. The smallest value is given the first rank, and the ranks are assigned in ascending order. The sum of the ranks in each group is taken and denoted by T_1 and T_2. Next, a U-value is calculated from the rank sums using equation (3-1) and taken as the smaller value of the calculated U-values. An expected value of U and a standard error is then calculated and used to

obtain a z value. Finally, a p-value is determined from the reference tables and evaluated against the z-value. If the p-value is less than the significance level of 0.05, the null hypothesis that the rank sums of the two groups are not different is accepted. The U-test was conducted on the *kOPI* and *kT* results to analyse the environmental exposure and w/c ratio variables.

$$U_{1,2} = n_1 \cdot n_2 + \frac{n_1(n_1+1)}{2} - T_{1,2} \qquad (3\text{-}1)$$

$n_{1,2}$ = number of group elements
$T_{1,2}$ = sum of the ranks in each group

3.8.4. Wilcoxon-signed rank test

The Wilcoxon test examines the difference between paired samples, much like the t-test for dependent samples. However, the test does not assume normality of the data but evaluates both the sign and ranks of the values in the sample groups. The null hypothesis is that the medians of the two dependent samples are equal. The present study used the Wilcoxon-signed rank and U-test to infer the differences in the *kT* and *kOPI* values at 28 and 56 days.

The Wilcoxon-signed rank calculates the difference between the paired samples and takes the absolute values of the differences in ranked order from the smallest to the largest. The sums of the positive and negative ranks are taken as W+ and W-, respectively (Bernstein & Bernstein, 1999). The sum with the smaller value is taken as the test statistic W, and reference tables are used to obtain the critical value of W at a 0.05 significance level.

3.8.5. Kruskal Wallis test

The Kruskal Wallis test checks the statistical significance between several non-dependent groups (DATAtab, 2023a). It follows on from the U-test and uses a similar procedure for ranking and obtaining the rank sums of the groups. The null hypothesis speculates that the independent samples have identical medians and are from the same population. The test statistic uses a sum of squares, in this case, the sum of squares of the ranks.

The test statistic, H, is given by;

$$H = \frac{12}{N(N+1)} \sum_{i=1}^{k} \left(\frac{R_i^2}{n_i} \right) - 3(N+1) \qquad (3\text{-}2)$$

where k = number of groups
n = number of observations in a group
R = group rank sum
N = sample size / total number of observations

H corresponds to the chi-square at (k-1) degrees of freedom; therefore, the chi-square distribution table (see Appendix B.7) is used to obtain the critical value for the test and compared to the H-value. The H-test was employed to test the statistical significance of the differences between the binder types used in the study.

3.8.6. Correlational analysis

One of the study aims was to investigate the relationship between the OPI and TPT methods based on field measurements. A correlation test assessed the relationship between the two methods without assuming causality. Due to the nature of the gas permeability data distribution, the Spearman rank correlation test was chosen, as it uses data ranks rather than raw values, making it a non-parametric alternative to Pearson's correlation (Lachenicht, 2013; Bhandari, 2022). First, a rank is assigned to each value of the tested samples from the smallest to the largest. Then, the assigned ranks from each data group are plotted against each other to distribute the data evenly and calculate the Pearson's correlation coefficient of the ranks, r_s (DATAtab, 2023b). The strength of the correlation is interpreted using Table 3-10.

Table 3-10 Interpretation of strength of correlation (adapted from DATAtab, 2023b)

Correlation coefficient	Strength of correlation
0 < 0.1	No correlation
0.1 < 0.3	Low correlation
0.3 < 0.5	Fair correlation
0.5 < 0.7	High correlation
0.7 < 1.0	Very high correlation

This study computed the correlation analysis using Microsoft Excel and DATAtab software. The significance of the correlation coefficient was assessed using the p-value at a 0.05 significance level to determine if the correlation differed significantly from zero.

3.9. Methodological limitations

The methodological limitations that were encountered are presented in this section.

3.9.1. Range of data set

The study focused on commonly used concrete mixes in South Africa. Therefore, the dataset generated did not evaluate an extensive range of binders, especially those with supplementary cementitious materials (SCMs).

The manufactured RC elements and test panels were aimed at simulating best concrete practices; thus, the sensitivity of the test methods to 'poor concrete' quality could not be investigated in-depth. Nevertheless, the data collected in the experimental program was still useful in providing valuable insights towards using NDT methods in the SADIA for durability assessment and quality control on site.

3.9.2. Sampling of test area and measurement points

The selected measurement points were limited to the sun-facing side of the test elements, as described in section 3.5.4. The decision meant that the effect of orientation could not be assessed. The test face was kept consistent for both the summer and periods. A micro-analysis of OPI

samples from sun-facing and non-facing sides was conducted. However, due to the small dataset, no inferences could be drawn.

3.10. Summary

This chapter described the experimental design and methods applied in the study. First, the five mix designs used in the experimental program were discussed, describing the material constituents, mix proportions, and procedures followed in constructing the test elements. Next, the experimental tests were presented, focusing on the OPI and the Torrent permeability tests. The experiments investigated the sensitivity of the gas permeability test methods to variables such as the w/c ratio, binder type, testing age, and environmental exposure. The strategies adopted in executing the tests were detailed, and justification was given for each instance. Lastly, the data processing techniques and statistical analysis tools utilised in the study were also discussed.

4. ANALYSIS AND DISCUSSION OF RESULTS

4.1. Introduction

This chapter presents the results of the experimental programme. The results of the OPI test and the TPT method are analysed and discussed based on the sensitivity of the two methods to the experimental variables, which included w/c ratio, binder type, environmental exposure, and concrete age. The outcomes from this chapter aim to answer how a joint durability assessment using the OPI and Torrent test method can be implemented on-site.

Name designations were assigned to the concrete mixes for easy reference. Three binders were chosen: CEM I 52.5N, CEM II/A-L 52.5N, and FA (70% CEM I 52.5N + 30% fly ash). The binders were used to prepare five mixes, namely a 30 MPa and 40 MPa CEM I 52.5N mix, a 30 MPa and 40 MPa CEM II/A-L 52.5N mix, and a blended mix consisting of 70% CEM I 52.5N and 30% fly ash of 30 MPa grade. Table 4-1 summarises the nomenclature used for the mixes.

Table 4-1 Concrete mix design nomenclature.

Description	Mix Designs				
	Mix 1	**Mix 2**	**Mix 3**	**Mix 4**	**Mix 5**
Binder	CEM I 52.5N	CEM II/A-L 52.5N	CEM I 52.5N	CEM II/A-L 52.5N	70% CEM I 52.5N + 30% FA
Concrete grade	40 MPa	40 MPa	30 MPa	30 MPa	30 MPa
Mix designation	40-PC-I	40-PC-II	30-PC-I	30-PC-II	30-FA

4.1.1. Statistical analysis methods used

Table 4-2 shows an overview of the statistical analysis methods applied in this study. The methods have been described in section 3.8 and Appendix B.4

Table 4-2 Statistical methods applied in the study.

Statistical test	Parameter	Variable
Parametric tests		
t-test	Compressive strength	concrete age, environmental exposure, w/c ratio
ANOVA	Compressive strength	Binder type
Non-parametric tests		
Mann Whitney/U-test	*kOPI, kT*	environmental exposure, w/c ratio
Wilcoxon signed rank	*kOPI, kT*	Concrete age
Kruskal Wallis	*kOPI, kT*	Binder type

4.2. Compressive strength

Figure 4-1 shows the compressive strength data (mean value obtained from three cubes) of the mixes taken at 28 days in the summer and winter.

4.2.1. Effect of experimental variables on compressive strength

The average compressive strengths across all mixes in both testing periods were higher than the design characteristic strengths specified for this study (i.e. 30 MPa and 40 MPa). All mixes exhibited the highest strength gain in the first three days of curing, with the higher 40 MPa mixes averaging more than 70% of their final strength. The compressive strength development over 3, 7, and 28 days is summarised in Appendix C.1.

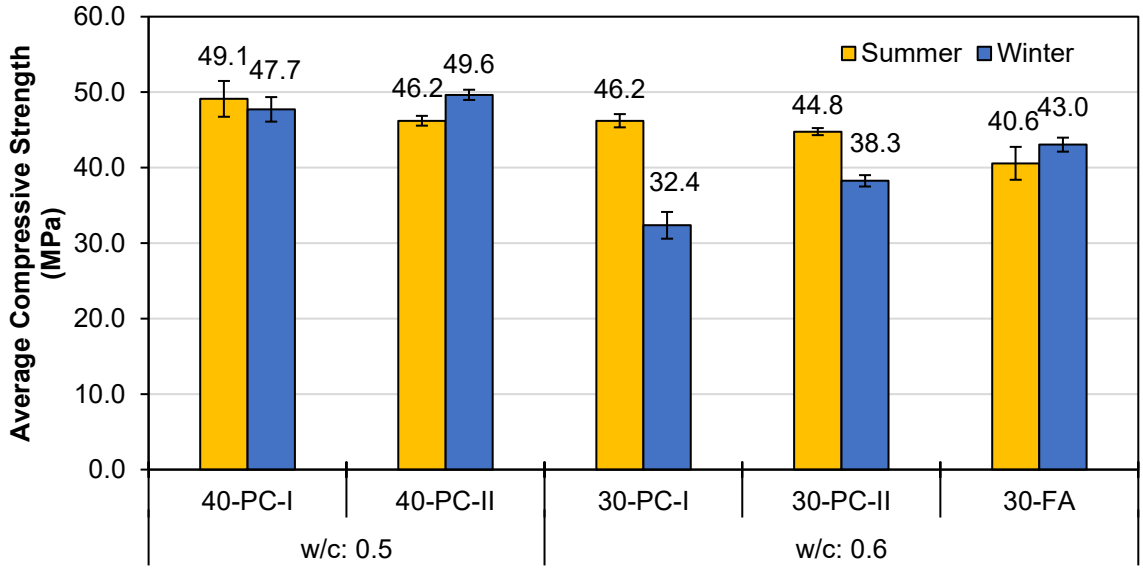

Figure 4-1 Compressive strength results at 28 days (error bars represent standard deviation).

The following analysis focuses on the effect of the w/c ratio, binder type, and testing period on the compressive strength results. A summary of the statistical analysis of the variables is presented in Appendix B.4.2.

As expected, the 0.5 w/c ratio mixes had higher strength, regardless of the binder type or the testing period. This trend is attributed to higher w/c ratios (0.6) having less dense cement matrices, inhibiting hydration product interaction to contribute to strength gain.

The 30-PC-I and 30-PC-II mixes had surprisingly low strength values in winter, likely due to batching variations (to compensate for cold weather and wet aggregates) and uncontrolled retempering of the mixes.

The strength results were influenced by seasonal temperatures, with the 40-PC-I, 30-PC-I, and 30-PC-II mixes exhibiting lower strength in winter. The effect can be explained by lower casting temperatures in winter slowing down the hydration process. However, the differences observed

were statistically insignificant, indicating the benefit of controlled curing temperatures in the curing tanks.

4.3. South African Durability Index (DI) test results

This section reports the findings from the OPI test, particularly the sensitivity of the OPI test to the w/c ratio, binder type, environmental exposure, and concrete age. The OPI tests were conducted on specimens extracted from the representative test panels as described in section 3.6.3.1.

4.3.1. Overview of OPI test results

The minimum OPI requirements for concrete structures exposed to carbonation-induced corrosion may be generalised as follows (COTO, 2020b):

- **OPI_{min} = 9.65 ($kOPI_{max}$ = 2.2 x 10^{-10} m/s);** recommended minimum cover depth = 40 mm; for moderate to severe exposure conditions XC3 – XC4.
- **OPI_{min} = 9.40 ($kOPI_{max}$ = 4.0 x 10^{-10} m/s);** recommended minimum cover depth = 40 mm; for moderate exposure conditions XC2.

The OPI values are derived from the logarithmic transformation of *kOPI* for practical use, as described in section 2.5.1.2. OPI values were calculated as the arithmetic mean of four determinations per mix. *kOPI* values were calculated as the geometric mean for direct comparison with Torrent *kT* values. The geometric mean minimises the effect of outliers, providing a more accurate representation of the central tendency for data that is not normally distributed.

Figure 4-2 and Figure 4-3 show that the permeability characteristics of all the concrete elements would be deemed acceptable for severe carbonation exposure classes (XC3 and XC4), indicating a generally low penetrability of the concrete with high resistance to the ingress of gases through permeation.

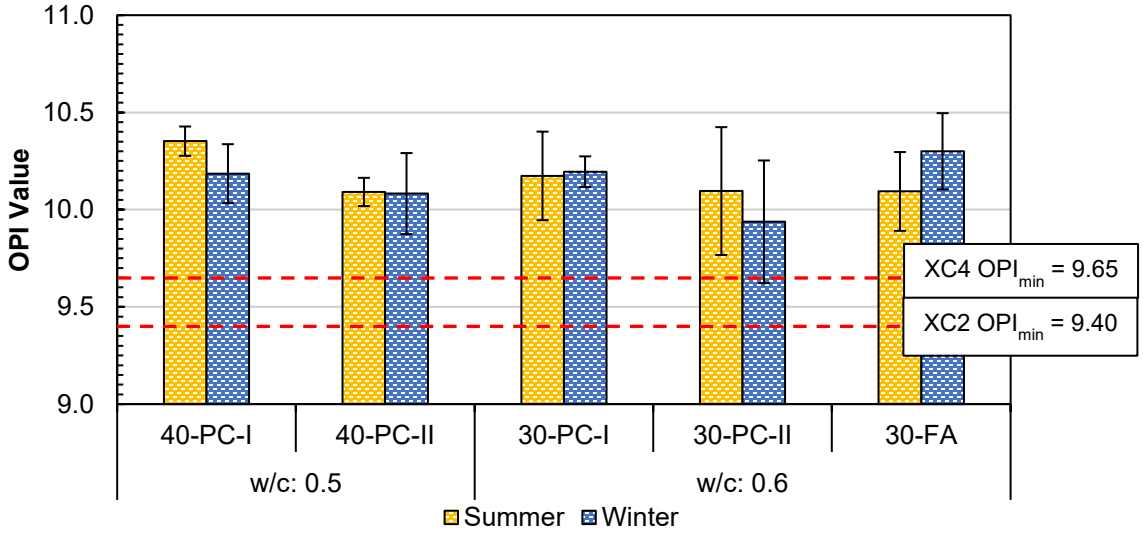

Figure 4-2 Overview of OPI experimental results at 28 days (error bars represent standard deviation).

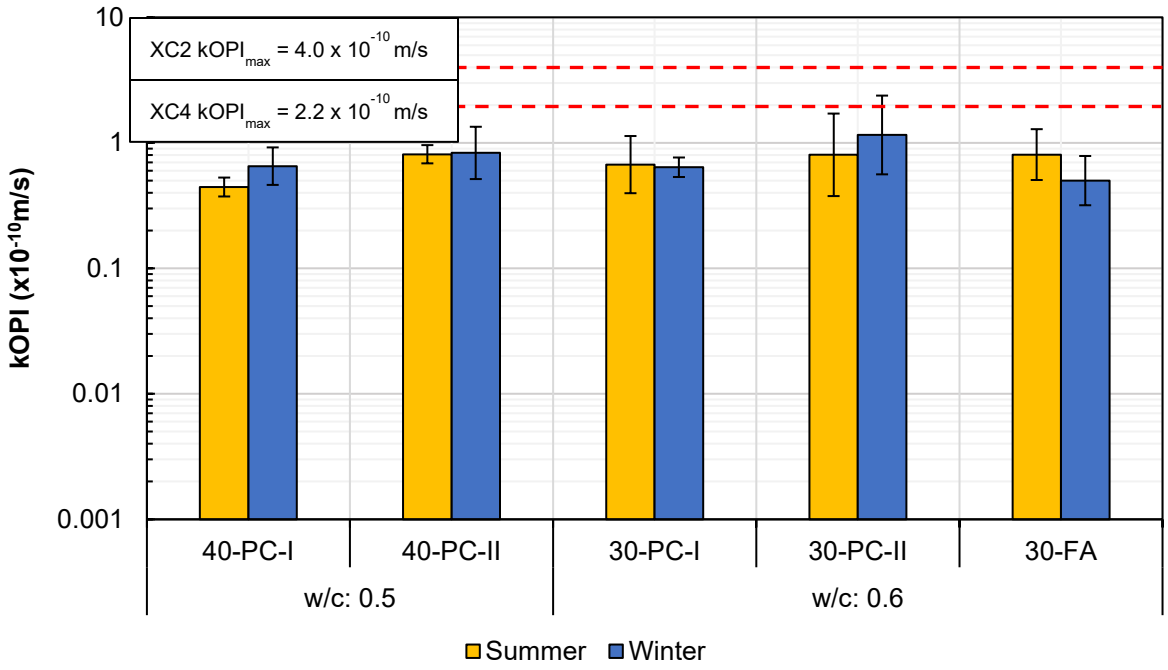

Figure 4-3 Overview of oxygen permeability coefficient results (kOPI) at 28 days (error bars represent geometric standard deviation).

Table 4-3 Numerical summaries of the OPI results at 28 days.

Mix	OPI_{Mean} (log scale)	Minimum	Maximum	Standard Deviation	CoV (%)
SUMMER					
40-PC-I	10.35	10.28	10.39	0.08	0.7
40-PC-II	10.09	10.07	10.19	0.07	0.7
30-PC-I	10.17	9.95	10.39	0.23	2.2
30-PC-II	10.10	9.89	10.40	0.33	3.3
30-FA	10.09	9.85	10.28	0.20	2.0
WINTER					
40-PC-I	10.19	9.96	10.28	0.15	1.5
40-PC-II	10.08	9.79	10.27	0.21	2.1
30-PC-I	10.20	10.10	10.26	0.08	0.8
30-PC-II	9.94	9.56	10.24	0.32	3.2
30-FA	10.30	10.03	10.45	0.20	1.9

The OPI values ranged between 9.9 (1.7 x 10^{-10} m/s) and 10.4 (0.5 x 10^{-10} m/s), falling between the good to excellent durability class. Recall that the higher the OPI or lower the *kOPI* value, the lower the permeability.

The coefficient of variability in the OPI values ranged between 0.7% - 3.3% at 28 days (Table 4-3). Reported repeatability and reproducibility values by Gouws et al. (2001), Stanish et al. (2006), Nganga et al. (2017), and the DI manual for site and ready-mix concrete data range between 1.0% - 3.0%. The OPI results from this study generally fall within the acceptable CoV

ranges in literature, except for the 30-PC-II mix, which had a slightly higher CoV than 3%. The *kOPI* values had high variability (see Appendix C.3) due to the dispersion of raw permeability values. The higher CoVs can be associated with the sensitivity of the test method to material variability, handling of the concrete onsite, and specimen preparation.

Hereafter, the analysis of the OPI test results relates to the *kOPI*, which will be used to analyse its association with *kT*. The *kOPI* values are the untransformed permeability coefficients, thus allow direct comparison with the Torrent *kT* values. Detailed test results, including the log-transformed OPI data, are presented in Appendix C.3.

4.3.2. Influence of experimental variables on the OPI test results

w/c ratio

0.5 w/c ratio mixes exhibited lower *kOPI* values than the 0.6 mixes, as seen in Figure 4-3. However, the difference in the two w/c ratio groups was found to be insignificant based on the Mann-Whitney U-test (section 3.8.3) for both the summer ($p = 0.34$) and winter ($p = 0.85$).

Binder type

Figure 4-3 shows that the PC-I mixes performed better than the PC-II mixes, regardless of the w/c ratio or the concrete grade. In the winter period, the 30-FA mix had the lowest *kOPI*. A Kruskal-Wallis test was computed to compare the differences in the binders, revealing no significant difference (Summer – $p = 0.26$; Winter – $p = 0.06$). Summarised tables showing the data from the statistical analysis are presented in Appendix B.7.1.

Environmental exposure

The *kOPI* recorded in the summer and winter were compared to observe the influence of natural exposure on the permeability of the concrete mixes. A curing compound was applied to the concrete elements in both periods to minimize early-age moisture loss. The summer data had lower kOPI values than the winter group except for the 30-PC-I and 30-FA mixes, but a Mann-Whitney test showed no significant differences between the two data sets ($U = 185$; $n1 = 20$, $n2 = 20$; $p = 0.69$). The concrete elements were exposed to 9.7 mm of rainfall in summer and 34 mm in winter during the respective 28-day curing periods and brief periods of wet coring during sample preparation. There was a 9°C difference between the average site temperature in summer and winter. Details of the rainfall and temperature data recorded during the tested period are presented in Appendix C.2.

Concrete age

Figure 4-4 shows the differences between the *kOPI* values at 28 and 56 days. The permeability increased with age in summer, as observed for the 40-PC-I, 30-PC-I, and 30-PC-II mixes. In winter, the gas permeability generally reduced with age, albeit slightly for the 40-PC-I and 30-FA, while the 30-PC-II mix increased. Nonetheless, the *kOPI* results at the two concrete ages were

not significantly different regardless of the binder type or w/c ratio (summer – W = 104, p = 0.97; winter – W = 77; p = 0.29) based on a Wilcoxon signed-rank test.

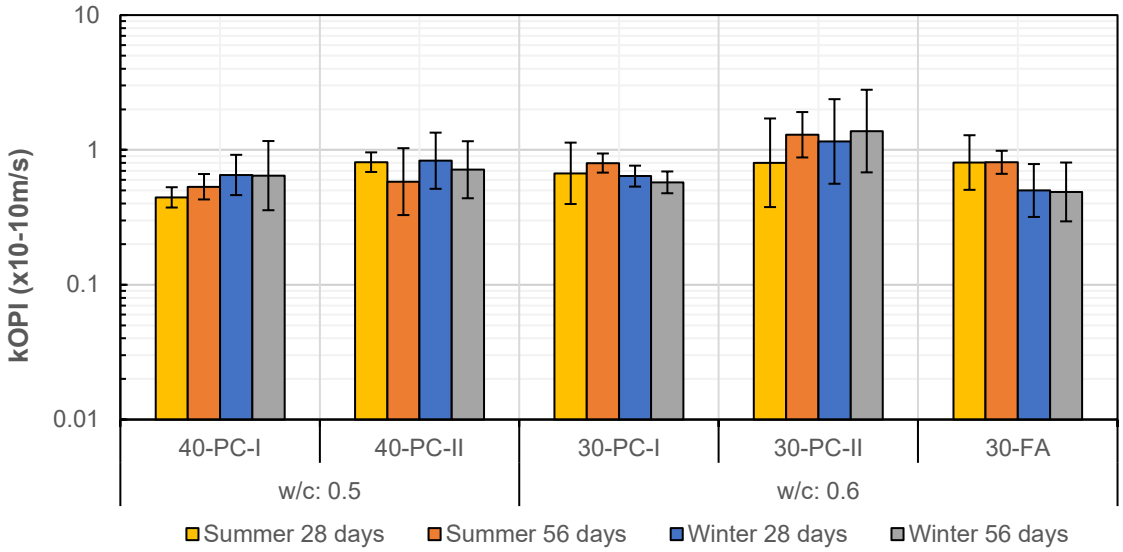

Figure 4-4 Permeability coefficients (kOPI) results at 28 and 56 days.

4.3.3. Discussion

The study compared the oxygen permeability characteristics of concrete mixes with different w/c ratios, binder types, exposure environment, and age. This section explains the findings and discusses the results' practical implications.

The results showed that the 0.5 w/c mixes had lower *kOPI* than those with a 0.6 ratio. However, the differences were statistically insignificant. This was an unexpected observation. The 0.5 mixes would be expected to have better permeability performance due to the formation of a denser microstructure with fewer capillary pores and pore interconnections. It is possible that the lack of difference between the 0.5 and 0.6 mixes was influenced by the presence of the chemical admixtures improving the pore structure in the higher w/c ratio mixes. The 0.6 mixes had a slightly higher admixture dosage than the 0.5 mixes. It can also be deduced that concrete mixes with higher w/c ratios (within prescribed specifications) can achieve similar gas permeabilities to lower w/c ratio mixes, provided they are well compacted and adequately cured.

The PC-I mixes exhibited lower gas permeability than the PC-II mixes in both testing periods. The results can be attributed to the formation of a denser C-S-H gel matrix in the CEM I mixes from the higher concentration of reactive clinker minerals. The higher clinker concentration facilitates a faster rate of hydration, promoting pore filling at early ages, thus leading to lower initial gas permeability. Interestingly, the 30-FA mix had the lowest gas permeability in winter. This finding might result from the pore-filling effect of the fly ash outweighing the contribution of the calcium hydroxide formation during the hydration of the other mixes. Nonetheless, the observed differences in the results were found to be insignificant through statistical analysis. It can be inferred that the gas permeability results of this study were less sensitive to the effect of binder type. Similar results were reported by Starck (2013), Dhanya (2015), Kanjee (2015), Omar (2018),

and Gilayeneh (2022), to a varying degree, but contradict findings by Bahurudeen (2014), Bustos (2015), and Zhang (2019). The discrepancies can be explained by the differences in binder types and replacement levels used in the other studies.

The environmental exposure conditions did not significantly influence the gas permeability results. Note that the effect of moisture at the time of testing was not expected to influence the *kOPI* results due to the oven drying preconditioning. During the initial curing period (7 days), very low rainfall was recorded in summer and winter (Appendix C.2), limiting the moisture available for curing. The lower permeability coefficients recorded in summer can be ascribed to increased cement hydration rates due to higher temperatures outweighing the effects of moisture loss. All the mixes still achieved low gas permeability characteristics in both periods. It is also possible that the curing compound and environmental moisture (relative humidity) influenced the gas permeability of the mixes in the initial curing period. Previous studies by Krook (1995) and Surana (2017a,b) demonstrated the benefit of curing compounds on gas permeability over air curing. The findings of this study suggest that field concrete requires supplementary curing techniques to compensate for the variations in ambient conditions that influence natural curing.

The gas permeability of the concrete mixes increased with age in summer except for the 30-FA and 40-PC-II blended mixes. The observed increase can be attributed to the drying effect in the summer, resulting in a higher number of capillary pores in the concrete. Further, the concrete elements likely experienced greater internal stresses in summer, potentially leading to the development of microcracks, particularly in the interfacial region (ITZ). The microcracking would increase internal connectivity, thus increasing the gas permeability. Conversely, the blended cements (40-PC-II and 30-FA) were less affected by drying at later ages due to pore-filling from finer particles and delayed pozzolanic reactions. The reduction in *kOPI* in winter at 56 days is likely due to favourable ambient conditions facilitating continued hydration and reducing pore sizes and interconnections within the microstructure. Even so, the OPI method showed the detrimental effect of handling the 30-PC-II mix discussed in section 4.2.1. Statistical analysis indicated that the gas permeability results at 28 and 56 days were not significantly different. It can be inferred that concrete age has an appreciable effect on gas permeability, due to the curing conditions and type of cement. The findings from this study agree with the results of Kropp (1995) and Starck (2013).

4.3.4. Summary and practical implications

The OPI test method showed sensitivity to the experimental variables (w/c ratio, binder type, exposure environment, and age). However, the observed differences in the results for each variable were statistically insignificant. The lack of significant difference can be linked to the generally good control of concreting procedures at the pre-cast site in using ready-mix concretes and curing compounds to supplement the natural curing. Several practical implications can be deduced from the outcomes of the OPI investigations in this study.

The OPI method demonstrated that concrete mixes with higher w/c ratio and lower grades, within applicable levels, can exhibit good gas permeability characteristics, provided that effective on-site quality control is implemented. This highlights the importance of ensuring proper compaction and

adequate curing methods to achieve good concrete quality. The results also suggested that chemical admixtures may benefit the microstructure of concrete. However, this benefit is thought to be highly dependant on the type and dosage of admixture used.

Using SCMs such as FA can potentially improve the long-term durability of concrete by reducing gas permeability due to the dilution effect. However, it is crucial to assess the impact of SCMs on the specific deterioration mechanisms in the concrete's environment. Studies have shown that FA particles (in high calcium fly ash) can also create additional nucleation sites for CO_2 absorption, leading to faster carbonation rates. Factors such as FA type, fineness, and replacement level should be carefully considered as potential means to counteract the adverse effects of increased carbonation.

4.4. Swiss Torrent test results

This section presents the findings from data obtained from the Torrent test method. The Torrent tests were conducted on the same representative test panels as the OPI test and the median barriers, which served as the as-built structural elements (section 3.5.2).

4.4.1. Overview of Torrent results

Under the Swiss standard SIA 262/1 (2019), recommendations for structures designed to resist carbonation-induced corrosion are summarised as follows:

- $\boldsymbol{kT_{i,min} = 2 \times 10^{-16}\ m^2}$ for severe carbonation exposure environment XC4. Exposure conditions XC1-XC3 do not have a specified *kT* limiting value.

The *kT* values were taken as the geometric mean of all the determinations for each mix. The lowest mean *kT* value on the test panels and the barriers was 0.006×10^{-16} m^2 (winter). The highest recorded *kT* measurement (summer) was 0.469×10^{-16} m^2 and 0.377×10^{-16} m^2 on the panels and barriers, respectively. Figure 4-5 and Figure 4-6 show that all the concrete elements would be acceptable for the most severe carbonation exposure class (XC4), ranging between 'Very Low' to 'moderate' permeability characteristics (Table 4-4).

Table 4-4 Torrent permeability classes (adapted from Torrent et al. (2022).

kT value (10^{-16} m^2)	Permeability class	
< 0.001	PK0	Negligible
0.001 – 0.01	PK1	Very low
0.01 – 0.1	PK2	Low
0.1 – 1.0	PK3	Moderate
1.0 - 10	PK4	High
10 - 100	PK5	Very high
> 100	PK6	Ultra-high

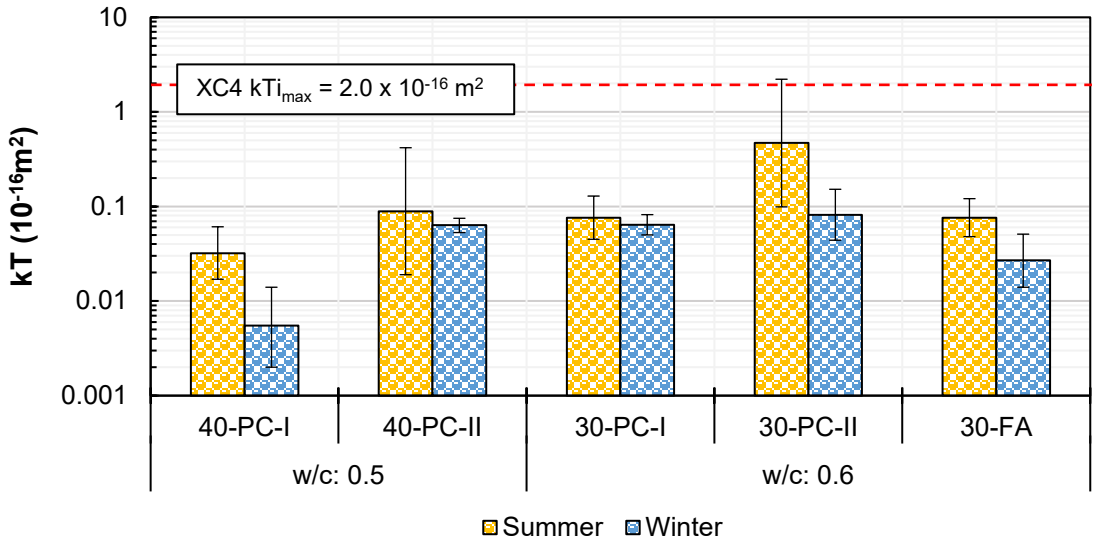

Figure 4-5 Overview of the Torrent permeability (kT) results obtained from the test panels at 28 days (error bars represent geometric standard deviation).

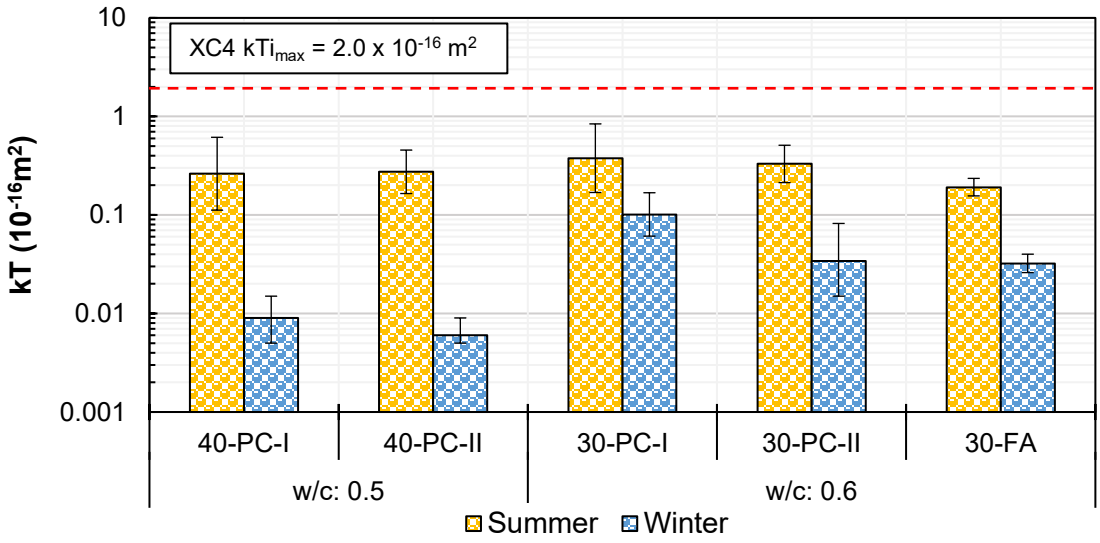

Figure 4-6 Overview of the Torrent permeability (kT) results obtained from the median barriers at 28 days (error bars represent geometric standard deviation).

The scatter of the *kT* data was generally within the range of variability data reported by Jacobs et al. (2009) and SIA 262/1 (2019). Table 4-5 shows the distribution of variability in Jacob's study, represented by the standard deviation of the logarithms of *kT* measurements (sLOG/geometric standard deviation) obtained on 52 structures (Torrent, Neves & Imamoto, 2022b). The sLOG for the test panels ranged between 0.03 and 0.68, while the variability of *kT* data from the median barriers ranged between 0.09 and 0.38 from the complete data set. An overview of the *kT* numerical summaries at 28 days is presented in Table 4-6. Further details on the *kT* variability can be found in Appendix C.4.

Table 4-5 Site variability of kT measurements (Jacobs et al., 2009).

Concrete source	sLOG (x10^{-16}m^2)		
	Minimum	Maximum	Average
Site data	0.09	1.13	0.43

Table 4-6 Variability (based on geometric standard deviation/sLOG) of kT results at 28 days.

Mix	Minimum (x10^{-16} m^2)	Maximum (x10^{-16} m^2)	kT_{gm} (x10^{-16} m^2)	sLOG (x10^{-16} m^2)	Minimum (x10^{-16} m^2)	Maximum (x10^{-16} m^2)	kT_{gm} (x10^{-16} m^2)	sLOG (x10^{-16} m^2)
SUMMER	TEST PANELS				BARRIERS			
40-PC-I	0.017	0.062	0.032	0.281	0.099	1.100	0.262	0.370
40-PC-II	0.035	0.530	0.089	0.671	0.160	0.540	0.275	0.220
30-PC-I	0.054	0.140	0.076	0.230	0.110	1.200	0.377	0.348
30-PC-II	0.078	1.200	0.469	0.675	0.180	0.620	0.330	0.190
30-FA	0.045	0.110	0.076	0.202	0.160	0.280	0.191	0.089
WINTER								
40-PC-I	0.002	0.014	0.006	0.393	0.003	0.016	0.009	0.241
40-PC-II	0.056	0.077	0.063	0.074	0.004	0.009	0.006	0.146
30-PC-I	0.049	0.079	0.064	0.106	0.058	0.200	0.101	0.220
30-PC-II	0.041	0.140	0.081	0.272	0.012	0.160	0.034	0.375
30-FA	0.013	0.044	0.027	0.279	0.022	0.039	0.032	0.093

4.4.2. Sensitivity of Torrent test to experimental variables

w/c ratio

The concrete mixes with a lower w/c ratio (0.5) had lower kT values than the 0.6 w/c ratio for both the panels and the barriers, irrespective of the season. Statistical analysis using the Mann-Whitney U-test revealed that the difference between the 0.5 w/c ratio and the 0.6 ratio mixes was significant for the summer test panels ($U = 10$, $p = 0.05$) and winter barriers ($U = 1.5$, $p = < 0.001$). This contrasted with the OPI results, which showed no statistical difference between the two w/c ratios.

Binder type

PC-I mixes had lower *kT* than PC-II mixes and 30-FA. The PC-II mixes had a larger scatter than the PC-I and FA mixes, particularly for the summer test panels. The results for the barriers were less distinguishable between binder types in summer. Overall, no clear distinction between the three binder types was detected for either the panels or the barriers, regardless of the environmental exposure. A Kruskal-Wallis test analysis showed no statistical difference between the binder types used (panels: summer – $p = 0.35$, winter – $p = 0.09$; barriers: summer – $p = 0.22$, winter – $p = 0.17$). Further details on the statistical analysis are presented in Appendix B.7.2.

Environmental exposure

The effect of curing conditions was analysed by comparing the summer and winter *kT* results. The test panels and barriers were oriented in a northeasterly direction where the test faces would be exposed to most of the sunlight. At 28 days, the panels were transferred to the UCT site to enable extraction of cores for the OPI tests. The panels were exposed to rainfall at the UCT site before any measurements were taken due to the limitations described in section 3.6.3.1. The summer data had slightly higher *kT* values than the winter results on the test panels. In contrast, a more notable difference in *kT* results was observed for the barriers. A U-test analysis showed a statistically significant difference between the summer and winter *kT* data for barriers but no difference for the panels. The effect of surface moisture content at the time of testing was also investigated to analyse the difference between exposure conditions further.

Concrete age

Figure 4-7 and Figure 4-8 show how the concrete age affects *kT* results for the panels and barriers. *kT* generally decreased between 28 and 56 days, except for the summer *kT* on the test panels. A Wilcoxon rank sum test found significant differences in the *kT* results between the two testing ages despite contrasting observations from the panels' summer *kT* results.

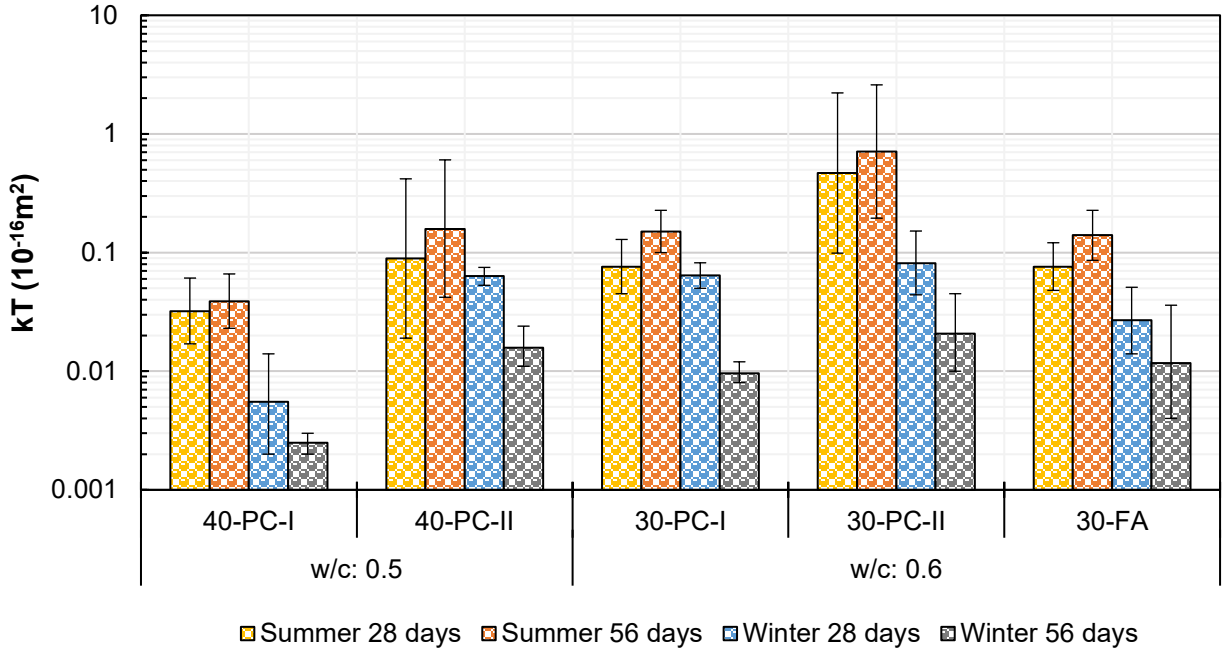

Figure 4-7 Effect of concrete age on Torrent (kT) results (test panels).

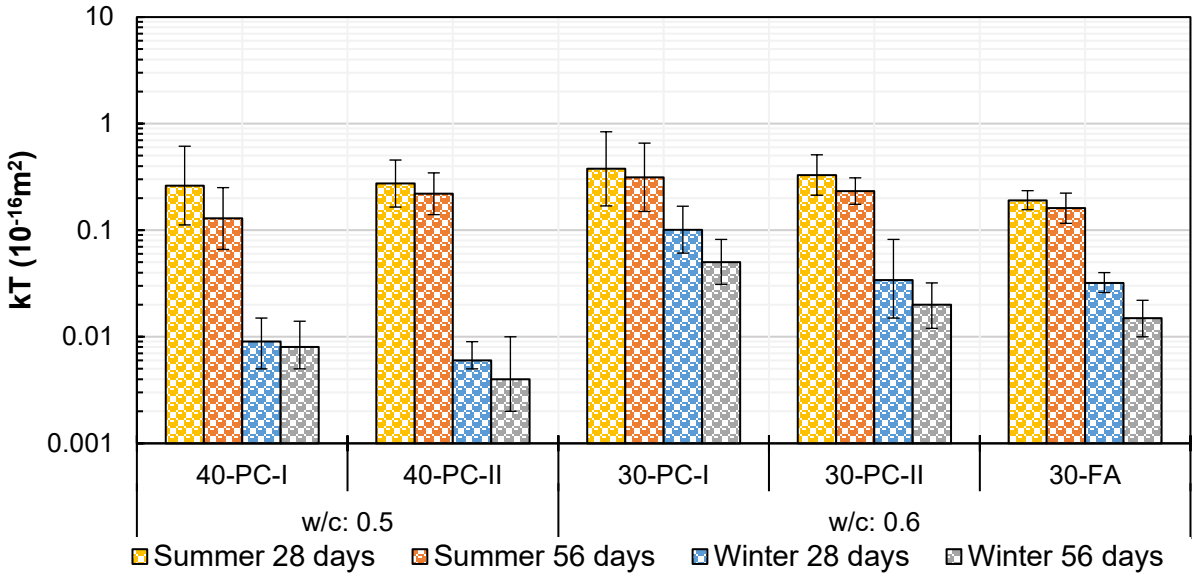

Figure 4-8 Effect of concrete age on Torrent (kT) results (barriers).

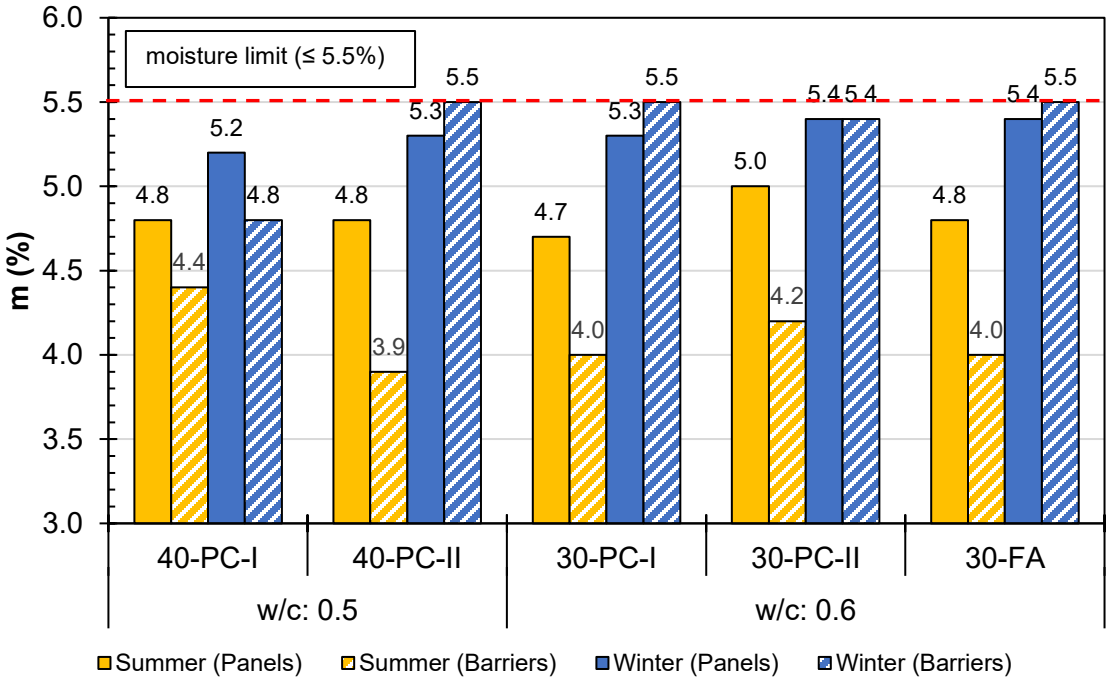

Figure 4-9 Overview of surface moisture content results taken at 28 days on the test panels and the barriers.

4.4.3. Analysis of moisture content

The surface moisture content was measured to ensure it did not exceed 5.5% during testing. The highest recorded surface moisture content per test element was taken as the moisture value as per the user manual. Figure 4-9 displays the moisture values during testing, ranging between

3.5% and 5.5%. The winter results were less distinguishable between the panels and barriers but markedly higher than in the summer. During summer, the rewetting of the panels at the UCT site possibly influenced the higher surface moisture on the panels compared to the barriers. The test elements with surface moisture values exceeding 5.5% were monitored until the levels were ≤ 5.5%. Air permeability measurements were taken only after the permissible levels were recorded. The complete dataset of the surface moisture determinations is presented in Appendix C.5.

4.4.3.1. Correlation between moisture content and measured kT

Both test panels and barriers showed a complex, non-linear relationship between moisture content and *kT* (Figure 4-10 and Figure 4-11). There was a scatter in the moisture values of the panels and a more clustered distribution for the panels. While *kT* consistently increased as concrete dried, there seemed to be no apparent connection between moisture content and *kT* during winter months when viewed independently. It was also observed that a higher surface moisture content did not always translate to less penetration depth of the test (Appendix C.5.1). A Spearman's rank correlation test revealed a significant negative relationship between *kT* and surface moisture across the dataset (Table 4-7). This inference suggests that while the relationship may not be immediately apparent over shorter periods, there is a link between moisture content and air permeability in concrete over time.

Table 4-7 Summary of the moisture (m%) and kT correlation analysis (Spearman's rank correlation).

Concrete element	Sample size (N)	Spearman's rho (r)	p-value
Test panels	60	-0.57	< 0.001
Barriers	120	-0.74	< 0.001

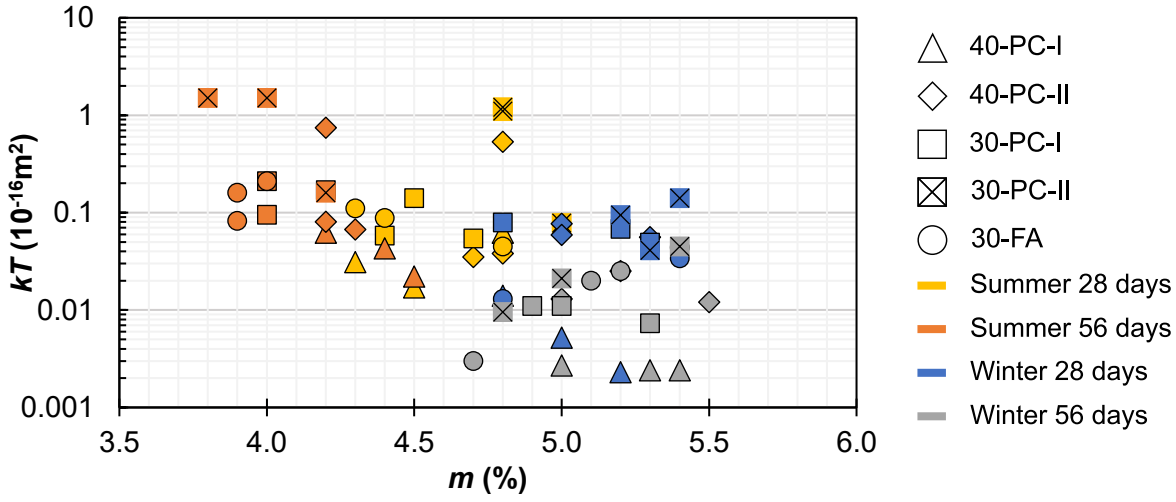

Figure 4-10 Relation between surface moisture content and kT results on the test panels (complete data sets).

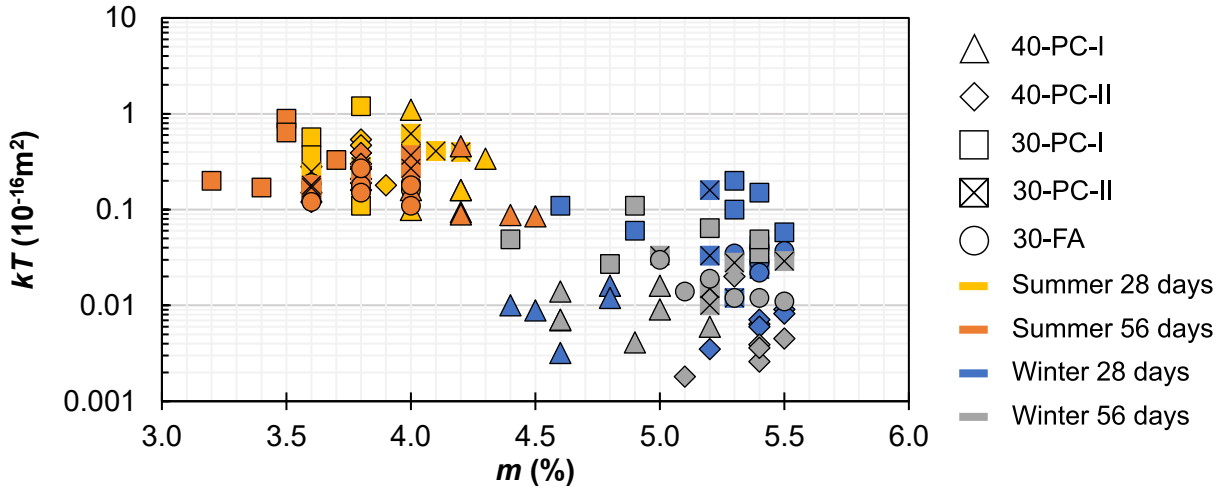

Figure 4-11 Correlation between surface moisture content and kT results on the barriers (complete data sets).

4.4.4. Comparison between test panels and median barriers

Generally, the *kT* results for the panels were lower than the *kT* for the barriers in summer, except for the 30-PC-II mix (Figure 4-12). In winter, no distinct trend was identified between the test elements. Note that only three measurements could be taken on each test panel due to limitations in the size of the panels, while six measurements were taken on each barrier. A Spearman correlation analysis revealed no significant correlation between the panel results and the barriers (summer: r = 0.16; winter: r = -0.28).

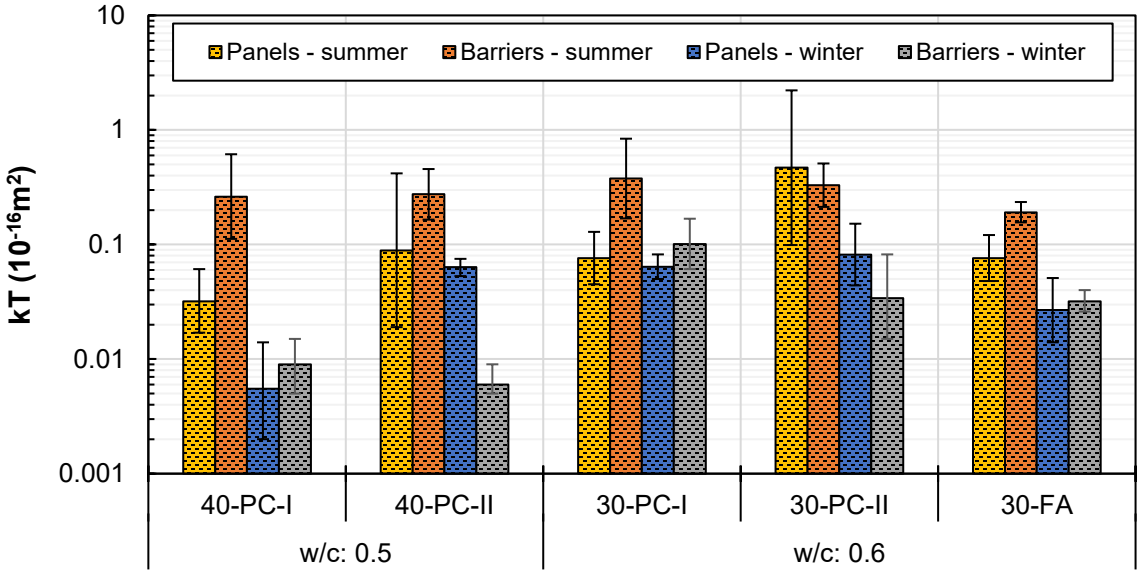

Figure 4-12 Comparison between kT results for the representative panels and the median barriers at 28 days.

4.4.5. Discussion

4.4.5.1. Sensitivity of Torrent test to the experimental variables

This section discusses the findings from the Torrent tests on the representative panels and the median barriers.

Concrete mixes with lower w/c ratio exhibited lower *kT* regardless of testing period. The difference was statistically significant for summer panels and winter barriers. These trends agree with the literature, which suggests higher w/c ratio concretes have increased capillary pore volume, size, and interconnections, leading to higher *kT* values. (Torrent, Neves & Imamoto, 2022b). Higher w/c ratios can also increase capillary suction, accelerating water loss and air permeability. Jacobs et al. (2009) reported that variations in materials, preparation, and experimental conditions, including ambient conditions, can also influence the rate of water loss and mask the impact of w/c ratio on *kT*. These disparities explain the observations of the statistical analysis for the summer panels and winter barriers. Therefore, while w/c ratio influences air permeability, other factors can mask its effect.

The air permeability characteristics of the different binder types used in the study were statistically identical. The PC-I mixes were expected to exhibit lower kT values at an early age due to faster hydration and the formation of hydration products. However, the blended cement mixes could achieve similar *kT* from the filling effect in the microstructure. The blended cement's influence is expected to become apparent at later ages, as they initially form fewer hydrates in the cement paste. Factors such as w/c ratio, moisture effect, sample size difference, and proportion in the blended cements likely influenced the observed trends for the panels and barriers. The findings seem to contradict studies by Starck (2013), Bahurudeen (2014) and various sources reported in Torrent (Torrent, Neves & Imamoto, 2022b). However, this discrepancy can be explained by the different SCMs and unconventional binders used in those studies. The current results align with findings by Glinicki (2013) and Dhanya (2015), where no clear distinction between cement types was found. Therefore, the benefits of binder choice on air permeability may depend on the proportioning of cement and replacement levels of the SCMs and the anticipated exposure conditions.

Higher *kT* was observed in summer for both test panels and, more significantly, in barriers. The higher *kT* values were due to higher summer temperatures leading to faster drying and increased pore openness. Additionally, higher water vapour pressure would be expected in summer, increasing the pressure of the measuring chambers and *kT* measurements. During the first 7 days after casting in summer, no rainfall was recorded, suggesting hydration development relied on initial moisture in the mixes and curing compound. Winter concrete likely benefited from initial water curing due to rainfall. The insignificant difference in panel *kT* results is likely due to the element’s exposure to rainfall in summer during transfer to the laboratory and overlapping kT ranges. The panels were air-dried in the laboratory environment before testing. The drying rate was likely slower than the rates the panels would have dried in ambient conditions. The

overlapping panel *kT* ranges can be attributed to variable surface moisture and fewer test points than median barriers.

The median barriers showed a more significant *kT* difference than panels due to winter moisture availability and surface moisture conditions at testing (see Figure 4-12). Slower drying rates due to barrier size may have influenced observed trends. The results indicate that surface moisture content appreciably affects air permeability. These findings are consistent with Starck's (2013) and Surana's (2017a) work.

Air permeability generally decreased between 28 and 56 days, with significant differences in *kT* results between the two testing ages. However, an increase in air permeability was observed in the summer *kT* results of the panels. This can be explained by the competing effects in early-age concrete drying in summer. There is reduced *kT* from hydration-induced pore refinement and increased *kT* from drying-induced pore openness. The summer panels exhibited increased gas permeability due to the dominant effect of drying over pore refinement. Additionally, the panels were kept in a laboratory environment between 28 and 56 days without exposure to any wetting from rainfall. The reduction in *kT* with age in winter appears to be strongly linked to the increased moisture availability to facilitate continued hydration and the surface moisture content during testing (from the morning condensation on the concrete surface). Statistical analysis showed that regardless of the testing period, air permeability is influenced by concrete age.

4.4.5.2. Effect of moisture content on measured kT

The surface moisture was higher in the winter due to the rainfall and morning condensation. Even so, the recommended moisture limits were achieved without requiring an extended drying period. The observed relationship between moisture content and measured *kT* (Figure 4-10 and Figure 4-11) was consistent with findings from Bueno et al. (2021). There was no distinct trend in the winter data, suggesting that the low air permeabilities obtained were not influenced by the surface moisture content alone. The measurements of penetration depth supported this observation. Higher moisture content led to deeper penetration into the concrete cover in some cases. One possible explanation for this could be the variable surface tension of the moisture within the pores and differences in the pore structure development.

Compared to the summer data, the winter results showed significantly lower permeability. This was primarily due to the continued hydration and moisture pore-blocking effect. Moisture can significantly affect the Torrent test, but the method can still distinguish the pore microstructure within recommended limits, even at high moisture content. The discrepancy in the winter data requires further investigation to understand the interaction between *kT* and moisture content.

4.4.5.3. Relationship between test panels and median barriers

The test panels had lower air permeability than the barriers, likely due to the differences in compaction effort, reinforcement in the barriers, and element size. The barriers' irregular, inclined shape hinders compaction, leading to air void formation and potentially higher porosity and air permeability. Inadequate compaction has been reported to cause insufficient water tightness,

resulting in higher porosity and pore connectivity (Torrent, Neves & Imamoto, 2022b). Thus, the resulting concrete mass may have been less homogenous in terms of compaction quality.

The reinforcement cage in the barriers may have caused concrete segregation around the bars, affecting permeability measurements. However, measurement points were selected between reinforcement spacing to minimise any obstruction to airflow into the measurement chambers.

The size difference between the test panels and the barriers likely contributed to the discrepancies between the measured *kT* values. On the one hand, a greater degree of scatter was found in the measurements for the panels, ascribed to the variable concrete quality at the selected points (top, middle, and bottom). Poorer concrete quality would be expected at the upper parts of the elements due to any uneven settling and segregation of materials. Bleed channels may have formed, increasing the pore network in these areas (Torrent, Neves & Imamoto, 2022b).

The measurement points for the barriers were generally at a fixed height, thus exhibiting less scatter. On the other hand, the different thicknesses between the panels and barriers would translate to different interactions with the exposure environment in terms of drying and rates of moisture loss. However, these parameters were not investigated in this study.

4.4.6. Summary and practical implications

The Torrent test method showed strong sensitivity to environmental exposure and concrete age. In contrast, its sensitivity to w/c ratio binder type had varying degrees of significance on the measured *kT*. The strong sensitivity to environmental exposure was linked to the concrete elements' moisture state.

Surface moisture significantly affected winter kT results. However, higher moisture did not have a pore-blocking effect in some cases, possibly due to variable surface tension and differences in the pore structure development.

The measured *kT* on the test panels and the barriers were statistically different, attributable to the disparity in size and thickness of the elements and compaction.

It could be deduced that parameters such as w/c ratio and binder type have some influence on the measured air permeability, but their influences may be challenging to isolate. Thus, to optimize concrete mix design for durability performance, the binder choice, w/c ratio, and proportioning of materials should be considered collectively.

Representative test panels for air permeability measurement can provide valuable baseline information on the penetrability of the as-built structural element; however, careful interpretation of the results is essential when measurements of the actual structure are not taken. Material consistency, concreting, and sampling are crucial for a reliable representation of the actual structure.

4.5. Relationship between *kOPI* and *kT* results

A key research question of this study was whether there is a relationship between DI results obtained with the OPI and Torrent methods on site-tested elements. Thus, the following section compares the results from the two methods.

w/c ratio

The OPI and TPT methods had similar responses to the w/c ratio. Statistical analysis indicated a distinct difference only in the *kT* summer data.

Binder type

The OPI and Torrent tests had comparable findings between the different binder types used in the study.

Environmental exposure

The OPI test yielded marginally lower coefficients of permeability in the summer compared to the winter, while the TPT had marginally higher coefficients in the summer data. Nonetheless, both methods revealed no significant difference between the exposure environments.

Concrete age

The *kT* tended to increase with concrete age in the summer, while the opposite was observed for the winter data. Interestingly, *kOPI* results at 28 and 56 days were comparable regardless of the testing period. It was inferred that the difference in *kT* was statistically significant, whilst the difference in *kOPI* was insignificant.

4.5.1. Correlation between kOPI and TPT

From a permeability classification perspective, the OPI and Torrent tests placed the concrete mixes in similar categories, as shown in Table 4-8. The 'Excellent' category for the OPI encompasses the 'Very Low – Moderate' permeability classes of the Torrent method.

Table 4-8 Comparison of kT and kOPI permeability classes based on DI results.

Binder type	Concrete age	Air permeability (TPT)		Oxygen permeability (OPI)	
		SUMMER	WINTER	SUMMER	WINTER
40-PC-I	28 days	Low	Very Low	Excellent	Excellent
	56 days	Low	Very Low	Excellent	Excellent
40-PC-II	28 days	Low	Low	Excellent	Excellent
	56 days	Moderate	Very Low	Excellent	Excellent
30-PC-I	28 days	Low	Low	Excellent	Excellent
	56 days	Moderate	Low	Excellent	Excellent

Binder type	Concrete age	Air permeability (TPT)		Oxygen permeability (OPI)	
		SUMMER	WINTER	SUMMER	WINTER
30-PC-II	28 days	Moderate	Low	Excellent	Good
	56 days	Moderate	Low	Good	Good
30-FA	28 days	Low	Low	Excellent	Excellent
	56 days	Moderate	Low	Excellent	Excellent

Figure 4-13 and Figure 4-14 show the relationship between the OPI test and the Torrent test method for the aggregated summer and winter data. It was found that a power function achieves the best fit for the presented data, yielding a high coefficient of determination in the summer (R^2 = 0.74) but a low coefficient from the winter data (R^2 = 0.14). A Spearman's correlation analysis suggested a high positive correlation r(8) = 0.57 for the summer data but a statistically insignificant relationship p = 0.08. The study of the winter data suggested a moderate correlation r(8) = 0.32 with no significant association between the *kOPI* and the *kT* values.

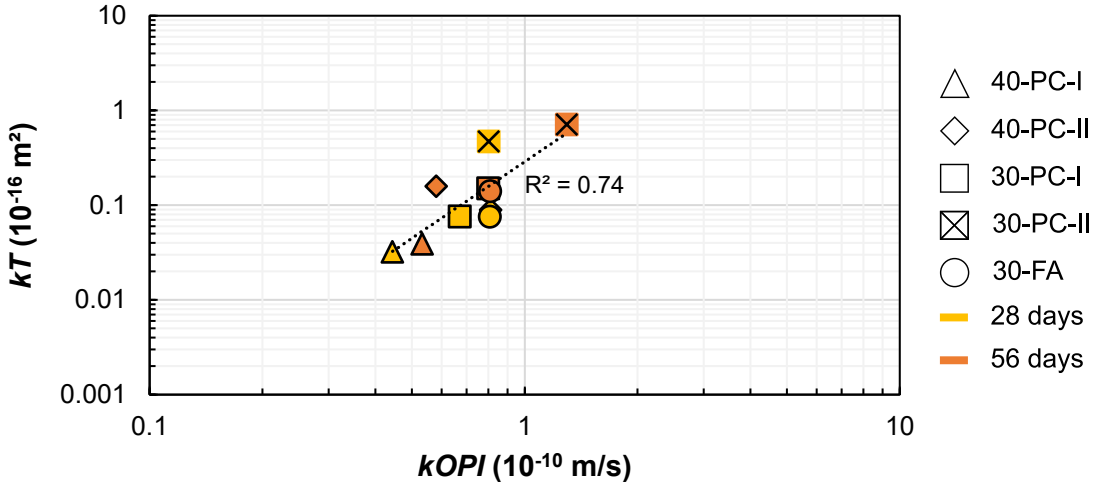

Figure 4-13 Correlation between kT and kOPI (summer data).

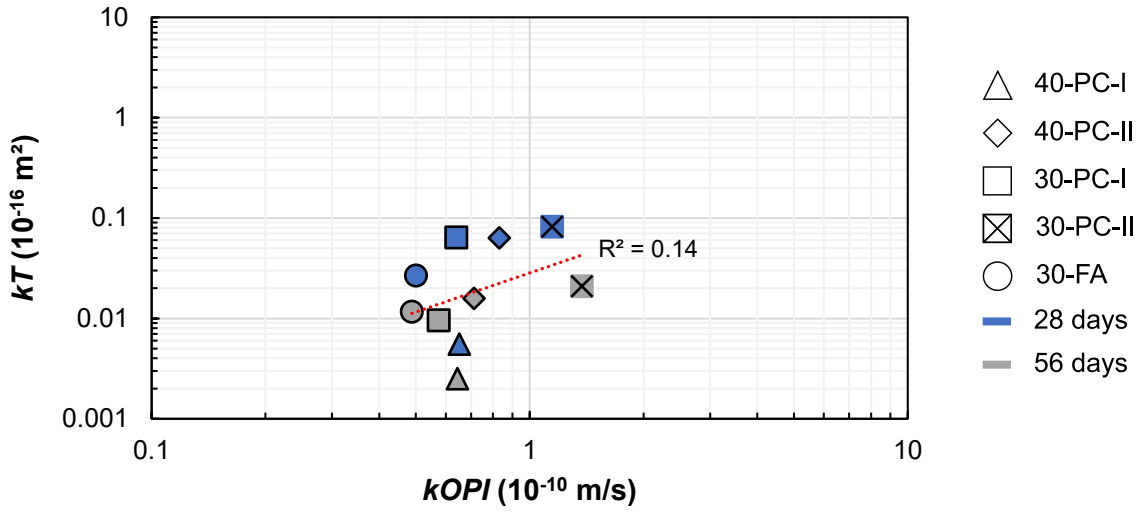

Figure 4-14 Correlation between kT and kOPI (winter data).

4.5.2. Effect of moisture correction on kOPI vs kT

A proposed moisture correction by Bueno et al. (2021) gives an adjusted *kT* value based on a reference surface moisture value (5%). This study applied the approach to analyse the correlation between *kOPI* and *kT*.

Figure 4-15 and Figure 4-16 show the effect of the moisture adjustment on the correlation between the *kOPI* and *kT* data. A downward shift was observed in the data cluster in Figure 4-15 within the range of 0.01 x 10^{-16} m^2 – 0.1 x 10^{-16} m^2, and the 30-PC-II mix at 28 days deviated from the trend. A significant change in the correlation was observed for the summer, while the winter data had a negligible change. The coefficient of determination for the summer data had a marked decrease (R^2 = 0.13), while a slight increase was detected for the winter data (R^2 = 0.16).

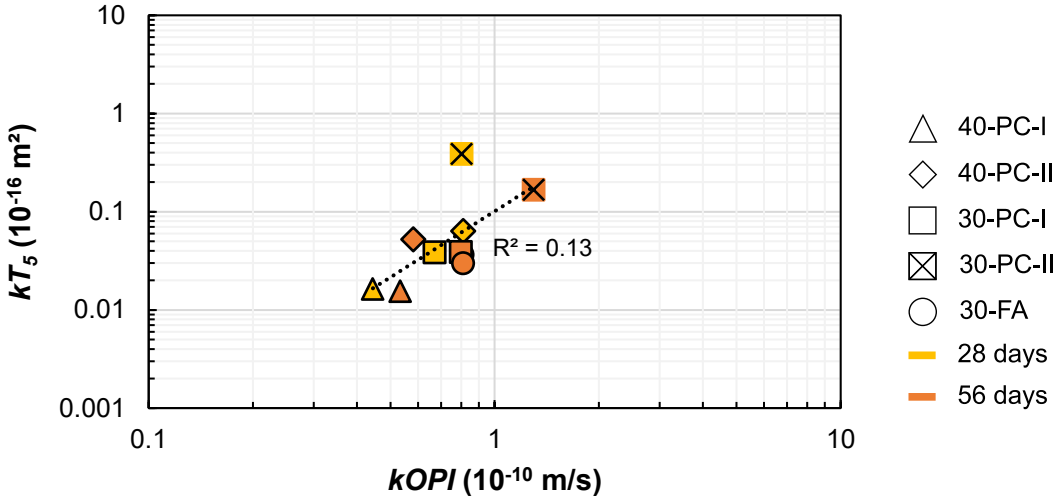

Figure 4-15 Correlation between kT_5 and kOPI (summer data).

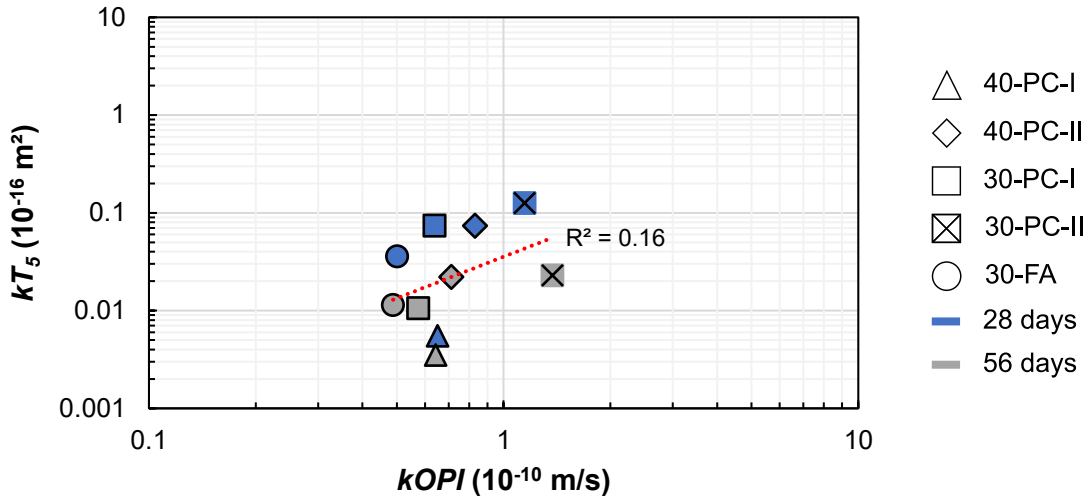

Figure 4-16 Correlation between kT_5 and kOPI (winter data).

4.5.3. Discussion

The OPI and Torrent tests generally responded similarly to the experimental variables, except for the environmental exposure and the concrete age. The differences observed can be interpreted as follows.

Both methods showed that isolating w/c ratio and binder type is a complex issue with respect to permeability. The interplay of the mix design parameters and influences from the concrete's handling, placing, and compaction can mask the influence of these variables on air or gas permeability results.

The observations for the influence of environmental exposure suggest that the curing conditions had similar effects on the measured air and gas permeabilities. This outcome is interesting as the same statistical inference was drawn for the OPI and TPT method despite the *kT* results being influenced by moisture at the time of testing. The OPI results were not influenced by moisture due to the oven-drying preconditioning of the samples. The significant difference observed for the barrier's *kT* results cannot be ignored as they indicate the appreciable effect of moisture, particularly in the winter period. Thus, further exploration is needed to understand the impact of environmental exposure, especially varying moisture conditions, on OPI and TPT methods. A more comprehensive range of curing conditions is also essential to explore.

The OPI and TPT methods showed similar trends with concrete age, but the findings differed during winter because of increased rainfall. The *kT* results were influenced by the loss of pore water in the summer and likely benefitted from continuous hydration in the winter. There was also a pore-blocking effect from moisture despite the surface moisture contents being within permissible limits at the testing time. The more prevalent action of these superimposed effects was assumed to control the effect on air permeability. For the OPI test, the oven drying conditioning suggests the effective removal of any influence from pore moisture. Hence, the results were statistically the same between 28 and 56 days.

4.5.3.1. Correlation between kT and kOPI

Table 4-8 compares the permeability classes of the OPI and Torrents for the results obtained in this study. The Torrent method has a stricter evaluation of concrete quality, with the 'excellent' category of the OPI test equating to three categories of the TPT method. The differences in the two test approaches can explain this discrepancy. The outer 5 mm layer is removed from the sample surface of OPI specimens to eliminate the influence of surface treatments and any handling damage on the measured *kOPI*. On the other hand, measurements are taken directly on the surface using the TPT method. This 'outer layer' is assumed to have poorer quality than that of the core of the concrete structure due to microcracks, bleed channels, and finishing inconsistencies, among other factors. The heterogeneities in the layer are expected to cover a wide range of pore sizes, thus requiring a wide range of permeability categories to interpret the concrete quality (Torrent & Frenzer, 1995; Torrent, Neves & Imamoto, 2022b). Even so, the TPT and OPI methods typically assess the same concrete depths: 30 mm (OPI) and up to 40 mm (TPT) for dry concrete. Therefore, a refinement of OPI categories can be explored in future studies to eliminate the classification disparities between the two methods.

A correlation analysis showed a strong relationship between the *kT* and *kOPI* results in summer but none in winter. This suggests that moisture-induced pore blocking in winter obscured the TPT method's sensitivity despite staying within the specified surface moisture limits. A moisture correction method proposed by Bueno et al. (2021) was applied to the *kT* results to observe any changes in the correlation between the two methods.

4.5.3.2. Effect of moisture correction

There was a marginal improvement in the correlation for the winter data from (R^2 = 0.14) to (R^2 = 0.16). The findings support Bueno's deductions that at high moisture contents, the change in *kT* has no practical significance. A remarkable change was observed for the summer data, where the correlation dropped sharply from (R^2 = 0.74) to (R^2 = 0.13) likely linked to the surface moisture variations between 2 and 56 days. This indicates that the moisture state of the concrete may govern the relationship between the OPI and TPT methods at the time of testing. The OPI and TPT methods likely showed an excellent correlation only in the summer due to similar sample dryness.

The 30-PC-II data point at 28 days in Figure 4-15 skews the correlation. The *kT* value remained unchanged after moisture correction due to its initial 5% moisture content. This highlights the impact of moisture on kT measurement and underscores the need for moisture compensation, especially considering the questionable handling of the 30-PC-II mix during delivery on-site.

Further research is necessary to confirm if the summer data correlation is consistent in a larger data set. The moisture correction method can improve *kT* result interpretation, but the 5% reference surface moisture may need adjustment for local climates. A better understanding of moisture content variations and depths of moisture penetration under different environmental conditions is required to calibrate moisture compensation more accurately. Studies can be

conducted to determine surface moisture content from oven-dried OPI samples, allowing for the conversion into a reference moisture value to correct site *kT* results in moist or wet environments.

Based on the results of this study, a clear relationship between the OPI and TPT method could only be confirmed in the summer site investigations.

4.6. Comparison of experimental results with Starck (2013)

The study aimed to validate Starck's (2013; 2017) findings. Figure 4-17 and Figure 4-18 illustrate Starck's data overlaid on the results of the present study. The summer correlation data fill out a further portion on the line of best fit in Starck's data cluster. The current data comprised lower gas and air permeability coefficients, indicating better concrete quality. Variable compaction in Starck's study may have contributed to higher permeability results. Furthermore, the difference in the binder types and the mix compositions may have also affected the data correlation. Nonetheless, the summer data aligns very well with Starck's correlation.

The winter data from this study also merged reasonably well with Starck's data, albeit with higher scatter. The low scatter in Starck's data may be attributed to the simulated winter exposure conditions, where there was some degree of control in the amount of moisture wetting the concrete elements.

Starck's study found a strong correlation between the OPI and Torrent method regardless of the exposure environment, but the current study could not achieve as strong an association with field concrete elements in local winter conditions. The strength of the relationship between the OPI and Torrent tests appears to be linked to the moisture state of the tested samples. Thus, using the Torrent method as a complementary method to the OPI test must be implemented carefully, especially in moist site conditions.

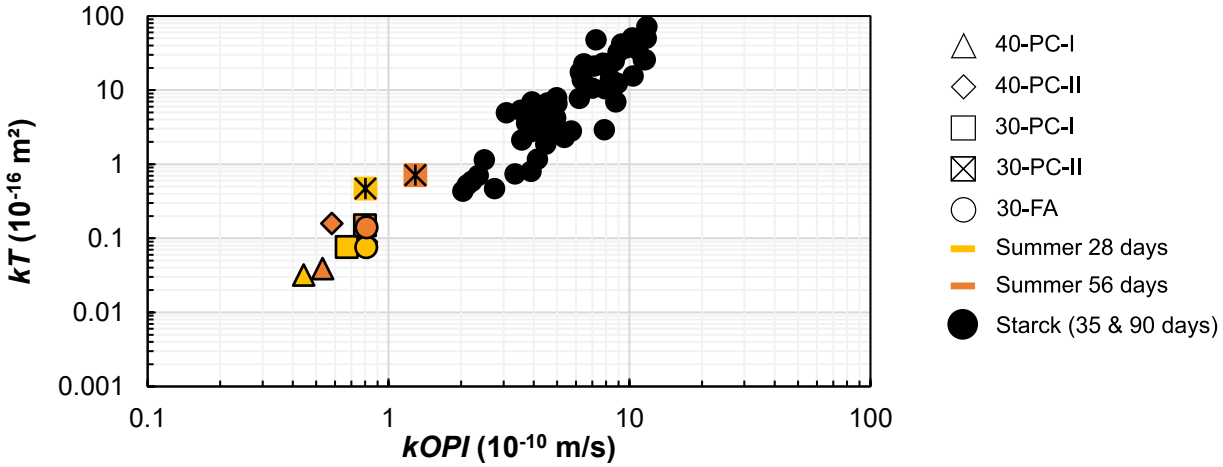

Figure 4-17 Comparison of previous research versus current study correlation (summer data).

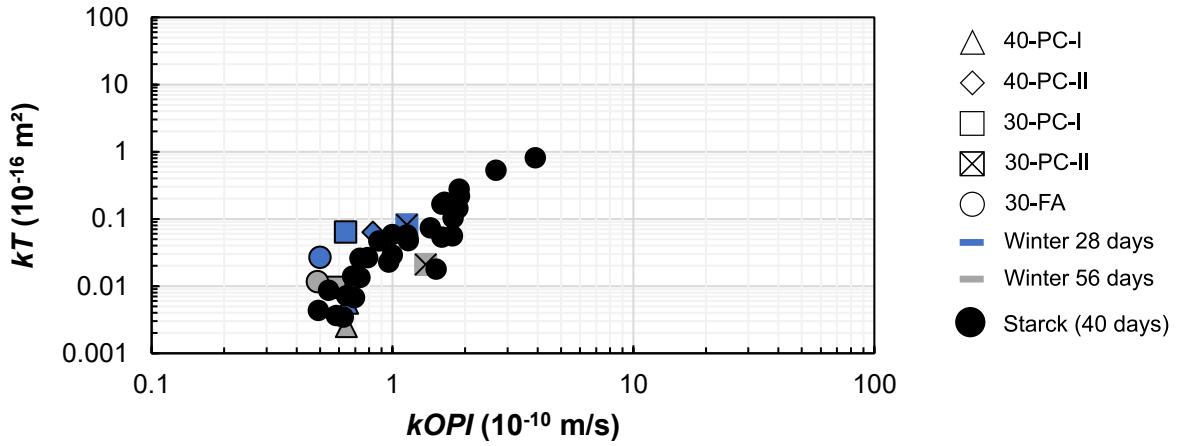

Figure 4-18 Comparison of previous research versus current study correlation (winter data).

4.7. Towards site implementation of a combined approach

While this study did not find a strong winter correlation between OPI and Torrent methods, a combined approach may still be applicable on-site. A joint strategy presents a progressive step towards faster local durability performance assessments. Careful interpretation of results obtained in moist conditions is essential to avoid inaccurate concrete quality assessment. Importantly, a better understanding of the surface moisture values of concrete in dry and moist environments is needed.

A proposed site strategy is presented in Chapter 5. Furthermore, the following areas of study can be explored to refine the approach and increase its reliability.

- Extensive site investigations of *kT* and *kOPI* measurements in varying local exposure conditions and under different curing regimes can contribute to a larger gas and air permeability database to better understand typical site DI values, particularly *kT* coefficients.
- Investigation of the reference surface moisture value (5%) proposed by Bueno et al. (2021) as an applicable reference value for moisture correction of local concretes. Such investigations may involve determining site-specific "dry and wet" surface moisture content for different concrete types on test panels.
- Conversion of the *kOPI* coefficients to *kT* units derived from the governing equations. Such a conversion would not rely on establishing correlations based on experimental data. The current study showed that environmental exposure (ambient conditions) affects the relationship between the OPI and the Torrent method.

4.8. Limitations of the study

The following factors were limitations of the methodology applied in this study.

- The small sample size in the study limited the ability to interpret trends and patterns.
- Minimal rainfall limited the exploration of the full effect of moisture on the Torrent method.

- A direct *kOPI-kT* comparison for barriers was impossible due to a lack of barrier core samples for kOPI measurement.
- The influence of the concrete's handling, placing and compaction most likely affected the measured DI results; however, this effect could not be quantified.

4.9. Chapter summary

The chapter presented the sensitivity of the OPI and Torrent tests to w/c ratio, binder type, environmental exposure, and age. The OPI and TPT methods generally displayed good responsiveness to the test variables, and statistical analyses were computed to check the significance of the differences observed. Table 4-9 summarises the findings from the study.

1. The compressive strength analysis revealed significant influences from w/c ratio and binder type, as expected.
   - Higher w/c ratio resulted in lower strength, attributed to the ITZ effect (increased porosity in the aggregate paste zones).
   - FA mix showed lower early strength gain than PC mixes, which was believed to be linked to slower hydration rates. However, better strength results were observed in winter, likely due to the change in the FA quality.
   - PC-I and PC-II mixes had similar strengths, but winter mixes showed more significant variation due to batching inconsistencies during cold weather adjustments.
   - Seasonal variations appeared to impact the strength results, but the controlled curing temperatures were believed to mitigate the effect, leading to similar strength outcomes between summer and winter results.
2. The sensitivity of the OPI method to the test variables generated the following findings:
   - Lower w/c ratios decreased gas permeability. However, the results showed no significant differences, suggesting that adequate compaction and proper curing can offset the impact of higher w/c ratios on concrete microstructure.
   - PC-I mixes generally had lower gas permeability than PC-II and FA mixes, but the differences were insignificant.
   - Environmental conditions had minimal impact on the gas permeability results, indicating that the extent of curing in the summer and winter produced similar gas permeability characteristics.
   - Gas permeability generally increased with age due to drying and microcracking, while blended mixes benefited from pore filling.
3. The TPT response to the test variables revealed the following findings:
   - Lower w/c ratios resulted in lower air permeability. However, a significant difference was only observed in the summer test period for the panels and winter for the barriers.
   - No significant differences were found in the *kT* results between binder types. It was concluded that binder influence likely depends on replacement levels in blended cement mixes.

- Summer conditions generally led to higher air permeability due to drying and increased water vapour pressure. However, the surface moisture content at the time of testing had an appreciable effect on the measured permeability in winter.
- *kT* decreased with age between 28 and 56 days, particularly in the winter test period. The observed trend was linked to increased moisture availability, which enabled continued hydration and higher surface moisture content during testing (pore-blocking effect).
- Moisture blocked pores, affecting air permeability. However, the Torrent method could still assess pore structure within moisture limits and penetrate deeper into the cover layer.
- The measured air permeability on the panels was lower than the median barriers, attributed to discrepancies in the element size and compaction effort.

4. The following can be summarised on the comparative analysis of the OPI and TPT results.

- Both methods showed that the influence of w/c ratio and binder type on air or gas permeability is challenging to assess in isolation due to extrinsic factors.
- Curing conditions in summer and winter had similar effects on permeability despite the TPT results being influenced by moisture in winter.
- The two methods exhibited similar responses to the effect of concrete age; however, the trend became skewed for the Torrent method in winter, owing to the influence of moisture.
- There was a strong correlation between the OPI and TPT method in summer, while a weaker association was found for the winter data. The discrepancies indicated that TPT sensitivity was masked in winter, even with specified surface moisture levels.
- The moisture correction approach showed the usefulness of moisture compensation in better interpreting air permeability in varying environmental conditions, particularly in dry conditions.

Although the study could not establish a conclusive relationship between the OPI and Torrent in winter, a combined approach suited to site conditions was deemed viable.

Table 4-9 Summary of findings from the present study.

Test Variable	Compressive Strength	OPI Method	TPT Method (Panels)
w/c ratio	- Lower w/c had higher strength in summer and winter.	- Lower w/c ratio had lower permeability.	- Lower w/c ratio had lower permeability.
Statistical significance	- Significant in both test periods.	- Insignificant in both test periods.	- Significant in summer, non-significant in winter.
Binder type	- PC-I and PC-II mixes had similar strengths but were higher than the FA mix.	- PC-I mixes had lower permeability than PC-II and FA in summer. FA mix is lowest in winter.	- PC-I mixes had lower air permeability than PC-II mixes and 30-FA.
Statistical significance	- Significant in summer, insignificant in winter.	- Insignificant in both test periods.	- Insignificant in both test periods.
Environmental exposure	- Summer period had higher strength.	- Summer mixes had lower permeability than winter mixes.	- Winter mixes had lower permeability than summer mixes.
Statistical significance	- -Insignificant.	- Insignificant.	- Insignificant.
Concrete age	-	- Mixes at 28 days had lower permeability than 56 days.	- Mixes at 28 days had lower permeability than 56 days in summer, while the opposite was observed in winter.
Statistical significance	-	- Insignificant in both test periods.	- Significant in both test periods.

5. CONCLUSION AND RECOMMENDATIONS

5.1. Introduction

This study aimed to combine the OPI and Torrent test methods for site application in local durability assessment strategies. The results showed that the two methods responded similarly to the experimental variables. However, the effect of moisture tended to skew the association of the OPI and TPT, especially on the responsiveness to the exposure environment. Thus, in proposing an integrated approach, the influence of moisture must be considered. This chapter concludes the study by outlining the key findings from the experimental programme and proposes a framework for implementing non-destructive testing in local DI assessment of concrete. Suggested future research work is proposed.

5.2. Background

The study investigated the relationship between the oxygen permeability (OPI) and Torrent permeability (TPT) indicators measured on site concrete elements to develop guidelines for a combined permeability index testing approach. The two methods have emerged as well-established standardised approaches for qualifying the potential durability performance of concrete, concerning gas and air permeability, respectively.

Previous studies have shown that the OPI and TPT methods are sensitive to cement type, w/c ratio, environmental exposure and concreting practices. Starck (2013; 2017) reported a good correlation between the two methods based on laboratory investigations under simulated environmental exposure conditions. But, the practical implementation of a combined approach has not been explored. Thus, there was a great need to evaluate the relationship between the OPI and TPT methods on site, in ambient conditions, and propose practical guidelines for the current South African durability index approach (SADIA).

Five mixes were used to make reinforced concrete barriers and representative test panels. The mixes comprised 30 and 40 MPa grades of CEM I, CEM II/A-L, and a blended mix of CEM I and FA. The concrete elements were manufactured in the summer and winter seasons of Cape Town and cured on site, at a precast plant in Airport Industria in Cape Town. The OPI and TPT tests were carried out at 28 and 56 days in both seasons to evaluate the sensitivity of the methods to environmental exposure, as well as w/c ratio, cement type, and age. The main findings and conclusions drawn are presented in the following sections.

5.3. General findings and conclusions

5.3.1. State-of-the-art in performance-based durability approaches

One of the study objectives was to review the state-of-the-art and practice in performance-based durability design and testing. A literature review was carried out on approaches used in different regions of the world. The review showed a global shift towards performance-based approaches,

but significant variation and inconsistency remain in their standardisation and implementation. It was found that South Africa and Switzerland have well-established testing methodologies, with the SADIA and Torrent approaches increasingly relied upon for concrete durability prediction.

5.3.2. Sensitivity of the OPI and Torrent methods to test variables

Lower w/c ratio (0.5) and higher concrete grade (40 MPa) translated to lower *kOPI* and *kT* values. This was attributed to the formation of denser microstructures with fewer capillary pores and pore connectivity in the mixes with lower w/c and higher grades. The results corroborated the findings in the literature. However, the differences in the results between the w/c ratios and grades used were statistically negligible. It can be concluded that mixes with 0.5 and 0.6 w/c ratios and grades of 30 MPa and 40 MPa can achieve similar gas and air permeability characteristics with good compaction and adequate curing.

The OPI and TPT methods were less sensitive to the influence binder types used in this study than the other test variables. There was a general trend of lower *kT* and *kOPI* in the PC-I (CEM I) mixes compared to the PC-II (CEM II A/L) and FA (CEM I + FA) mixes. Even so, the statistical differences between the binder types were found to be insignificant for both test methods. The findings suggest that the combined effects of the binder type used, the proportioning, and the replacement levels of SCMs must be considered carefully to achieve optimal permeability characteristics.

Despite varying environmental conditions, both test methods had no significant statistical differences in the measured permeability of the test panels. This indicated that the curing conditions of the elements in the summer and winter had similar effects, attributed in part to the curing compound applied to minimise moisture loss during the initial curing period. The Torrent method appeared to be influenced by the surface layer moisture at the time of testing, even within the permissible moisture levels. The effect was observed in the panels where exposure to rain during site transfer in summer and drying in the laboratory influenced the lower air permeability results, which overlapped with winter results. Significantly lower air permeability results were found for the barriers in winter compared to summer, reaffirming the influence of surface moisture. It was concluded that supplementary curing techniques are essential to compensate for variations in climatic conditions to achieve desired permeability characteristics.

The results showed increased air and gas permeability with age except for the winter Torrent results. The 30-FA and 40-PC-II mixes had greater resistance to drying effects, particularly in the OPI results, due to their finer particle sizes (pore filling) and delayed pozzolanic reactions. As the winter kT results improved with age, the effect of surface moisture during the winter period likely contributed to the deviation of the results from the general trends observed in the study. However, the observed differences were insignificant for the OPI results, while significant differences were observed for the Torrent results. The findings suggest that concrete age has a minor effect on gas permeability between 28 and 56 days under adequate concreting practice and curing

conditions. Further, surface moisture levels during testing can mask the effect of concrete age on air permeability results.

5.3.3. Correlation between kT and kOPI

A strong correlation between the two methods was observed in summer, while a weak correlation was found in the winter results due to the pore-blocking effect of surface moisture. Thus, the site relationship between the OPI and Torrent method is affected by moisture conditions. It can be concluded that a purely empirical relationship between the two methods may be difficult to achieve under different exposure environments; therefore, a link between the methods derived from theoretical equations should be explored instead.

5.3.4. Moisture correction on kT measurements

The moisture correction approach marginally improved the winter *kT-kOPI* correlation, while a significant change was observed in the summer correlation (from a strong to weak relationship). The findings further consolidated the conclusion that the moisture state influences the association between the OPI and Torrent method. Bueno's moisture correction approach was more responsive in adjusting *kT* results in dry conditions.

5.4. Overarching conclusions and practical implications

The conservative attitude towards adopting performance-based approaches requires a shift to advance the adoption of durability indicator methods. The action necessitates collaboration between academics and practitioners to refine current approaches and incorporate methodologies that assess critical parameters that affect concrete durability, particularly transport mechanisms in the microstructure.

The study results showed that the OPI and Torrent methods are sensitive to site concreting processes such as handling, placing, and compaction, though not exhaustively investigated in this research. These factors cause variations in the concrete quality and affect its durability performance. Therefore, using assessment methods such as the OPI and Torrent approaches is essential to address any shortcomings in handling fresh concrete on site that may affect the performance of the concrete in service.

While environmental conditions had a statistically insignificant impact on permeability, the benefits of supplementary curing techniques like curing compounds were highlighted in the different curing environments, having similar effects on the results. The surface moisture at the time of testing influenced the Torrent measurements appreciably, particularly in winter, reinforcing the difficulty of interpreting kT results under moist conditions. Therefore, additional methods such as the OPI test should be considered to obtain a more comprehensive assessment of the pore microstructure to minimise the impact of surface moisture.

The summer permeability correlation aligned with Starck's (2013; 2017) findings, while the winter data slightly deviated, suggesting that uncontrolled ambient variables, such as moisture, strongly influenced the association between the OPI and Torrent method. It was concluded that

determining empirical correlations on site using the OPI and Torrent methods may be complex considering the ever-changing environmental conditions on site. Thus, a combined approach using both methods, guided by site-specific conditions is strongly recommended. Further, an investigation into linking the two approaches based on theoretical equations should be explored.

The study showed that moisture compensation approaches, as postulated by Bueno et al. (2021), can also be useful in interpreting Torrent permeability results in extreme environmental conditions (dry conditions). However, the reference moisture value may not universally apply to all concrete types or conditions. A better understanding of moisture states in varying environmental conditions is required to calibrate the reference moisture values in the local context.

5.5. Practical implementation of a combined approach

Based on the findings in Chapter 4, the measured *kT* value should be ≤ 1.0 x 10^{-16} m^2 (see Figure 5-1) to qualify concrete quality for severe carbonation environments (i.e. environments with moderate humidity (50-85%RH) and cyclic wet and dry conditions). This limit falls within the 'Excellent' category for the OPI category. The permeability classification indicating the *kOPI* and *kT* limits is presented in Table 5-1. The concretes used were batched at a pre-cast plant with good quality control. Thus, the suggested *kT* limit may be considered strict and should be updated as more site data becomes available.

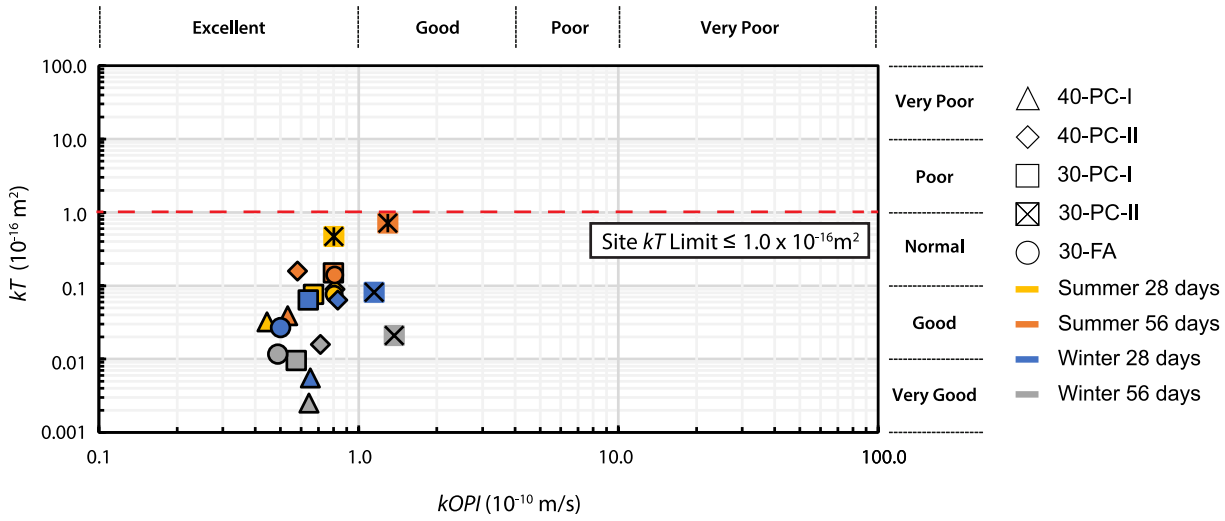

Figure 5-1 Site kT limit based on permeability data from the study. kT and kOPI data points based on geometric mean.

Table 5-1 Concrete Quality based on kT and kOPI.

Concrete quality	kOPI 10^{-10} m/s	OPI	Torrent kT 10^{-16} m^2
Excellent / Very Good	< 1.0	> 10	< 0.01
Good	3.2 – 1.0	9.5 - 10	0.01 – 0.1
Normal	---	---	0.1 – 1.0
Poor	10.0 – 3.2	9.0 – 9.5	1.0 - 10
Very Poor	> 10.0	< 9.0	> 10

It is proposed that the initial DI assessment on-site be conducted using the Torrent air permeability tester on the actual structure, using the relevant standards and user manuals. The concrete quality can be accepted if the results satisfy the testing conditions and are within acceptable limits ($kT_s \leq 1.0 \times 10^{-16}$ m^2). A sample of the Torrent test report sheet is presented in Appendix D.1.

Where the acceptable limit is exceeded, further testing is required to confirm the concrete's gas permeability characteristics. The testing will incorporate the OPI test, extracting cores from the structure at four of the highest *kT* measurements. This strategy will allow a direct and reliable evaluation of the concrete quality at questionable locations.

Clients may decline to have coring done on the actual structure; thus, test panels can be manufactured in consultation with the client before the concrete is placed.

The moisture conditions on site influence measured *kT*, especially in a moist environment such as the rainy winter of Cape Town. The summer surface moisture values averaged between 3.9 and 5.0%. It is proposed that the surface moisture content on the test area should not exceed the 5.5% prescribed in the Swiss standards. If the moisture limit is exceeded, sufficient time must be allowed for surface drying until acceptable moisture conditions are reached (usually 2-3 consecutive days after water contact). Where the waiting time extends beyond the monitoring period, the OPI test can be used to evaluate the gas permeability. Equally important is consideration for concrete with low moisture content. Moisture compensation using Bueno et al.'s approach is recommended to get a representative quality of the tested concrete, given that *kT* values from drier concrete may be conservative. Torrent (2022b) and Ptacek (2024) report the benefit of moisture compensation on the interpretation of *kT* for very dry concrete.

Figure 5-2 summarises the framework for the proposed approach.

5.6. Discussion of the proposed framework

The proposed combined approach offers a more comprehensive and faster DI assessment methodology. The Torrent test is executable within a significantly shorter time (1 hour 30 minutes per 6 determinations) than the OPI test. Thus, many more determinations can be made and rechecked quickly if required. Furthermore, using the Torrent test enables the testing of concrete elements that would not be suitable for investigation using intrusive methods such as thin concrete sections or elements in confined spaces. Even so, the OPI method remains a robust approach that should be relied on, especially where surface treatments and moisture may affect concrete's measured gas or air permeability.

An additional benefit of the integrated approach is reducing the number of cores to be extracted when evaluating the durability of the actual structure. With the successful implementation of a combined approach, the manufacture of test panels can be made optional.

The most significant benefit of the proposed framework is the actual structure instead of mock test panels. Measurements of the representative elements require some calibration to represent the concrete quality of the actual structure. Therefore, testing the actual structure non-destructively provides a more rational basis for durability assessments.

Successful implementation of the proposed methodology requires rigorous experimental studies in various exposure environments and consideration of other influencing factors on the measured DI parameters. Continued research on the OPI-Torrent association can refine the recommended approach, considering local moisture content and site *kT* limits in South Africa.

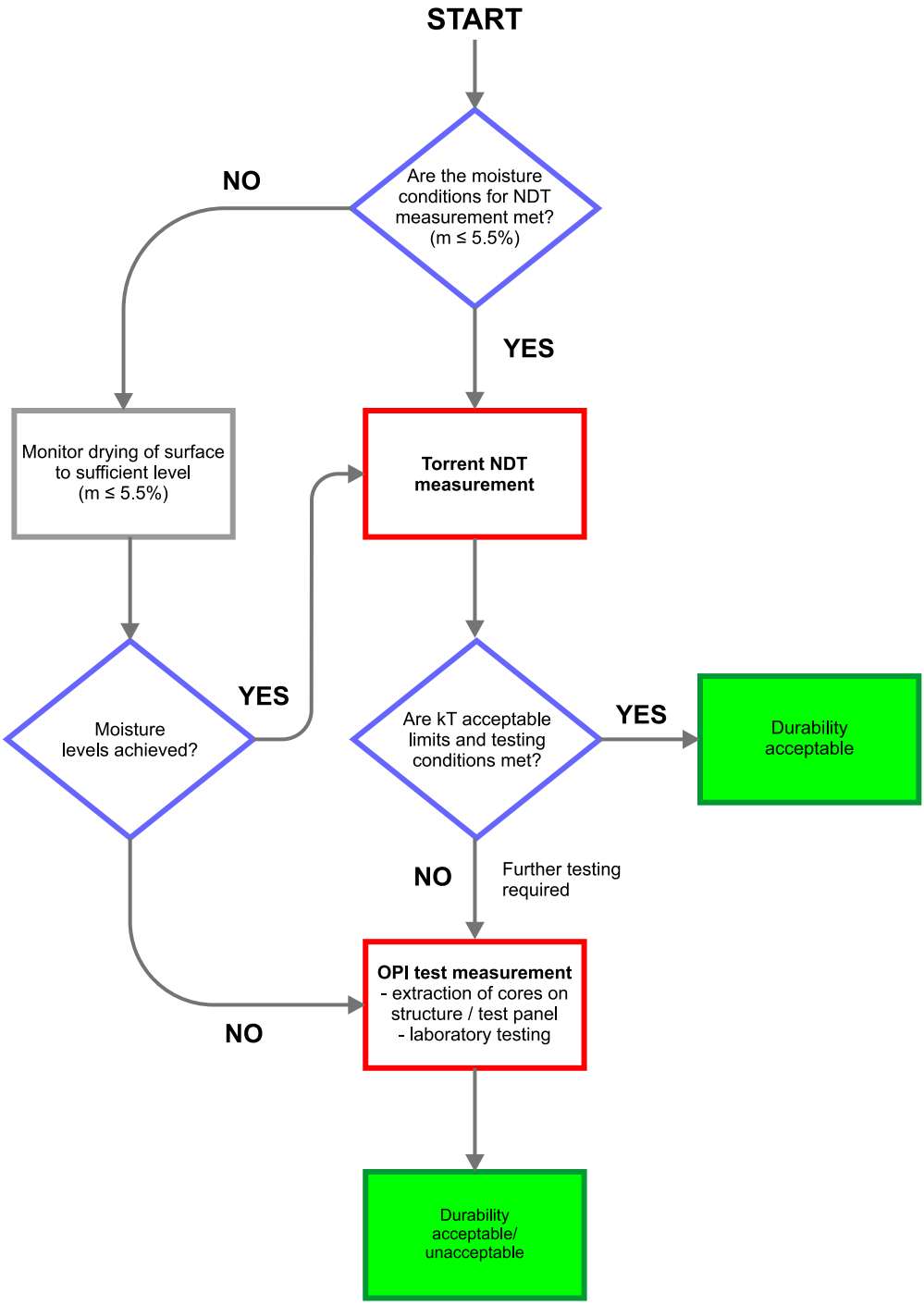

Figure 5-2 Proposed OPI-TPT integrated approach for durability assessment on site.

5.6.1. Summary of proposed combined approach

This study concluded that a combined permeability test approach using the OPI and Torrent method can be achieved on site using the following procedure:

i. Initial site assessment: The Torrent air permeability test is taken on the structure, following established procedures and standards. Where the specified limits are not met, and the moisture content levels cannot be achieved after extended monitoring, cores must be taken at locations of interest for evaluation via the OPI test.
ii. Acceptance criteria: Findings from this study suggest that a site *kT* value ≤ 1.0 x 10^{-16} m^2 is suitable for qualifying concrete quality in carbonation environments (areas with moderate to high humidity and exposed to wet and dry conditions).
iii. Moisture compensation: Moisture correction should be used to adjust *kT* to a reference moisture value for the interpretation of *kT* measurements.

5.7. Recommendations for future research

The following recommendations are put forward:

i. Larger sample sizes and range of concretes

The current study was limited to a small sample size and limited binder types. Thus, the inferences and implications of the results need to be verified more extensively. Further research is required using a more comprehensive range of concretes and a bigger sample size to validate the observations of this study.

ii. Investigations on actual structures

The *kT* and *kOPI* correlation was based on the representative test panels. Future work is recommended to investigate the OPI results obtained from actual structures to compare the *kOPI-kT* correlation of mock panels' and the correlation with the actual structure.

iii. Moisture correction investigations

The current study trialled a moisture correction approach proposed by Bueno et al. (2021) to adjust the *kT* results at a reference moisture content of 5%. However, the kT_5 values were not significantly different from the original data, a finding that was consistent with Bueno's study and attributed to high surface moisture contents (4.0%-5.5%). Therefore, future research focusing on drier site structures is required to fully evaluate the proposed moisture correction approach and its broader applicability. Such a study would allow a more robust assessment of the correction's effectiveness in adjusting *kT* measurements to represent standard moisture conditions.

Additional studies are needed to determine if the surface moisture of OPI pre-conditioned samples can be used as a reference to adjust site *kT* values. Subsequently, the correlation between the *kOPI* and adjusted *kT* can be evaluated.

iv. Refinement of OPI concrete classification

A notable inconsistency was observed in the concrete quality classification categories for the OPI and Torrent methods, ascribed to the different measurement approaches of the methods. This suggests a need to revise the OPI categories, as both methods generally show similar sensitivity to different concrete parameters. Further, the classifications should be linked with different carbonating environments.

v. Conversion of gas permeability units to air permeability units

The study could not conclusively find an empirical correlation between the OPI and TPT methods on site investigations, attributed to the influence of variable site conditions. Therefore, a more fundamental approach to linking the two methods could be explored based on derivations from governing equations. Such a study could make translating a specified OPI value or limits prescribed by SANRAL to expected site Torrent measurements easier.

5.8. Research contributions

The proposed combined approach using the Torrent test alongside the OPI method offers a significant advancement in assessing concrete durability indicators in South Africa. The speed and non-destructive nature of the Torrent Test enable comprehensive testing of various elements in confined spaces, reducing the need for core extraction and test panel fabrication. Importantly, evaluating the actual structure, instead of representative panels, provides a more representative assessment of concrete quality.

Further research is needed to consolidate application of the combined strategy in diverse environments.

REFERENCES

ACI Foundation. 2020. *Literature review of concrete durability and service life requirements in global codes and standards*.

Al-haddad, D.B. 2022. Comparison and Critique review of Durability Provisions and Design Requirements of Various International Design Codes and Standards. The British University in Dubai.

Alexander, M.G. 2018. Service life design and modelling of concrete structures – background, developments, and implementation. *Revista ALCONPAT*. 8(3):224–245. DOI: 10.21041/ra.v8i3.325.

Alexander, M.J. 2005. Durability indexes and their use in concrete engineering. 9–22. DOI: 10.1617/2912143586.002.

Alexander, M. & Beushausen, H. 2019. Durability, service life prediction, and modelling for reinforced concrete structures – review and critique. *Cement and Concrete Research*. 122(May):17–29. DOI: 10.1016/j.cemconres.2019.04.018.

Alexander, M.G., Mackechnie, J.R. & Ballim, Y. 1999.

Alexander, M.G., Gouws, S.M. & Maritz, G. 2001. Use of Durability Index Tests for the Assessment and Control of Concrete Quality on Site. *Concrete Beton*. 98(April):5–16. Available: www.concretesociety.co.za.

Alexander, M.G., Ballim, Y. & Stanish, K. 2008. A framework for use of durability indexes in performance-based design and specifications for reinforced concrete structures. *Materials and Structures/Materiaux et Constructions*. 41(5):921–936. DOI: 10.1617/s11527-007-9295-0.

Alexander, M.G., Santhanam, M. & Ballim, Y. 2010. Durability design and specification for concrete structures—the way forward. *International Journal of Advances in Engineering Sciences and Applied Mathematics*. 2(3):95–105. DOI: 10.1007/s12572-011-0027-x.

Alexander, M.G., Bentur, A. & Mindess, S. 2017. *Durability of concrete: Design and construction*. CRC Press - Taylor & Francis Group.

Alexander, M.G., Otieno, M. & Beushausen, H. 2021. Durability of Concrete. In *Fulton's Concrete Technology*. Tenth ed. M.G. Alexander, Ed. CRC Press, Taylor Francis Group. 441.

Alexander, M.G., Arito, P., Ballim, Y., Beushausen, H., Bonser, R., Boshoff, B., Brouard, B., Burwitz, S., et al. 2021. *Fulton's Concrete technology*. Tenth ed. M.G. Alexander, Ed. Cement & Concrete SA.

Angelucci, M. 2013. The influence of mix design parameters and compressive strength on durability indices. MSc. Thesis submitted to University of Cape Town.

Ash Resources. 2009. *Fly Ash Product Catalogue*. Ash Resources. Available: www.ashresources.co.za [2022, September 11].

ASTM F2659. 2010. *Guide for Preliminary Evaluation of Comparative Moisture Condition of Concrete, Gypsum Cement and Other Floor Slabs and Screeds Using a Non-Destructive Electronic Moisture Meter*. DOI: 10.1520/F2659-10R15.Copyright.

Bahurudeen, A. & Santhanam, M. 2014. Performance evaluation of sugarcane bagasse ash-based cement for durable concrete. *Proceedings of the 4th International Conference on the Durability of Concrete Structures, ICDCS 2014*. (July):275–281. DOI: 10.5703/1288284315412.

Ballim, Y. & Lampacher, B.J. 1996. Long-term carbonation of concrete structures in the Johannesburg environment. *SAICE Journal*.

Ballim, Y., Alexander, M. & Beushausen, H. 2009. Durability of concrete. In *Fulton's Concrete Technology*. 9th Editio ed. G. Owens, Ed. 155–188.

Barbara, S.V.G., Anya, L., Wu, B., Huet, B., Andrade, C., Thiel, C., Gruyaert, E., Vanoutrive, H., et al. 2020. Understanding the carbonation of concrete with supplementary cementitious materials : a critical review by RILEM TC 281-CCC. 53(136). DOI: 10.1617/s11527-020-01558-w.

Basheer, P.A.M. & Nolan, É. 2001. Near-surface moisture gradients and in situ permeation tests. *Construction and Building Materials*. 15(2):105–114. DOI: https://doi.org/10.1016/S0950-0618(00)00059-3.

Belgacem, M.E., Neves, R. & Talah, A. 2020. Service life design for carbonation-induced corrosion based on air-permeability requirements. *Construction and Building Materials*. 261:120507. DOI: 10.1016/j.conbuildmat.2020.120507.

Bernstein, S. & Bernstein, R. 1999. Non-parametric techniques. In *Elements of Statistics II: Inferential statistics, Schaum's Outlines*. McGraw-Hill. 389.

Beushausen, H. & Alexander, M.G. 2008. The South African durability index tests in an international comparison. *Journal of the South African Institution of Civil Engineering*. 50(1):25–31.

Beushausen, H. & Alexander, M.G. 2009. *Fultons Concrete Technology*. Cement & Concrete Institute, South Africa.

Beushausen, H. & Louw, W. 2021. Condition assessment and repair of concrete structures. In *Fulton's Concrete Technology*. Tenth ed. M.G. Alexander, Ed. Cement & Concrete SA. 1007–1009.

Beushausen, H. & Luco, L.F. 2015. *Performance-Based Specifications and Control of Concrete Durability: State-of-the-Art Report (RILEM TC 230-PSC)*. DOI: https://doi.org/10.1007/978-94-017-7309-6.

Beushausen, H., Torrent, R. & Alexander, M.G. 2019. Performance-based approaches for concrete durability: State of the art and future research needs. *Cement and Concrete Research*. 119(July 2018):11–20. DOI: 10.1016/j.cemconres.2019.01.003.

Bevans, R. 2022. *An Introduction to t Tests | Definitions, Formula and Examples*. Available: https://www.scribbr.com/statistics/t-test/ [2023, May 03].

Bhandari, P. 2022. *Correlational research | When & how to use*. Available: https://www.scribbr.com/methodology/correlational-research/ [2023, May 03].

Bonnet, S. & Balayssac, J.P. 2018. Combination of the Wenner resistivimeter and Torrent permeameter methods for assessing carbonation depth and saturation level of concrete. *Construction and Building Materials*. 188:1149–1165. DOI: 10.1016/j.conbuildmat.2018.07.151.

Bueno, V., Nakarai, K., Nguyen, M.H., Torrent, R.J. & Ujike, I. 2021. Effect of surface moisture on

air-permeability kT and its correction. *Materials and Structures/Materiaux et Constructions*. 54(2). DOI: 10.1617/s11527-021-01666-1.

Bustos, F., Martinez, P., Videla, C. & Lopez, M. 2015. Reducing concrete permeability by using natural pozzolans and reduced aggregate-to-pasteratio. *Journal of Civil Engineering and Management*. 21(2):165–176. DOI: 10.3846/13923730.2013.802719.

Chryso South Africa. 2020. *CHRYSO ® Plast Omega 174 Technical Data Sheet*. Chryso Southern Africa (Pty) Ltd.

Constro Facilitator. 2022. *An overview of fly ash; classification, advantage, and utlization*. Available: https://constrofacilitator.com/an-overview-of-fly-ash-classification-advantage-and-utlization/ [2022, September 28].

COTO. 2020a. Structures (Draft standard). In *Standard Specifications for Road and Bridge Works for South African Road Authorities*. The South African National Roads Agency SOC Ltd.

COTO. 2020b. Quality assurance (Draft standard). In *Standard Specifications for Road and Bridge Works for South African Road Authorities*. The South African National Roads Agency SOC Ltd.

DATAtab. 2023a. *Kruskal wallis test*. Available: https://datatab.net/tutorial/kruskal-wallis-test [2023, May 03].

DATAtab. 2023b. *Spearman correlation*. Available: https://datatab.net/tutorial/spearman-correlation [2023, May 03].

Dhanya, B.S. 2015. Study of the influence of supplementary cementitious materials on selected durability parameters of concrete. Indian Institute of Technology Madras.

Dlamini, N.N. 2019. A Critical Appraisal of the Developments in Durability of Concrete Structures in SA. University of the Witwatersrand.

Ekolu, S.O. 2018. Model for practical prediction of natural carbonation in reinforced concrete: Part 1-formulation. DOI: 10.1016/j.cemconcomp.2017.10.006.

Elsalamawy, M., Mohamed, A.R. & Kamal, E.M. 2022. The role of relative humidity and cement type on carbonation resistance of concrete. *Alexandria Engineering Journal*. 58(4):1257–1264. DOI: 10.1016/j.aej.2019.10.008.

Esau, D. 2022. *CEM I/CEM II SURETECH 52.5N Chemical composition sheets*. PPC Cement SA (Pty) Ltd.

Figg, J.W. 1973. Methods of measuring the air and water permeability of concrete. *Magazine of Concrete Research*. 25(85):213–219.

Fotso Lele, H.R. 2021. A Practical Carbonation Model for Service Life Design of Reinforced Concrete Structures. Available: http://hdl.handle.net/11427/36850.

Fotso Lele, H.R., Beushausen, H. & Alexander, M.G. 2023. A practical carbonation model for service life design of reinforced concrete structures. *Scientific African*. 20. DOI: 10.1016/j.sciaf.2023.e01677.

Freitag, S., Papworth, F. & Paull, R. 2016. Concrete durability: Concrete institute of Australia's recommended practice. In *The New Zealand concrete industry concference 2016*. Auckland, New Zealand.

Gilayeneh, V.S. & Nwaubani, S.O. 2022. Transport Properties of Pozzolanic Concrete Based on the South African Durability Indexes. *World Congress on Civil, Structural, and Environmental Engineering*. DOI: 10.11159/ICSECT22.116.

Glinicki, M. & Nowowiejski, G. 2013.

Gopinath, R. 2020. Concrete carbonation prediction for varying environmental exposure conditions. Ph.D Thesis submitted to University of Cape Town.

Gopinath, R. & Alexander, M. 2018. *Experimental investigation and modelling of natural carbonation of concrete*.

Gopinath, R., Alexander, M. & Beushausen, H. 2017. Predicting depth of carbonation of concrete for varying climatic conditions.

Govender, D. 2019. The design of a data model (DM) for managing durability index (DI) results for national road infrastructure. University of Cape Town.

Hooton, R.D. 2019. Future directions for design, specification, testing, and construction of durable concrete structures ☆. DOI: 10.1016/j.cemconres.2019.105827.

INSA Toulouse. 2022. *Concrete - Performance-based method for justifying concrete structures durability - FD P18-480*. Toulouse, France: l'Association Francaise de Normalisation (AFNOR).

Jacobs, R. & Kiliswa, M. 2021. Cementitious Materials. In *Fulton's Concrete Technology*. Tenth ed. M. Alexander, Ed. Cement & Concrete SA. 41–69.

Jacobs, F., Denarie, E., Teruzzi, T., Leemann, A. & Torrent, R.J. 2009. *Recommendations for quality control of concrete using air permeability measurements (translated from German)*. Bern, Switzerland.

Kanjee, J.P. 2015. Assessing the influence of crack width on the durability potential of cracked concrete using the durability index approach. MSc.Thesis submitted to University of Cape Town. Available: http://hdl.handle.net/11427/24308 [2024, June 16].

Kessy, J.G., Alexander, M.G. & Beushausen, H. 2015. Concrete durability standards : International trends and the South African context. 57(1135):47–58.

Kollek, J.J. 1989. The determination of the permeability of concrete to oxygen by the Cembureau method—a recommendation. *Materials and Structures*. 22(3):225–230. DOI: 10.1007/BF02472192.

Krook, A. 1995. An investigation of concrete curing practice in the Cape Town area. University of Cape Town.

Kropp, J. 1995. Relations between transport characteristics and durability. *Performance criteria for concrete durability, RILEM Report*. 12:97–137.

Kropp, J. & Alexander, M. 2007. Transport mechanisms and reference tests. *Non-Destructive Evaluation of the Penetrability and Thickness of the Concrete Cover - State-of-the-Art Report of RILEM Technical Committee 189-NEC*. (May):13–34.

Kumar, S., Gupta, R.C., Shrivastava, S., Csetenyi, L. & Thomas, B.S. 2016. Preliminary study on the use of quartz sandstone as a partial replacement of coarse aggregate in concrete based on clay content, morphology and compressive strength of combined gradation. *Construction and Building Materials*. 107:103–108. DOI: 10.1016/j.conbuildmat.2016.01.004.

Kurashige, I. 2015. Novel Non-destructive Test method to Evaluate Air-Permeability Distribution in Depth Direction in Concrete-Development of Triple-Cell Air-Permeability Tester (TCAPT). In *The Proceedings of the International Symposium Non-Destructive Testing in Cicil Engineering*.

Kwon, S.J. & Song, H.W. 2010. Analysis of carbonation behavior in concrete using neural network algorithm and carbonation modeling. *Cement and Concrete Research*. 40(1):119–127. DOI: 10.1016/J.CEMCONRES.2009.08.022.

Kwon, S.-J., Ahn, Y.H. & Rosen, M.A. 2017. Current Trends of Durability Design and Government Support in South Korea: Chloride Attack. DOI: 10.3390/su9030417.

Lachenicht, L. 2013. Correlation. In *Numbers, hypotheses, & conclusions: A course in statistics for the Social sciences*. Second ed. C. Tredoux & K. Durrheim, Eds. Cape Town, South Africa: Juta & Company Ltd.

Lampacher, B.J. 2000. Durability of concrete structures. Univeristy of the Witwatersrand, Johannesburg.

Leemann, A. & Moro, F. 2017. Carbonation of concrete: the role of CO2 concentration, relative humidity and CO2 buffer capacity. *Materials and Structures/Materiaux et Constructions*. 50(1). DOI: 10.1617/S11527-016-0917-2.

Li, K. 2022. M & S highlight : Kollek (1989), The determination of the permeability of concrete to oxygen by the Cembureau method — a recommendation. *Materials and Structures*. 55(2):1–4. DOI: 10.1617/s11527-021-01864-x.

Li, D., Chen, B., Sun, H., Memon, S.A., Deng, X., Wang, Y. & Xing, F. 2018. Evaluating the effect of external and internal factors on carbonation of existing concrete building structures. DOI: 10.1016/j.conbuildmat.2018.01.127.

Luo, D., Niu, D. & Dong, Z. 2014. Application of Neural Network for Concrete Carbonation Depth Prediction.

Mackechnie, J.R.. 2003. Quality of Western Cape Sandstone as Concrete Aggregate. *Concrete Beton*. 104(August):11–13.

Mackechnie, J.R. & Alexander, M.G. 2002. Durability Predictions Using Early-Age Durability Index Testing. In *9th International Conference on Durability of Building Materials and Components*.

Megamix. 2022. *Concrete Materials Data sheet*. Cape Town, South Africa.

Mehta, P.K. & Monteiro, P.J.M. 2001. *Concrete: Microstructure, Properties and Materials*.

Mehta, P.K. & Monteiro, P.J.M. 2006. *Concrete: Microstructure, Properties, and Materials*. Third ed.

Van der Merwe, J. 2019. Constitutive models towards the assessment of concrete spalling in fire. ETHZ, Zürich.

Moore, A.J., Bakera, A.T. & Alexander, M.G. 2021. A critical review of the Water Sorptivity Index (WSI) parameter for potential durability assessment: Can WSI be considered in isolation of porosity? *Journal of the South African Institution of Civil Engineering*. 63(2):27–34. DOI: 10.17159/2309-8775/2021/v63n2a4.

Mukadam, Z. 2014. Critical Review of the South African Concrete Durability Index Tests. MSc. Thesis submitted to University of Cape Town.

Neves, R., Santos, J. & Valente-Monteiro, A. 2011. *Estudo sobre a influência da compactação na resistência do betão à carbonatação*.

Neves, R., Branco, F. & De Brito, J. 2012. About the statistical interpretation of air permeability assessment results. *Materials and Structures/Materiaux et Constructions*. 45(4):529–539. DOI: 10.1617/s11527-011-9780-3.

Nganga, G.W. 2012. Practical implemenation of the durability index-based performance approach. MSc. Thesis submitted to University of Cape Town.

Nganga, G., Alexander, M. & Beushausen, H. 2013. Practical implementation of the durability index performance-based design approach. DOI: 10.1016/j.conbuildmat.2013.03.069.

Nganga, G., Alexander, M. & Beushausen, H. 2017. *Practical implementation of the durability index performance-based design approach: Current Experience*. ResearchGate. Available: https://www.researchgate.net/publication/257389869_Practical_implementation_of_the_durability_index_performance-based_design_approach [2021, March 01].

Nganga, G.W., Alexander, M.G., Moyana, P. & Beushausen, H. 2016. Practical implementation of durability index performance-based specifications: Current experience. *fib Symposium*. 150(September):18–22.

Nganga, G.W., Beuhausen, H. & Alexander, M.G. 2017. Practical implementation of durability index performance-based specifications: current experience. *Concrete Beton*. 18–22.

Nganga, G.W., Mumenya, S.W. & Abuodha, S.O. 2020. Design of Durable Concrete Mixes for Reinforced Concrete (RC) Structures. In *27th Institution of Engineers Kenya Conference Papers*. Nairobi. 1–5.

Nganga, G.W., Alexander, M.G. & Ballim, Y. 2022. Variability of oxygen permeability index values in concrete construction: A proposed approach for parameter margins to guide concrete mixture design. *Journal of the South African Institution of Civil Engineering*. 64(3):2–9.

Nguyen, M.H., Nishio, S. & Nakarai, K. 2022. Effect of temperature on nondestructive measurements for air permeability and water sorptivity of cover concrete. *Construction and Building Materials*. 334:2–8. DOI: 10.1016/j.conbuildmat.2022.127361.

Nilsson, L. 2003. Durability of concrete and concrete construction Durability concept ; pore structure and transport processes. In *Durability of concrete and concrete construction*.

Nilsson, L.O. 2019. Corrosion of steel in concrete. *Developments in the Formulation and Reinforcement of Concrete*. 115–129. DOI: 10.1016/B978-0-08-102616-8.00005-8.

Nishimura, K., Kato, Y. & Mita, K. 2015. Influence of construction work conditions on the relationship between concrete carbonation rate and the air-permeability of surface concret. In *International Conference on Regeneration and Conservation of Concrete Structures*. Nagasaki, Japan.

Nnodim, U.R. 2020. Effects of pore void saturation degree on nondestructive tests for durability assessment of concrete structures. (September).

Omar, N. 2018. Carbonation and permeability characteristics of modern South African concretes. MSc. Thesis submitted to University of Cape Town.

Otieno, M. & Walter, K. 2022. An assessment of a practical implementation of the deemed-to-satisfy durability design and specification approach in the Swakopmund–Walvis Bay Freeway

upgrade project in Namibia. *Journal of the South African Institution of Civil Engineering*. 64(2):28–37. DOI: 10.17159/2309-8775/2022/v64no2a3.

Owens, G. 2009. *Fulton's Concrete Technology*. Ninth ed. G. Owens, Ed. Cement & Concrete Institute.

Papworth, F. 2016. A whole of life approach to concrete durability—the CIA concrete durability series. In *Proceedings of the 4th International Conference on Concrete Repair, Rehabilitation and Retrofitting, ICCRRR 2015*. DOI: 10.1201/b18972-29.

Papworth, F. 2018. Australian Developments in Concrete Durability Consultancy. (May).

Papworth, F. & Matthews, S. 2018. fib Model Code 2020-Durability Design and Through Life Management of New and Existing Structures. In *Sixth International Conference on Durability of Concrete Structures*. Leeds, United Kingdom.

Park, S., Lee, E., Ko, J., Yoo, J. & Kim, Y. 2018. Rheological properties of concrete using dune sand. *Construction and Building Materials*. 172:685–695. DOI: 10.1016/j.conbuildmat.2018.03.192.

Parrot, L. 1994. Design for Avoiding Damage Due to Carbonation-Induced Corrosion. *Amercian Concrete Institute (ACI) - Special Publication*. 145:283–298. DOI: 10.14359/4466.

Parrott, L.J. 1989. Air permeability of cover concrete and the effect of curing. *Cement and Concrete Association Services, Report, UK*.

Parrott, L. & Hong, C.Z. 1991. Some factors influencing air permeation measurements in cover concrete. *Materials and Structures*. 24(6):403–408. DOI: 10.1007/BF02472013.

Ptacek, L., Strauss, A., Grba, D., Sattler, F., Macha, M., Kosta, A., Marchtrenker, S., Boisits, P., et al. 2024. Performance based concrete quality assessment with gas permeability testing on site. *Frontiers in Built Environment*. 10(May):1–14. DOI: 10.3389/fbuil.2024.1396801.

Richardson, M.G. 2002. *Fundamentals of Durable Reinforced Concrete*. 1st Editio ed. CRC Press. DOI: 10.1201/9781482272109.

RILEM Technical Committee. 2007. Comparative Test - Part I : " Penetrability " Test Methods - RILEM TC 189-NEC: State-of-the-Art Report. In *Non-Destructive Evaluation of the Penetrability and Thickness of the Concrete Cover*. RILEM. 157–185.

Romer, M. & Leemann, A. 2006. Sensitivity of a non-destructive vacuum test method to characterize concrete permeability. *Concrete Repair, Rehabilitation and Retrofitting - Proceedings of the International Conference on Concrete Repair, Rehabilitation and Retrofitting, ICCRRR 2005*. 177–179.

Saetta, A. V. & Vitaliani, R. V. 2005. Experimental investigation and numerical modeling of carbonation process in reinforced concrete structures: Part II. Practical applications. *Cement and Concrete Research*. 35(5):958–967. DOI: 10.1016/J.CEMCONRES.2004.06.023.

Salvoldi, B.G. 2010. Modelling the carbonation of concrete using early age oxygen permeability index tests. University of Cape Town.

Salvoldi, B.G., Beushausen, H. & Alexander, M.G. 2015. Oxygen permeability of concrete and its relation to carbonation. *Construction and Building Materials*. 85:30–37. DOI: 10.1016/j.conbuildmat.2015.02.019.

Sangoju, B., Gopal, R. & Bhajantri H, B. 2020. A review on performance-based specifications

toward concrete durability. *Structural Concrete*. (May):1–13. DOI: 10.1002/suco.201900542.

SANS 3001-CO3-1. 2015. *Civil engineering test methods - Part CO3-1 : Concrete durability index testing - Preparation of test specimens*.

SANS 3001-CO3-2. 2015. *Concrete durability index testing. Part CO3-2: Oxygen permeability test*.

SANS 50206. 2015. *Concrete - Specification, performace, production and conformity*. Brussels.

SANS 5862:1. 2006. *Concrete tests - Consistency of freshly mixed concrete: Slump test*.

SANS 5863. 2006. *Concrete tests - Compressive strength of hardened concrete*. Available: http://srvubupan001.uct.ac.za/sans/documents/SANS5863.pdf.

SANS 878. 2012. *Ready-mixed concrete*.

Scrivener, K.L., Crumbie, A.K. & Laugesen, P. 2004. The interfacial transition zone (ITZ) between cement paste and aggregate in concrete. *Interface Science*. 12(4):411–421. DOI: 10.1023/B:INTS.0000042339.92990.4C/METRICS.

SIA 262/1. 2013. *Construction en béton - Spécifications complémentaires*. Zurich.

SIA 262/1. 2019. *Construction en béton - Spécifications complémentaires. Annex E: 'Perméabilité à l'air dans les structures' (Extract)*. Zurich: Société suisse des ingénieurs et des Architectes.

Soutsos, M. 2010. *Concrete Durability - A Practical Guide to the Design of Durable Concrete Structures - Knovel*. ICE Publishing. Available: https://app-knovel-com.ezproxy.uct.ac.za/web/toc.v/cid:kpCDAPGDD5/viewerType:toc//root_slug:viewerType%3Atoc/url_slug:root_slug%3Aconcrete-durability-practical?kpromoter=federation [2021, May 15].

Stanish, K., Alexander, M.G. & Ballim, Y. 2006. Assessing the repeatability and reproducibility values of South African durability index tests. *Journal of the South African Institution of Civil Engineering*. 48(2):10–17.

Starck, S. 2013. The Integration of Non-Destructive test methods into the South African Durability Index Approach. MSc. Thesis submitted to University of Cape Town.

Starck, S., Beushausen, H., Alexander, M. & Torrent, R. 2017. Complementarity of in situ and laboratory-based concrete permeability measurements. *Materials and Structures/Materiaux et Constructions*. 50(3):1–15. DOI: 10.1617/s11527-017-1037-3.

Stefanoni, M., Angst, U. & Elsener, B. 2017. Corrosion rate of carbon steel in carbonated concrete-A critical review. DOI: 10.1016/j.cemconres.2017.10.007.

Sugandhini, H., Sivadas, N., Nayak, G. & Shetty, K.K. 2022. A review on concrete's durability in India- Framework for performance-based approach. DOI: 10.1016/j.matpr.2022.01.437.

Surana, S., Pillai, R.G. & Santhanam, M. 2017a. Performance evaluation of field curing methods using durability index tests. *Indian Concrete Journal*. 91(7):37–50.

Surana, S., Pillai, R.G. & Santhanam, M. 2017b. Performance evaluation of curing compounds using durability parameters. *Construction and Building Materials*. 148:538–547. DOI: 10.1016/j.conbuildmat.2017.05.055.

Szychowski, J. & Torrent, R.J. 2017. Innovation in air-permeability NDT: Concept and performance. In *14th International Conference on Durability of Building Materials and*

Components. Ghent: RILEM. 313.

Torrent, R. 2012. Non-Destructive Air-Permeability Measurement: From Gas-Flow Modelling To Improved Testing. *Microdurability*. (1):467–476. Available: www.m-a-s.com.ar/images/events/Microdurability Paper 151 - RT.pdf.

Torrent, R. 2015. Exp-Ref: A Simple, Realistic and Robust Method to Assess Service Life of Reinforced Concrete Structures. *Concrete*. (1).

Torrent, R.J. 1992. A two-chamber vacuum cell for measuring the coefficient of permeability to air of the concrete cover on site. *Materials and Structures*. 25:358–365.

Torrent, R.J. 2013. Service life prediction: Theorecrete, labcrete and realcrete approaches. *Sustainable Construction Materials and Technologies*. 2013-Augus.

Torrent, R. & Ebensperger, L. 1993. *Studie über Methoden zur Messung und Beurteilung der Kennwerte des Überdeckungsbetons auf der Baustelle: Forschungsauftrag Nr. 89/89*. Rapport No ed. Bern, Switzerland: Eidgenöss. Verkehrs-u. Energiewirtschaftsdep.

Torrent, R. & Luco, L.F. 2014. Service life assessment of concrete structures based on site testing. In *DBMC 2014 Conference*. Sao Paulo, Brazil. DOI: 10.1061/(ASCE)0733-947X(1990)116:2(252).

Torrent, R.J. & Frenzer, G. 1995. A method for the rapid determination of the coefficient of permeability of the “covercrete”. In *International Symposium on Non-destructive Testing in Civil Engineering (NDT-CE)*. 985–992.

Torrent, R., Moro, F. & Jornet, A. 2014. Coping with the Effect of Moisture on Air-Permeability measurements. *RILEM International workshop on performance-based specification and control of concrete durability*. (June):489–498.

Torrent, R., di Prisco, M., Bueno, V. & Sibaud, F. 2018. Site Air-Permeability of HPSFR and Conventional Concretes. *ACI SP-326*. 1–9.

Torrent, R., Bueno, V., Moro, F. & Jornet, A. 2019. Suitability of impedance surface moisture meter to complement air-permeability tests. *Rilem Pro*. 128(March):56–63.

Torrent, R., Neves, R. & Imamoto, K. 2022a. Durability performance of concrete structures. In *Concrete Permeability & Durability Performance: From Theory to Field Applications*. CRC Press, Taylor Francis Group.

Torrent, R.J., Neves, R.D. & Imamoto, K.-I. 2022b. *Concrete Permeability & Durability Performance: From Theory to Field Applications*. First ed. CRC Press - Taylor & Francis Group. DOI: https://doi.org/10.1201/9780429505652-5.

Tramex. n.d. *Concrete Moisture Encounter 4 (CME4): User Guide*. Tramex Ltd.

Ujike, I., Okazaki, S. & Nakamura, T. 2009. A study on the improvement of on-site air permeability tests for concrete structures. *Cement Science and Concrete Technology*. 63:189–195.

Wally, G.B., Magalhães, F.C., Pinto, C. & Filho, S. 2022. From prescriptive to performance-based: An overview of international trends in specifying durable concretes. DOI: 10.1016/j.jobe.2022.104359.

Walpole, R., Myers, R., Myers, S. & Ye, K. 2012. *Probability & Statistics for Engineers & Scientists*. 9th ed. Prentice Hall.

Wieland, M. 2009. A comparison of service life design approaches for reinforced concrete structures. University of Cape Town - University of Applied Sciences Karlsruhe.

WITS & UCT. 2018. *Durability Index Testing Procedure Manual*.

WITS & UCT. 2023. *Durability Index Testing Procedure Manual*.

Wu, K., Han, H., Li, H., Dong, B., Liu, T. & De Schutter, G. 2021. Experimental study on concurrent factors influencing the ITZ effect on mass transport in concrete. *Cement and Concrete Composites*. 123:104215. DOI: 10.1016/j.cemconcomp.2021.104215.

Yang, K., Basheer, P.A.M., Bai, Y., Magee, B.J. & Long, A.E. 2014. Development of a new in situ test method to measure the air permeability of high performance concretes. *NDT & E International*. 64:30–40. DOI: https://doi.org/10.1016/j.ndteint.2014.02.005.

Zhang, D. & Li, K. 2019. Concrete gas permeability from different methods: Correlation analysis. DOI: 10.1016/j.cemconcomp.2019.103379.

Zhou, Y., Gencturk, B., Asce, A.M., Willam, K., Asce, F. & Attar, A. 2015. Carbonation-Induced and Chloride-Induced Corrosion in Reinforced Concrete Structures. DOI: 10.1061/(ASCE)MT.1943-5533.0001209.

APPENDIX A. SUPPLEMENTARY LITERATURE REVIEW INFORMATION

A.1. Permeability classification kT vs kOPI

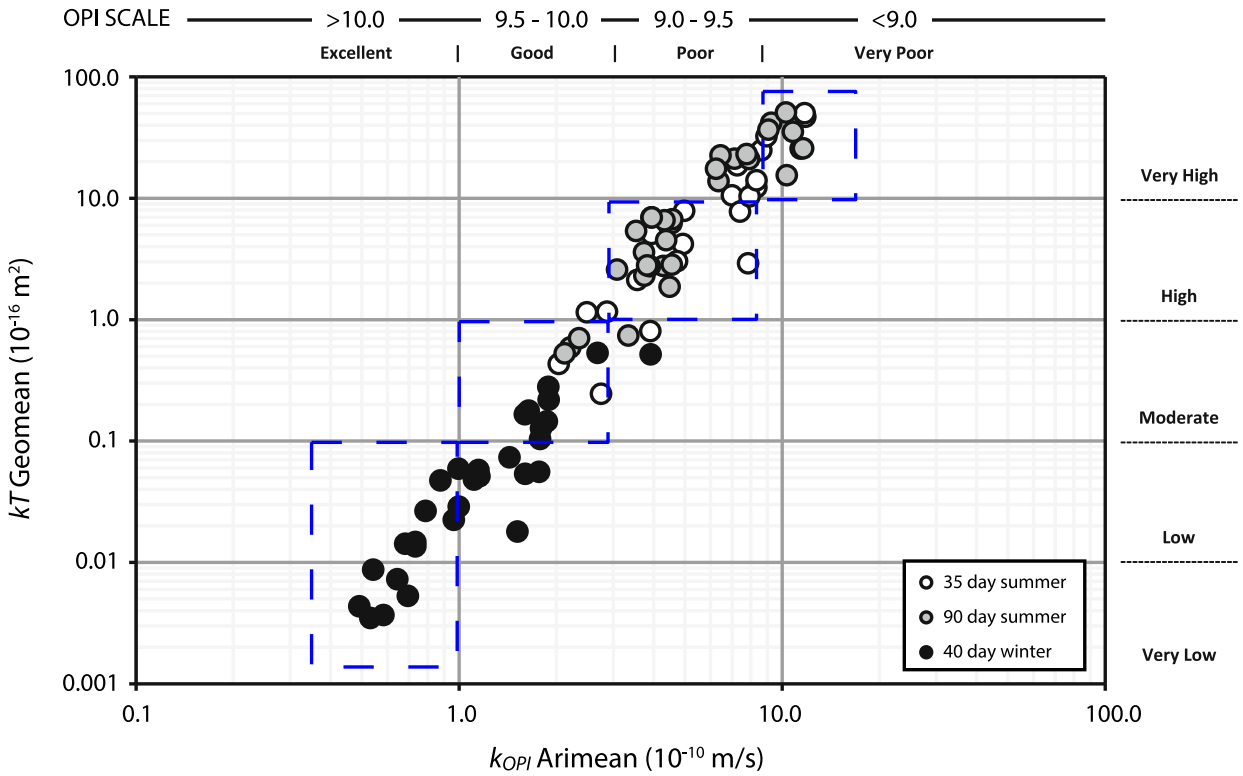

Figure A-1 kT - kOPI permeability classification criteria (adapted from Starck (2017).

A.2. South African environmental exposure classes and durability specifications

Table A-1 Environmental classes (adapted from COTO (2020a).

Environmental Class	Limited description
X0	No corrosion risk
Corrosion induced by carbonation	
XC1a	External concrete exposed to low humidity (<50% RH) and sheltered from moisture; arid areas; interior concrete
XC1b	Permanently wet or saturated damp
XC2	Wet, rarely dry
XC3	External concrete exposed to moderate humidity (50-85% RH) and sheltered from rain in non-arid areas
XC4	External concrete exposed to rain or condensation, or alternatively wet and dry conditions
Corrosion induced by seawater, sea spray, and saline groundwater	
XS1	Exposed to airborne salt but not in direct contact with seawater or inland saline water
XS2a	Permanently submerged in sea (or saline) water
XS2b	XS2a with abrasion
XS3a	Tidal, splash, and spray zones
XS3b	XS3a with abrsion

Table A-2 Durability Index and cover specification for concrete in typical chloride environments (adapted from COTO (2020a).

Environmental class	Cover (mm), as specified	Chloride Conductivity (mS/cm)			
		Typical Cementitious Binder System[3]			
		Fly ash (30 %)	Blastfurnace slag (50 %)	Corex slag (50 %)	Silica fume (10 %)
For 100 year service life					
XS1	40	1,20	1,30	1,60 [2]	n/a [1]
	50	1,85 [2]	1,95 [2]	2,20 [2]	0,40
	60	2,15 [2]	2,35 [2]	2,75 [2]	0,65
XS2a	50	0,85	1,00	1,20	n/a [1]
	60	1,25	1,45 [2]	1,70 [2]	n/a [1]
XS2b	60	1,10	1,30	1,55 [2]	n/a [1]
XS3a	50	0,65	0,80	0,95	n/a [1]
	60	0,95	1,10	1,40	n/a [1]
XS3b	60	0,85	1,00	1,30	n/a [1]

1) n/a refers to cementitious binder system not suitable for the indicated purpose.

2) Maximum water: cementitious binder ratio for all binder systems shall be maximum 0,550.

A.3. Compliance and conditional acceptance criteria

Table A-3 Limiting values implemented by SANRAL for performance specification and reduced payment conditions (adapted from COTO (2020b).

	Oxygen permeability index	Chloride conductivity Index	Water sorptivity index	
	OPI (log scale)	**CCI (mS/cm)**	**WSI ($mm/hr^{0.5}$)**	**Percentage Payment**
Full acceptance	$\geq (OPI_{spec} - B_{ave})$	$\leq (CCI_{spec} + B_{ave})$	$\leq (CCI_{spec} + B_{ave})$	100%
Conditional acceptance [a]	$\geq L_r \leq (OPI_{spec} - B_{ave})$	$>(CCI_{spec} + B_{ave}) \leq L_r$	$>(CCI_{spec} + B_{ave}) \leq L_r$	80%
Rejection	$< L_r$	$> L_r$	$> L_r$	N/A

[a] incurs reduced payment

- B_{ave} = prescribed tolerance values for assessment of durability parameters
- $OPI/CCI/WSI_{spec}$ = specified durability indicator value
- L_r = rejection limit

Table A-4 Tolerance values and rejection limits for DI test evaluations (adapted from COTO (2020b).

Specified concrete durability property	Unit	Tolerance (B_{ave})	Rejection Limit (L_r)
Oxygen permeability index	log scale	0,25	Specified OPI - 0,40
Chloride conductivity index	mS/cm	0,20	Specified CCI + 0,40
Water sorptivity index	$mm/hr^{0.5}$	1,50	Specified WSI + 2,50

The acceptability of Durability indicator test outcomes will be evaluated according to the predetermined requirements in the COTO specifications to ensure conformity with the specified conditions and restrictions (COTO, 2020b).

APPENDIX B. SUPPLEMENTARY MATERIALS AND METHODS INFORMATION

B.1. Concrete mix designs

Table B-1 Batched concrete mixes used in summer (materials in kg/m³).

Description	Mix Designs				
	Mix 1	**Mix 2**	**Mix 3**	**Mix 4**	**Mix 5**
Mix designation	**40-PC-I**	**40-PC-II**	**30-PC-I**	**30-PC-II**	**30-FA**
Design Strength (MPa)	40	40	30	30	30
CEM I 52.5N	355	0	285	0	210
CEM II/A-L 52.5N	0	355	0	285	0
Fly Ash	0	0	0	0	90
Coarse aggregate	1100	1100	1080	1080	1080
Dune Sand	515	515	570	570	615
Crusher Sand	220	220	245	245	215
Omega 174 (% Binder)	0.60	0.60	0.65	0.65	0.60
Water	175	175	175	175	175
W/C	0.50	0.50	0.60	0.60	0.60
Slump (mm)	170	150	170	120	200

Table B-2 Batched concrete mixes used in winter (materials in kg/m³).

Description	Mix Designs				
	Mix 1	**Mix 2**	**Mix 3**	**Mix 4**	**Mix 5**
Mix designation	**40-PC-I**	**40-PC-II**	**30-PC-I**	**30-PC-II**	**30-FA**
Design Strength (MPa)	40	40	30	30	30
CEM I 52.5N	355	0	285	0	215
CEM II/A-L 52.5N	0	348	0	298	0
Fly Ash	0	0	0	0	90
Coarse aggregate	1130	1176	1082	1156	1083
Dune Sand	530	498	571	546	617
Crusher Sand	226	232	245	244	215
Omega 174 (% Binder)	0.65	0.55	0.65	0.58	0.60
Water	170	168	175	160	160
W/C	0.50	0.50	0.60	0.55	0.55
Slump (mm)	190	150	100	110	170

B.2. Concrete moisture meter (electrical impedance method)

The Tramex concrete moisture meter (CME4) is a non-destructive test device used to measure the surface moisture in the concrete. As mentioned in section 3.6.4.3, the instrument is based on non-destructive impedance measurement. The device has transmitting and receiving electrodes fitted with spring-loaded contacts at the base. The electric impedance is measured by transmitting low-frequency signals between the electrodes passing through the concrete surface, as shown in Figure B-1. The alternate current flowing in the material is inversely proportional to the impedance of the material (Tramex, n.d.). Therefore, a change in impedance is experienced in the presence of moisture, detecting a moisture value on the device's scale (0% - 6%).

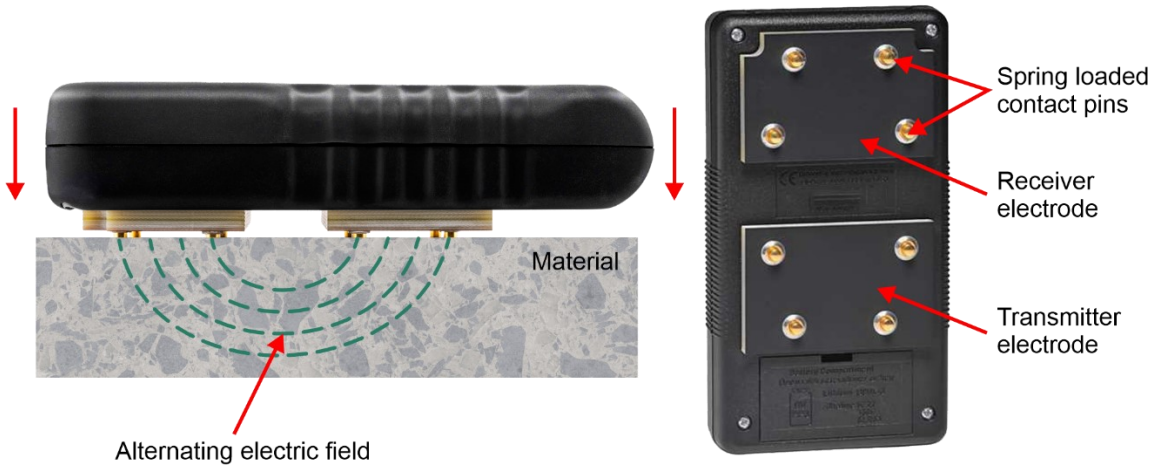

Figure B-1 Concrete moisture meter operation (adapted from Tramex user guide).

Testing procedure

In the study, the surface of the measurement points was first cleaned to remove any dust. The device was then powered on and pressed directly on the test points with all the spring-loaded pins on the electrodes fully compressed. At each location, moisture readings were taken by pausing the meter reading once the pins were compressed and the pointer on the scale was stable. Six readings were taken for each barrier, and three readings for the panel; the highest recorded value on each test element was taken as the moisture value.

B.3. Surface resistivity measurement (Wenner method)

The resistivity measurements were conducted using a Wenner four-probe device. The resistivity meter comprises four probes that enable current transmission in the outer conductors and measures the potential difference between the inner probes (Figure B-2 Schematic diagram of the Wenner resistivity meter (extracted from Screening Eagle technologies).). The measurement indicates the ease of ionic movement in the concrete pore solution (Starck, 2013). The concrete's electrical resistance depends on factors such as the concrete cover layer's microstructure, the pore liquid's conductivity, and the concrete's saturation levels (Beushausen & Louw, 2021). Thus, the resistivity measurements can be used to inform the potential durability of concrete.

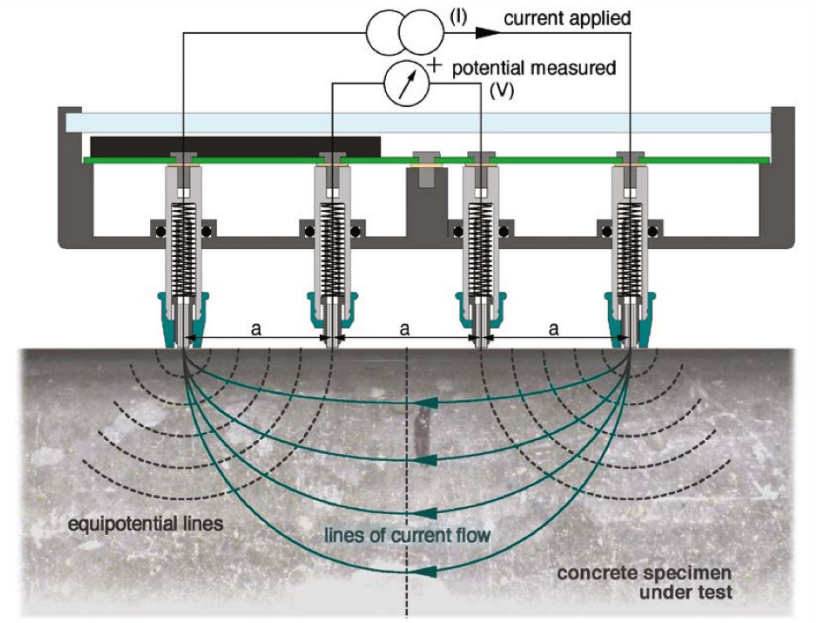

Figure B-2 Schematic diagram of the Wenner resistivity meter (extracted from Screening Eagle technologies).

The following measurement procedure was undertaken:

The resistivity meter was first calibrated using a calibration plate. Then, two readings were taken at each test point by wetting the tips of the four electrodes in water (to enhance electrical contact) and pressing the device against the concrete surface. The device was pressed diagonally on the surface to minimise any influence from the rebars. Twelve readings per median barrier and six readings per panel were taken, and the arithmetic mean of the readings was taken as the surface resistivity of the concrete.

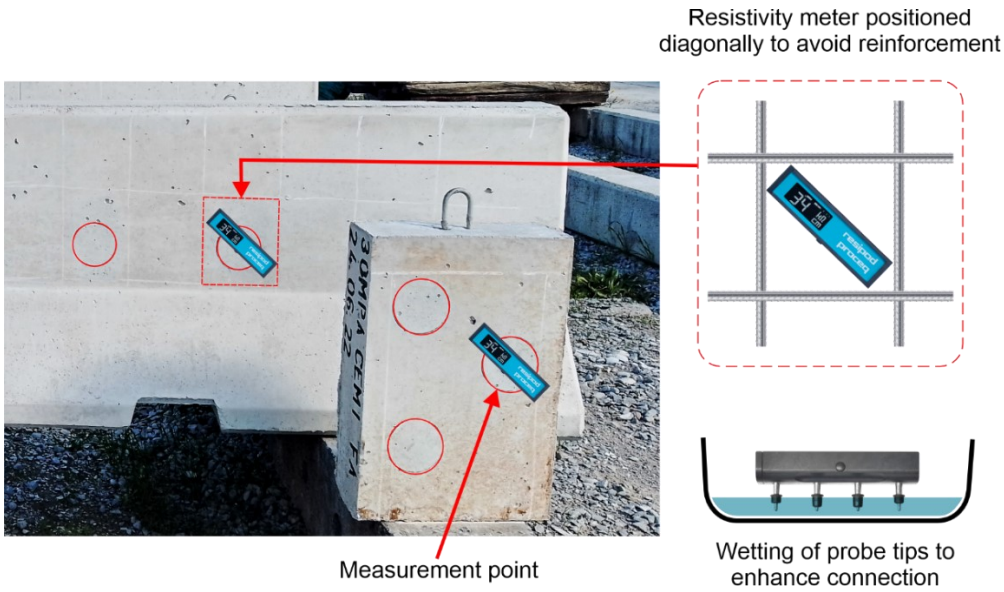

Figure B-3 Resistivity measurement on-site.

B.4. Statistical analysis methods

B.4.1. t-test

The t-test procedure involves the calculation of a t-statistic and comparison against a critical value obtained from the t-distribution tables. The t-statistic represents the actual difference between the means of the two data groups relative to the variability within each group (Bevans, 2022). Microsoft Excel was used to compute the t-tests for the data groups. The equations used in t-test calculations are expressed as:

$$t = \frac{\overline{x_1} - \overline{x_2}}{\sqrt{(S_P{}^2(\frac{1}{n_1} + \frac{1}{n_2}))}} \qquad (B\text{-}1)$$

$$S_P = \frac{(n_1 - 1){S_1}^2 + (n_2 - 1){S_2}^2}{n_1 + n_2 - 2} \qquad (B\text{-}2)$$

Where $\overline{x_1}, \overline{x_2}$ represent the means of the groups
S_P = the pooled standard deviation,
S_1, S_2 = sample or group standard deviation and,
n_1, n_2 = sample sizes

B.4.2. Summary of compressive strength statistical analysis

Table B-3 t-test results for compressive strength data.

Variable	Parameter		T-statistic	df*	P-value	Significance
w/c ratio, concrete grade (summer)	0.5 40 MPa	0.6 30 MPa	2.77	13	0.016	Significant
w/c ratio, concrete grade (winter)	0.5 40 MPa	0.6 30 MPa	5.31	13	<0.001	Significant
Environmental exposure	Summer	Winter	1.67	20.07	0.110	Not significant

**df represents degrees of freedom.*

Table B-4 ANOVA results for compressive strength data.

	Parameters			Sum of squares	df*	Mean square	F-value	p-value	Significance
SUMMER									
Binder type	PC-I	PC-II	FA	100.44	2	50.22	15.28	<0.001	
Residual				39.44	12	3.29			Significant
Total				139.88	14				
WINTER									
Binder type	PC-I	PC-II	FA	48.71	2	24.35	0.52	0.609	
Residual				564.48	12	47.04			Not Significant
Total				613.18	14				

B.5. Mann Whiney U-test

B.5.1. Summary of kOPI statistical analysis

Table B-5 Mann Whitney analysis for influence of w/c ratio, concrete grade, and environmental exposure on kOPI results.

Variable	Parameter		n_1	n_2	Mean ranks		Sum of ranks		U	z	p	Significance
					1	2	T_1	T_2				
w/c ratio, grade (summer)	0.5 40 MPa	0.6 30 MPa	8	12	8.88	11.58	71	139	35	-1	0.316	Not significant
w/c ratio, grade (winter)	0.5 40 MPa	0.6 30 MPa	8	12	10.88	10.25	87	123	45	-0.23	0.851	Not significant
Environmental exposure	summer	winter	20	20	19.75	21.25	395	425	185	-0.41	0.698	Not significant

**Notes:*

U-value represents the Mann-Whitney statistic;

z-value represents the standard deviation from the mean in a normal distribution and is used to determine the significance of the U-value.

B.5.2. Summary of kT statistical analysis

Table B-6 Mann Whitney analysis for influence of w/c ratio, concrete grade, and environmental exposure on kT results (panels).

Variable	Parameter		n_1	n_2	Mean ranks		Sum of ranks		U	z	p	Significance
					1	2	T_1	T_2				
w/c ratio, grade (summer)	0.5 40 MPa	0.6 30 MPa	6	9	5.17	9.89	31	89	10	-2	0.05	Significant
w/c ratio, grade (winter)	0.5 40 MPa	0.6 30 MPa	6	9	6.33	9.11	38	82	17	-1.18	0.272	Not significant
Environmental exposure	summer	winter	15	15	18.03	12.97	270.5	194.5	74.5	-1.58	0.116	Not significant

B.6. Willcoxon-signed rank test

B.6.1. Summary of kOPI statistical analysis

Table B-7 Wilcoxon statistical analysis for the influence of concrete age on kOPI results.

		n	Mean rank	Sum of ranks	W	z	p	Significance
SUMMER								
28 – 56 days	Negative ranks	9	11.56	104	104	-0.04	0.970	Not significant
	Positive ranks	11	9.64	106				
	Ties	0						
	Total	20						
WINTER								
28 – 56 days	Negative ranks	14	9.50	133	77	-1.05	0.296	Not significant
	Positive ranks	6	12.83	77				
	Ties	0						
	Total	20						

**Notes:*

W represents the Wilcoxon test statistic.

Negative ranks: kOPI 56 days < kOPI 28 days

Positive ranks: kOPI 56 days > kOPI 28 days

Ties: kOPI 56 days = kOPI 28 days

B.6.2. Summary of kT statistical analysis

Table B-8 Wilcoxon statistical analysis for the influence of concrete age on kT results.

		n	Mean rank	Sum of ranks	W	z	p	Significance
SUMMER								
28 – 56 days	Negative ranks	1	2.00	2	2	-3.17	0.002	Significant
	Positive ranks	13	7.92	103				
	Ties	1						
	Total	15						
WINTER								
28 – 56 days	Negative ranks	14	7.50	105	0	-3.30	0.001	Significant
	Positive ranks	0	0	0				
	Ties	1						
	Total	15						

Negative ranks: kT 56 days < kT 28 days

Positive ranks: kT 56 days > kT 28 days

Ties: kT 56 days = kT 28 days

Table B-9 Critical values of the W test statistic using the Wilcoxon signed-rank test (extracted from (Walpole et al., 2012).

n	One-Sided $\alpha = 0.01$ Two-Sided $\alpha = 0.02$	One-Sided $\alpha = 0.025$ Two-Sided $\alpha = 0.05$	One-Sided $\alpha = 0.05$ Two-Sided $\alpha = 0.1$
5			1
6		1	2
7	0	2	4
8	2	4	6
9	3	6	8
10	5	8	11
11	7	11	14
12	10	14	17
13	13	17	21
14	16	21	26
15	20	25	30
16	24	30	36
17	28	35	41
18	33	40	47
19	38	46	54
20	43	52	60
21	49	59	68
22	56	66	75
23	62	73	83
24	69	81	92
25	77	90	101
26	85	98	110
27	93	107	120
28	102	117	130
29	111	127	141
30	120	137	152

B.7. Kruskal-Wallis test

B.7.1. Summary of kOPI statistical analysis

Table B-10 Kruskal Wallis analysis of binder type effect on kOPI results.

	n	Median	Mean Rank	Chi^2	df	p-value	Significance
SUMMER							
PC-I	8	0.48	7.88	2.72	2	0.256	Not significant
PC-II	8	0.84	11.88				
FA	4	0.78	13				
Total	20	0.61					
WINTER							
PC-I	8	0.57	9.63	5.64	2	0.06	Not significant
PC-II	8	0.76	13.88				
FA	4	0.44	5.50				
Total	20	0.63					

B.7.2. Summary of kT statistical analysis

Table B-11 Kruskal Wallis analysis of binder type effect on kT results.

	n	Median	Mean Rank	Chi^2	df	p-value	Significance
SUMMER							
PC-I	6	0.06	6.00	2.10	2	0.350	Not significant
PC-II	6	0.30	9.67				
FA	3	0.09	8.67				
Total	15	0.06					
WINTER							
PC-I	6	0.03	6.50	4.73	2	0.094	Not significant
PC-II	6	0.07	11.00				
FA	3	0.03	5.00				
Total	15	0.05					

Table B-12 Chi-squared distribution table (extracted from (DATAtab, 2023a).

Significance level Alpha	0.995	0.975	0.2	0.1	0.05	0.025	0.02	0.01	0.005
Degrees of freedom									
1	0	0.001	1.642	2.706	3.841	5.024	5.412	6.635	7.879
2	0.01	0.051	3.219	4.605	5.991	7.378	7.824	9.21	10.597
3	0.072	0.216	4.642	6.251	7.815	9.348	9.837	11.345	12.838
4	0.207	0.484	5.989	7.779	9.488	11.143	11.668	13.277	14.86
5	0.412	0.831	7.289	9.236	11.07	12.833	13.388	15.086	16.75
6	0.676	1.237	8.558	10.645	12.592	14.449	15.033	16.812	18.548
7	0.989	1.69	9.803	12.017	14.067	16.013	16.622	18.475	20.278
8	1.344	2.18	11.03	13.362	15.507	17.535	18.168	20.09	21.955
9	1.735	2.7	12.242	14.684	16.919	19.023	19.679	21.666	23.589
10	2.156	3.247	13.442	15.987	18.307	20.483	21.161	23.209	25.188

APPENDIX C. SUPPLEMENTARY RESULTS AND ANALYSIS INFORMATION

C.1. Compressive strength data

Table C-1 Summary of compressive strength results at 28 days.

Mix	w/c ratio	Minimum (MPa)	Maximum (MPa)	Mean (MPa)	Std. Deviation (MPa)
SUMMER					
40-PC-I	0.5	46.8	51.6	49.1	2.4
40-PC-II	0.5	45.5	46.8	46.2	0.7
30-PC-I	0.6	45.6	47.2	46.2	0.9
30-PC-II	0.6	44.3	45.3	44.8	0.5
30-FA	0.6	38.3	42.6	40.6	2.2
WINTER					
40-PC-I	0.5	46.6	49.6	47.7	1.6
40-PC-II	0.5	48.9	50.1	49.7	0.7
30-PC-I	0.6	30.3	33.5	32.4	1.8
30-PC-II	0.6	37.7	39.1	38.3	0.7
30-FA	0.6	42.2	44.0	43.1	0.9

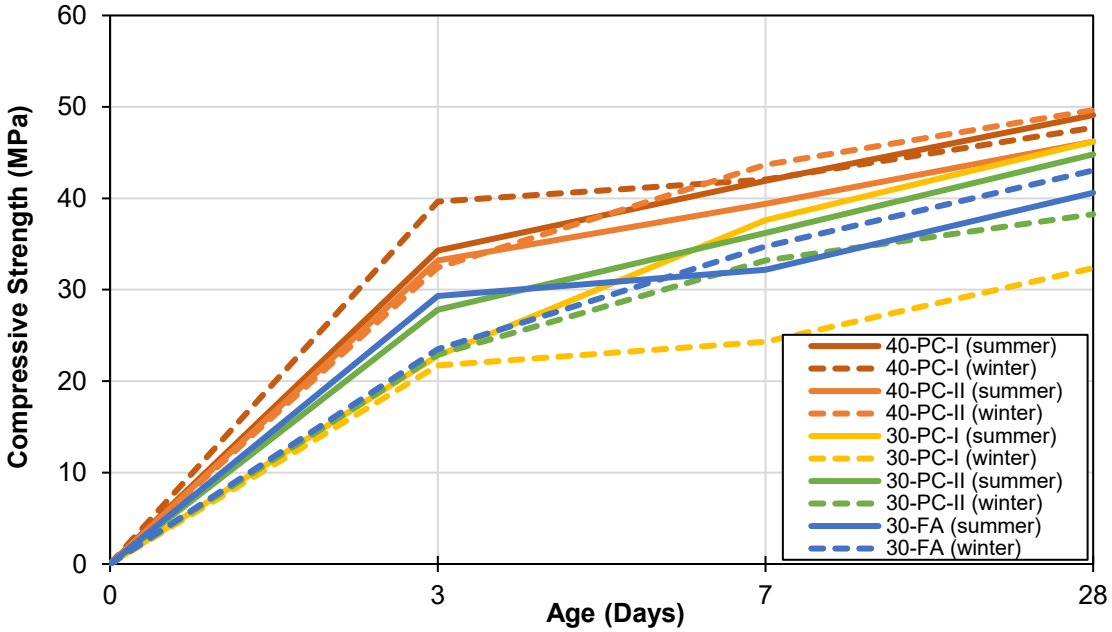

Figure C-1 Compressive strength development over 28 days.

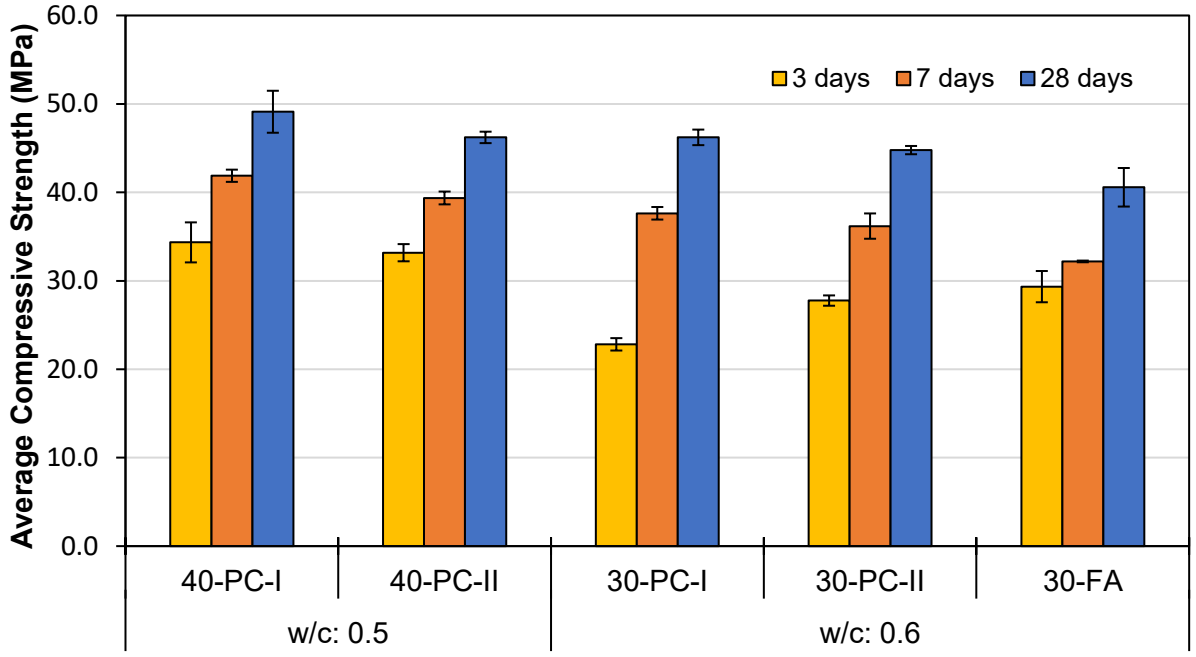

Figure C-2 Strength development of concrete mixes (Summer).

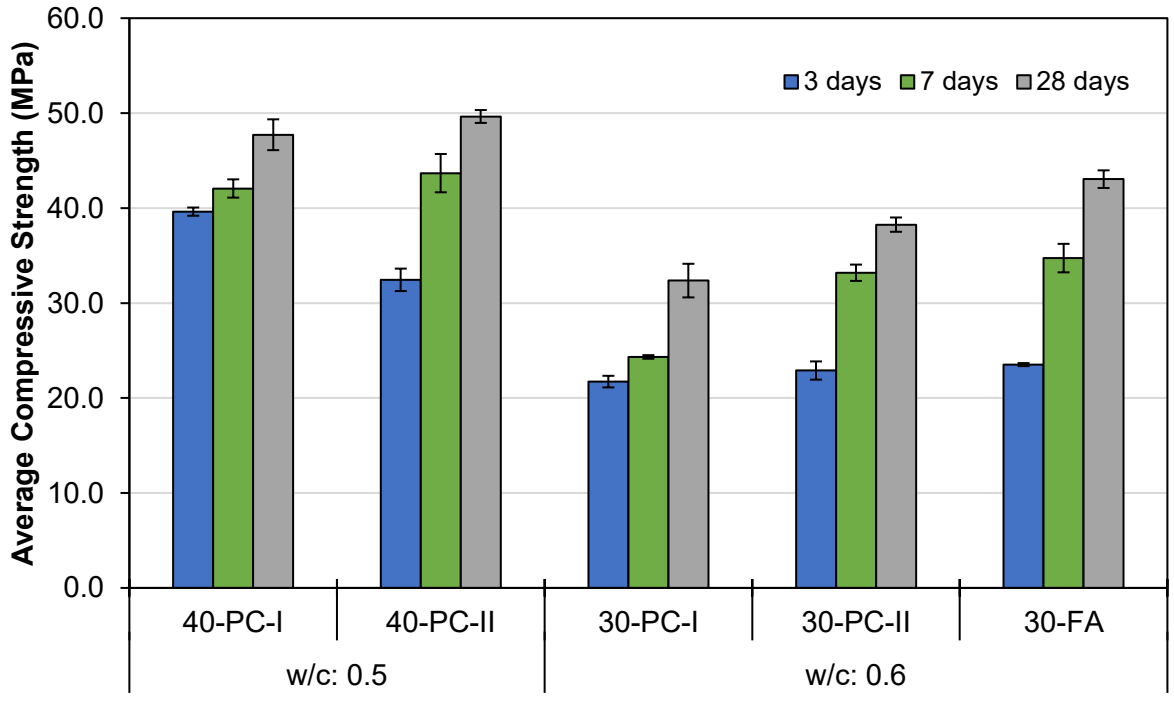

Figure C-3 Strength development of concrete mixes (winter).

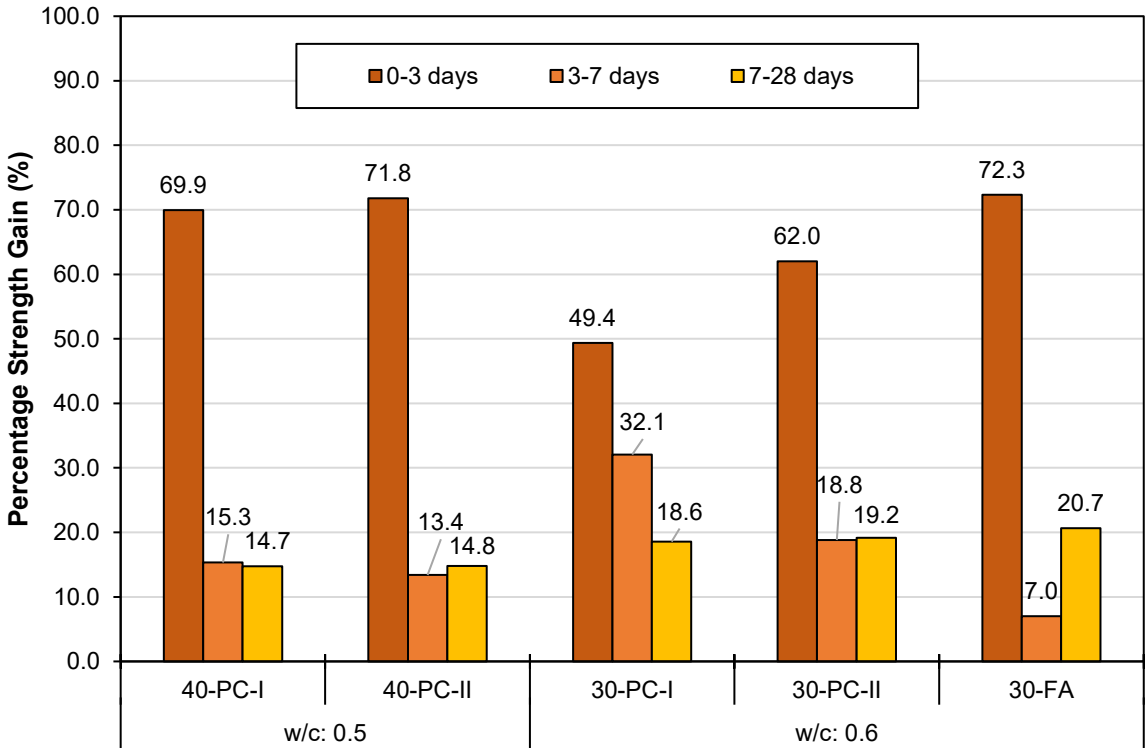

Figure C-4 Percentage strength gain of concrete mixes (summer).

C.2. Rainfall and temperature data

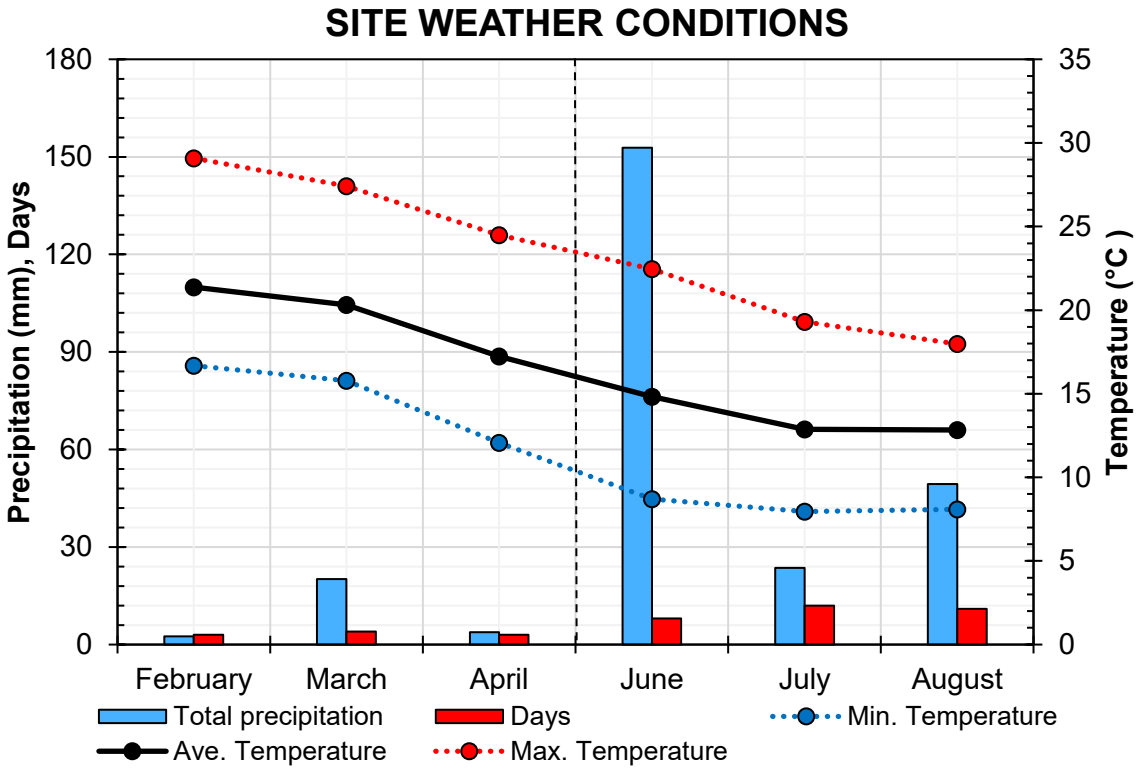

Figure C-5 Site temperature and rainfall data during experimental programme.

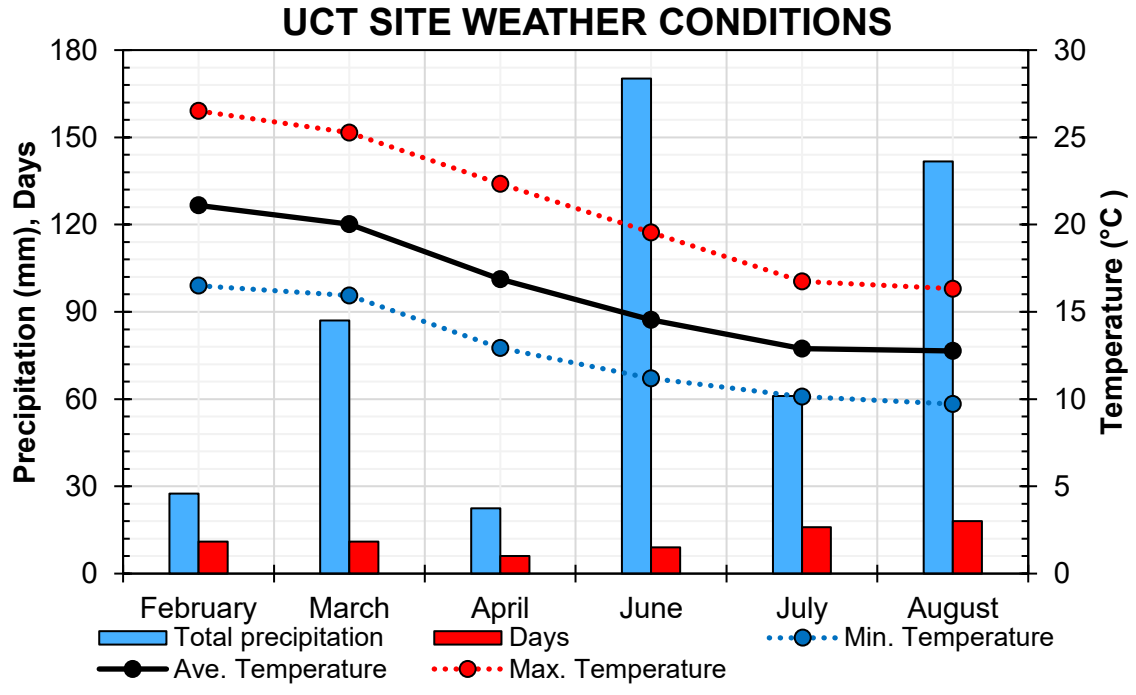

Figure C-6 Site temperature and rainfall data during the experimental programme.

C.3. Oxygen permeability index data

Table C-2 Oxygen permeability index raw data - Log transformed.

Log kOPI (x10^{-10}m/s)							
Mix	**Sample 1**	**Sample 2**	**Sample 3**	**Sample 4**	**Geomean***	**GSD****	**CoV (%)**
SUMMER (28 DAYS)							
40-PC-I	-0.284	-0.441	-0.296	-0.387	0.445	0.08	17.0
40-PC-II	-0.022	-0.079	-0.069	-0.193	0.811	0.07	9.0
30-PC-I	-0.003	0.047	-0.392	-0.347	0.671	0.23	34.0
30-PC-II	0.258	-0.398	-0.352	0.110	0.803	0.33	41.0
30-FA	-0.007	0.150	-0.233	-0.285	0.806	0.20	25.1
SUMMER (56 DAYS)							
40-PC-I	-0.228	-0.369	-0.164	-0.332	0.533	0.09	17.7
40-PC-II	0.132	-0.319	-0.338	-0.415	0.582	0.25	42.6
30-PC-I	-0.117	-0.128	0.007	-0.152	0.799	0.07	8.9
30-PC-II	0.096	0.205	0.266	-0.117	1.295	0.17	13.0
30-FA	-0.159	-0.098	-0.141	0.031	0.809	0.09	10.6
WINTER (28 DAYS)							
40-PC-I	0.036	-0.279	-0.231	-0.269	0.652	0.15	22.9
40-PC-II	-0.093	-0.265	-0.177	0.214	0.831	0.21	25.1
30-PC-I	-0.256	-0.261	-0.160	-0.101	0.639	0.08	12.2
30-PC-II	0.202	0.437	-0.239	-0.149	1.155	0.31	27.2
30-FA	-0.450	-0.442	-0.281	-0.031	0.500	0.20	39.2
WINTER (56 DAYS)							
40-PC-I	-0.336	-0.398	0.175	-0.205	0.644	0.26	39.8
40-PC-II	0.035	-0.319	-0.341	0.037	0.713	0.21	29.7
30-PC-I	-0.333	-0.278	-0.201	-0.151	0.575	0.08	14.1
30-PC-II	-0.047	0.067	-0.052	0.592	1.380	0.31	22.2
30-FA	-0.468	-0.501	-0.247	-0.031	0.488	0.22	44.7

**GeoMean represents the geometric mean*

***GSD represents geometric standard deviation.*

Table C-3 Oxygen permeability index raw data – OPI values.

	OPI Value						
Mix	**Sample 1**	**Sample 2**	**Sample 3**	**Sample 4**	**Average**	**SD**	**CoV (%)**
SUMMER (28 DAYS)							
40-PC-I	10.28	10.44	10.30	10.39	10.35	0.08	0.7
40-PC-II	10.02	10.08	10.07	10.19	10.09	0.07	0.7
30-PC-I	10.00	9.95	10.39	10.35	10.17	0.23	2.2
30-PC-II	9.74	10.40	10.35	9.89	10.10	0.33	3.3
30-FA	10.01	9.85	10.23	10.28	10.09	0.20	2.0
SUMMER (56 DAYS)							
40-PC-I	10.23	10.37	10.16	10.33	10.27	0.09	0.9
40-PC-II	9.87	10.32	10.34	10.42	10.24	0.25	2.4
30-PC-I	10.12	10.13	9.99	10.15	10.10	0.07	0.7
30-PC-II	9.90	9.80	9.73	10.12	9.89	0.17	1.7
30-FA	10.16	10.10	10.14	9.97	10.09	0.09	0.8
WINTER (28 DAYS)							
40-PC-I	9.96	10.28	10.23	10.27	10.19	0.15	1.5
40-PC-II	10.09	10.27	10.18	9.79	10.08	0.21	2.1
30-PC-I	10.26	10.26	10.16	10.10	10.20	0.08	0.8
30-PC-II	9.80	9.56	10.24	10.15	9.94	0.32	3.2
30-FA	10.45	10.44	10.28	10.03	10.30	0.20	1.9
WINTER (56 DAYS)							
40-PC-I	10.34	10.40	9.83	10.20	10.19	0.26	2.5
40-PC-II	9.96	10.32	10.34	9.96	10.15	0.21	2.1
30-PC-I	10.33	10.28	10.20	10.15	10.24	0.08	0.8
30-PC-II	10.05	9.93	10.05	9.40	9.86	0.31	3.1
30-FA	10.47	10.50	10.25	10.03	10.31	0.22	2.1

C.4. Torrent air permeability data

Table C-4 Torrent air permeability raw data for test panels.

SUMMER (28 DAYS)						**SUMMER (56 DAYS)**				
Mix	**kT ($x10^{-16}m^2$)**					**kT ($x10^{-16}m^2$)**				
	Sample 1	**Sample 2**	**Sample 3**	**GeoMean***	**sLOG**	**Sample 1**	**Sample 2**	**Sample 3**	**GeoMean***	**sLOG**
40-PC-I	0.031	0.062	0.017	0.032	0.281	0.043	0.062	0.022	0.039	0.228
40-PC-II	0.530	0.038	0.035	0.089	0.671	0.740	0.067	0.080	0.158	0.581
30-PC-I	0.058	0.054	0.140	0.076	0.230	0.210	0.095	0.170	0.150	0.178
30-PC-II	1.100	1.200	0.078	0.469	0.675	1.500	1.500	0.160	0.711	0.561
30-FA	0.110	0.088	0.045	0.076	0.202	0.160	0.082	0.210	0.140	0.210
WINTER (28 DAYS)						**WINTER (56 DAYS)**				
40-PC-I	0.002	0.014	0.005	0.006	0.393	0.002	0.003	0.002	0.002	0.030
40-PC-II	0.077	0.056	0.059	0.063	0.074	0.025	0.013	0.012	0.016	0.175
30-PC-I	0.068	0.079	0.049	0.064	0.106	0.011	0.011	0.007	0.010	0.103
30-PC-II	0.140	0.094	0.041	0.081	0.272	0.045	0.021	0.010	0.021	0.338
30-FA	0.044	0.034	0.013	0.027	0.279	0.025	0.020	0.003	0.011	0.506

**GeoMean represents the geometric mean*

**sLOG represents the geometric standard deviation (standard deviation of the log kT measurements).*

Table C-5 Torrent air permeability raw data for median barriers.

Mix	kT ($x10^{-16}m^2$)							
	Sample 1	Sample 2	Sample 3	Sample 4	Sample 5	Sample 6	GeoMean*	sLOG
SUMMER (28 DAYS)								
40-PC-I	0.160	0.340	0.340	1.100	0.160	0.099	0.262	0.370
40-PC-II	0.540	0.180	0.160	0.280	0.210	0.470	0.275	0.220
30-PC-I	0.110	0.570	1.200	0.250	0.370	0.410	0.377	0.348
30-PC-II	0.250	0.280	0.400	0.180	0.410	0.620	0.330	0.190
30-FA	0.190	0.160	0.190	0.160	0.190	0.280	0.191	0.089
SUMMER (56 DAYS)								
40-PC-I	0.085	0.094	0.088	0.460	0.160	0.089	0.129	0.289
40-PC-II	0.390	0.150	0.280	0.190	0.120	0.300	0.220	0.196
30-PC-I	0.170	0.330	0.890	0.150	0.640	0.200	0.314	0.320
30-PC-II	0.240	0.270	0.220	0.180	0.170	0.370	0.233	0.124
30-FA	0.180	0.150	0.110	0.120	0.180	0.270	0.161	0.141
WINTER (28 DAYS)								
40-PC-I	0.009	0.007	0.003	0.016	0.012	0.010	0.009	0.241
40-PC-II	0.006	0.007	0.009	0.004	0.006	0.008	0.006	0.146
30-PC-I	0.058	0.200	0.100	0.150	0.060	0.110	0.102	0.214
30-PC-II	0.012	0.024	0.026	0.042	0.033	0.160	0.034	0.375
30-FA	0.039	0.028	0.034	0.037	0.022	0.035	0.032	0.093
WINTER (56 DAYS)								
40-PC-I	0.016	0.006	0.004	0.014	0.009	0.007	0.008	0.225
40-PC-II	0.004	0.005	0.003	0.002	0.004	0.020	0.004	0.359
30-PC-I	0.035	0.110	0.060	0.049	0.027	0.049	0.050	0.209
30-PC-II	0.028	0.015	0.015	0.029	0.010	0.033	0.020	0.208
30-FA	0.019	0.012	0.014	0.011	0.012	0.030	0.015	0.167

C.5. Moisture content data

Table C-6 Concrete surface moisture data - test panels.

Mix	m (%)									
	1	2	3	4	5	6	Minimum	Maximum	Mean	Standard Deviation
SUMMER (28 DAYS)										
40-PC-I	4.3	4.5	4.8	4.6	4.5	4.4	4.3	4.8	4.5	0.2
40-PC-II	4.8	4.6	4.8	4.8	4.7	4.6	4.6	4.8	4.7	0.1
30-PC-I	4.4	4.4	4.7	4.6	4.5	4.6	4.4	4.7	4.5	0.1
30-PC-II	4.8	4.8	5.0	5.2	5.0	5.2	4.8	5.2	5.0	0.2
30-FA	4.3	4.4	4.2	4.4	4.8	4.6	4.2	4.8	4.5	0.2
SUMMER (56 DAYS)										
40-PC-I	4.4	4.4	4.2	4.5	4.2	4.5	4.2	4.5	4.4	0.1
40-PC-II	4.2	4.3	4.0	4.2	4.3	4.2	4.0	4.3	4.2	0.1
30-PC-I	4.2	4.2	4.0	4.2	4.2	4.0	4.0	4.2	4.1	0.1
30-PC-II	4.0	3.8	4.0	4.2	4.0	4.2	3.8	4.2	4.0	0.2
30-FA	3.9	3.8	3.9	4.0	3.8	4.0	3.8	4.0	3.9	0.1
WINTER (28 DAYS)										
40-PC-I	5.2	5.0	4.8	4.8	5.0	5.2	4.8	5.2	5.0	0.2
40-PC-II	5.0	5.2	5.3	5.2	5.0	5.0	5.0	5.3	5.1	0.1
30-PC-I	5.2	4.8	5.0	5.2	4.8	5.3	4.8	5.3	5.1	0.2
30-PC-II	5.4	5.2	5.4	5.3	5.2	5.2	5.2	5.4	5.3	0.1
30-FA	5.4	4.8	5.0	53.4	5.0	4.9	4.8	5.4	5.1	0.3
WINTER (56 DAYS)										
40-PC-I	5.4	5.0	5.2	5.4	5.0	5.3	5.0	5.4	5.2	0.2
40-PC-II	5.2	5.2	5.0	5.5	5.2	5.3	5.0	5.5	5.2	0.2
30-PC-I	5.0	5.0	4.9	5.3	5.2	5.0	4.9	5.3	5.1	0.2
30-PC-II	5.4	5.0	5.2	4.8	5.0	5.4	4.8	5.4	5.1	0.2
30-FA	5.2	5.0	5.2	4.7	4.8	5.1	4.7	5.2	5.0	0.2

Table C-7 Concrete surface moisture data - median barriers.

Mix	m (%)															
	1	2	3	4	5	6	7	8	9	10	11	12	Min	Max	Mean	S.D
SUMMER (28 DAYS)																
40-PC-I	3.9	4.4	3.7	2.9	4.3	4.1	4.1	4.3	3.4	3.7	4.4	3.9	2.9	4.4	3.9	0.5
40-PC-II	3.8	3.8	3.9	3.8	3.8	3.8	3.6	3.8	3.8	3.9	3.8	3.8	3.6	3.9	3.8	0.1
30-PC-I	3.8	4.0	3.6	3.6	3.8	3.8	3.8	3.8	3.6	3.6	4.0	3.8	3.6	4.0	3.8	0.1
30-PC-II	3.6	4.0	3.8	4.1	4.2	3.8	3.8	4.2	4.1	3.8	4.0	3.6	3.6	4.2	3.9	0.2
30-FA	3.6	3.8	3.8	3.6	4.0	4.0	4.0	3.8	3.6	3.8	3.8	3.6	3.6	4.0	3.8	0.2
SUMMER (56 DAYS)																
40-PC-I	4.5	4.2	4.2	4.0	4.4	4.2	4.4	4.4	4.0	4.2	4.5	4.2	4.0	4.5	4.3	0.2
40-PC-II	3.8	3.8	3.6	3.6	3.8	3.8	3.6	3.6	3.8	3.8	3.6	3.6	3.6	3.8	3.7	0.1
30-PC-I	3.4	3.2	3.7	3.5	3.5	3.6	3.6	3.5	3.5	3.7	3.2	3.4	3.2	3.7	3.5	0.2
30-PC-II	3.8	4.0	4.0	3.6	3.8	3.6	3.6	3.8	4.0	4.0	3.8	3.8	3.6	4.0	3.8	0.2
30-FA	3.8	3.8	3.8	4.0	4.0	3.6	3.6	4.0	4.0	3.8	3.8	3.8	3.6	4.0	3.8	0.1
WINTER (28 DAYS)																
40-PC-I	4.5	4.6	4.6	4.4	4.6	4.8	4.6	4.5	4.4	4.8	4.6	4.5	4.4	4.8	4.6	0.1
40-PC-II	5.4	5.4	5.2	5.4	5.5	5.2	5.4	5.5	5.2	5.4	5.5	5.4	5.2	5.5	5.4	0.1
30-PC-I	5.5	5.4	5.3	5.4	4.9	4.6	5.0	5.4	5.5	5.2	5.0	4.9	4.6	5.5	5.2	0.3
30-PC-II	5.3	5.2	5.4	5.4	5.4	5.2	5.2	5.2	5.4	5.3	5.4	5.3	5.2	5.4	5.3	0.1
30-FA	5.4	5.4	5.3	5.5	5.4	5.4	5.5	5.3	5.4	5.4	5.5	5.4	5.3	5.5	5.4	0.1
WINTER (56 DAYS)																
40-PC-I	5.0	5.2	4.9	4.6	5.0	4.9	5.0	5.0	4.9	4.9	5.0	5.2	4.6	5.2	5.0	0.2
40-PC-II	5.4	5.5	5.4	5.4	5.4	5.1	5.3	5.1	5.4	5.4	5.4	5.5	5.1	5.5	5.4	0.1
30-PC-I	5.4	4.9	5.2	5.4	5.4	4.8	5.0	4.4	4.8	5.2	5.4	5.0	4.4	5.4	5.1	0.3
30-PC-II	5.3	5.2	5.2	5.2	53.3	5.2	5.5	5.3	5.0	5.2	5.2	5.3	5.0	5.5	5.2	0.1
30-FA	5.2	5.4	5.2	5.1	5.5	5.3	5.5	5.0	5.2	5.1	5.4	5.1	5.0	5.5	5.3	0.2

C.5.1. Surface moisture content vs penetration depth

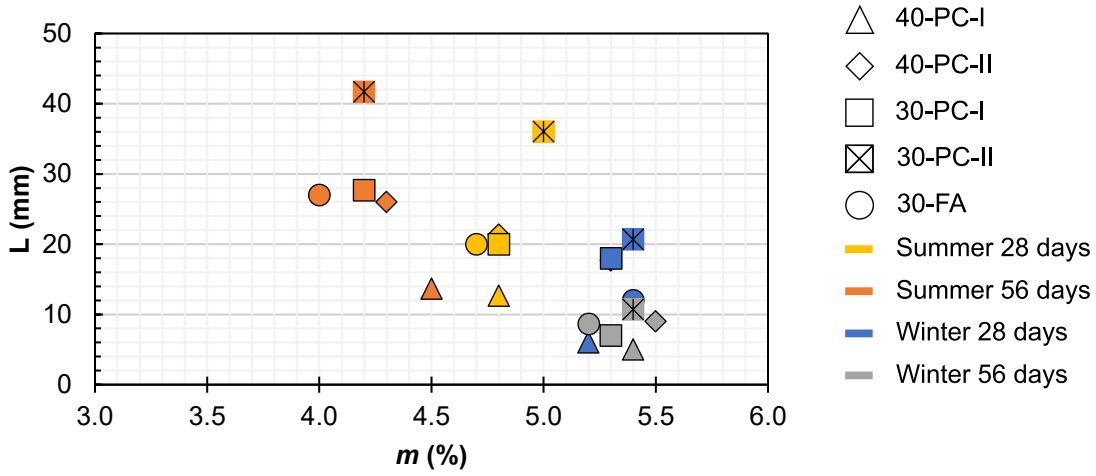

Figure C-7 Measured kT vs penetration depth (test panels).

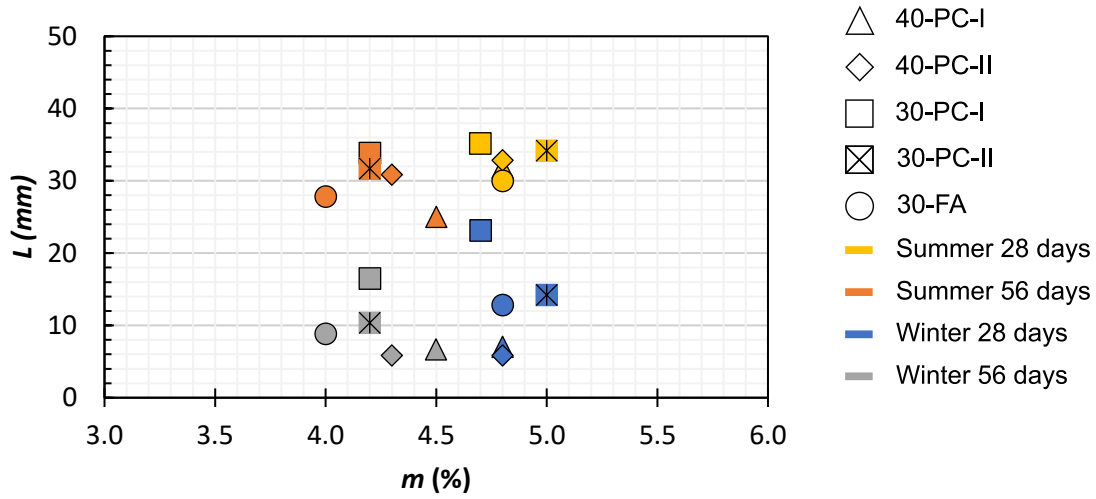

Figure C-8 Measured kT vs penetration depth (median barriers).

APPENDIX D. ADDITIONAL INFORMATION

D.1. Torrent permeability recording sheet

Test Report for Air-permeability after Standard SIA 262/1- E

Ordered by:……
Jobsite:……
Construction element: ……..
Concrete Composition / Properties:……
Date of Concreting of the element:……

Element exposure to weather:..... .....
Weather last 2 days:……..……..
Weather during test:…….... ....
Air temperature at …. hour … °C at …. hour … °C
Element temperature at …. hour … °C at …. hour … °C

Measured on …….. from …. until …. hour
Measured by: …… Company: ……

Air-permeability Instrument: …… .
Moisture meter: ……

Preparation of the Surface (e.g. polishing):……
Remarks (existence of cracks, surface protection systems, etc.): ……
……
Results of the Calibration……

Measure-ment Point [-]	Centre of Vacuum cell: Distance from …… [m]	Centre of Vacuum cell: Height from Floor [m]	Instrument Test No. [-]	Air-permeability kTi [10^{-16} m^2]	Elect. Resistivity [kΩcm]	Moisture content]%[	Comments

Number of results > kTs: …..	kTs = ….. 10^{-16} m^2	Conformity: Y / N

Number of results > kTs: …..		Conformity: Y / N

Conditions for Measurement acceptable: Y / N / partly due to …….

Remarks	Signature

APPENDIX E. ETHICS CLEARANCE

ETHICS APPLICATION FORM

Please Note:
Any person planning to undertake research in the Faculty of Engineering and the Built Environment (EBE) at the University of Cape Town is required to complete this form **before** collecting or analysing data. The objective of submitting this application *prior* to embarking on research is to ensure that the highest ethical standards in research, conducted under the auspices of the EBE Faculty, are met. Please ensure that you have read, and understood the **EBE Ethics in Research Handbook** (available from the UCT EBE, Research Ethics website) prior to completing this application form: http://www.ebe.uct.ac.za/ebe/research/ethics1

APPLICANT'S DETAILS		
Name of principal researcher, student or external applicant		SEAN THABANI ALFRED
Department		CIVIL ENGINEERING
Preferred email address of applicant:		ALFSEA001@myuct.ac.za
If Student	Your Degree: e.g., MSc, PhD, etc.	MSc.(Eng) CIVIL INFRASTRUCTURE MANAGEMENT AND MAINTENANCE
	Credit Value of Research: e.g., 60/120/180/360 etc.	120
	Name of Supervisor (if supervised):	PROF. MARK ALEXANDER
If this is a researchcontract, indicate the source of funding/sponsorship		
Project Title		Integrating Non-Invasive Test Methods to the SA Durability Index Approach

I hereby undertake to carry out my research in such a way that:

- there is no apparent legal objection to the nature or the method of research; and
- the research will not compromise staff or students or the other responsibilities of the University;
- the stated objective will be achieved, and the findings will have a high degree of validity;
- limitations and alternative interpretations will be considered;
- the findings could be subject to peer review and publicly available; and
- I will comply with the conventions of copyright and avoid any practice that would constitute plagiarism.

APPLICATION BY	Full name	Signature	Date
Principal Researcher/ Student/External applicant	SEAN THABANI ALFRED		11/02/22
SUPPORTED BY	Full name	Signature	Date
Supervisor (where applicable)	PROF. MARK ALEXANDER		11/02/22

APPROVED BY	Full name	Signature	Date
HOD (or delegated nominee) Final authority for all applicants who have answered NO to all questions in Section 1; and for all Undergraduate research (Including Honours).	Prof. Alphose Zingoni		04/04/2022
Chair: Faculty EIR Committee For applicants other than undergraduate students who have answered YES to any of the questions in Section 1.			

RE: Mix designs: UCT Research Project

MA **Mark Alexander <mark.alexander@uct.ac.za>**
2/11/2022 9:56 AM

To: Sean Alfred

EBE EiRC signature form...
199.62 KB

Herewith – and take this email as 'proof' of signature.

Prof Alexander

Emeritus Prof Mark G Alexander
Department of Civil Engineering, University of Cape Town
Private Bag X3
7701 Rondebosch, South Africa

Tel: +27 (0)21 650 4012 Fax: +27 (0)86 425 8652 Cell: +27 (0)76 426 1088
Email: mark.alexander@uct.ac.za
URL: www.civil.uct.ac.za ; www.comsiru.uct.ac.za

From: Sean Alfred <ALFSEA001@myuct.ac.za>
Sent: Friday, 11 February 2022 12:53 PM
To: Mark Alexander <mark.alexander@uct.ac.za>
Subject: RE: Mix designs: UCT Research Project

My apologies Prof,

I have attached the form now.

I agree, we must come up with something. Perhaps we can discuss when you are back?

Best regards,
Sean

Sent from Mail for Windows